Characterization and Optimization of Polyethylene Blends

Marlene J. Cran

Submitted for the degree of
Doctor of Philosophy
December 2004

School of Molecular Sciences
Victoria University

Cran, Marlene J
Characterization and
optimization of polyethylene

Declaration

I, Marlene Cran, declare that the PhD thesis entitled "Characterization and Optimization of Polyethylene Blends" is no more than 100,000 words in length, exclusive of tables, figures, appendices, references and footnotes. This thesis contains no material that has been submitted previously, in whole or in part, for the award of any other academic degree or diploma. Except where otherwise indicated, this thesis is my own work.

[redacted]

30th May, 2005

Signature

Date

Abstract

Several series of polyethylene (PE) blends were prepared where one component is a conventional PE and the second is a conventional linear low-density polyethylene (LLDPE) or a metallocene-catalyzed LLDPE. A two-step isothermal annealing (TSIA) procedure is developed enabling the satisfactorily resolution of endothermic peaks of blends of low-density polyethylene with LLDPE using standard thermo-analytical techniques. The TSIA procedure enables the quantification of components in an unknown, previously calibrated blend. The quantitative analysis of PE blends by Fourier-transform infrared (FT-IR) spectroscopy is explored and achieved by the development of a linear relationship based on the ratio of two absorbances in an FT-IR spectrum. The method exhibits potential for routine analyses of PE blends that have been previously calibrated. Chemiluminescence (CL) monitoring is successfully applied to study the oxidative degradation of PE blends. The CL data are consistent with the thermal and physicomechanical properties of the blends with a decreased blend miscibility reflected in the CL data as a departure from the idealized behaviour observed for more miscible blends. The physicomechanical and optical properties of PE blends are investigated and the results used to optimize the composition of particular film blends and assess the effects of downgauging the film thickness.

Publications Arising from this Work

Papers in Refereed Journals

Marlene J. Cran, Peter K. Fearon, Norman C. Billingham, and Stephen W. Bigger, "The Application of Chemiluminescence to Probe Miscibility in Metallocene-Catalyzed Polyethylene Blends", *J. Appl. Polym. Sci.*, 89, 3006-3015 (2003).

Marlene J. Cran and Stephen W. Bigger, "Quantitative Analysis of Polyethylene Blends by Fourier-Transform Infrared Spectroscopy", *Appl. Spectrosc.*, 57, 928-932 (2003).

Marlene J. Cran and Stephen W. Bigger, "The Effect of Metallocene-Catalyzed Linear Low-Density Polyethylene on the Physicomechanical Properties of its Film Blends with Low-Density Polyethylene", *J. Mater. Sci.*, 40, 621-627 (2005).

Marlene J. Cran and Stephen W. Bigger, "The Effect of Downgauging on the Physicomechanical Properties of Film Blends of Linear Low-Density Polyethylene with Low-Density Polyethylene", *J. Elast. and Plast.*, 37, 229-236 (2005).

Marlene J. Cran, Stephen W. Bigger and John Scheirs, "Characterizing Blends of Linear Low-Density and Low-Density Polyethylene by Differential Scanning Calorimetry", *J. Therm. Anal. and Cal.*, 81, 321-327 (2005).

Marlene J. Cran and Stephen W. Bigger, "The Effect of Metallocene-Catalyzed Polyethylene on the Physicomechanical Properties of Blends with Conventional Polyethylenes", *J. Plast. Film Sheeting* (submitted May 2005).

Conference/Symposium Presentations

David B. Barry, Wayne Laughton, Olga Kravaritis, Marlene J. Cran and Stephen W. Bigger, "Properties of Metallocene and Low-Density Polyethylene Blends", presented at 22nd Australasian Polymer Symposium, The University of Auckland, Auckland, NZ, February, 1997.

Marlene J. Cran, Stephen W. Bigger, David B. Barry, Kathleen Boys and Wayne R. Laughton, "Blending Metallocene-Catalyzed Polyethylene with Low-Density Polyethylene to Improve Physicomechanical Properties", presented at "Macro98", the 37th International Symposium on Macromolecules, IUPAC World Polymer Congress, Gold Coast, Australia, 12th-17th July, 1998.

Marlene J. Cran, Stephen W. Bigger, David B. Barry, Kathleen V. Boys and Bill Tassigiannakis, "Blending Low-Density Polyethylene with Metallocene-Catalyzed Linear Low-Density Polyethylene to Improve Film Properties", presented at the 217th National Meeting of the American Chemical Society, Anaheim, USA, 21st-25th March, 1999.

Marlene J. Cran, Stephen W. Bigger, R. John Casey, David B. Barry, Kathleen V. Boys and Bill Tassigiannakis, "Blending Metallocene-Catalyzed Polyethylene with Conventional Polyethylene to Improve Physicomechanical Properties", presented at the 23rd Australasian Polymer Symposium, Deakin University, Geelong, Australia, 28th November-2nd December, 1999.

Stephen W. Bigger, Marlene J. Cran, Peter K. Fearon and Norman C. Billingham, "Use Of Chemiluminescence Techniques for Analyzing the Stability of Polymer Blends", presented at11th Annual Conference on Polymer Additives, Clearwater Beach, Florida, USA, 24th-27th March, 2002.

Conference Proceedings

Marlene J. Cran, Stephen W. Bigger, Kathleen V. Boys, Bill Tassigiannakis and David B. Barry, "Blending Low-Density Polyethylene with Metallocene-Catalyzed Linear Low-Density Polyethylene to Improve Film Properties", *ACS Div. Polym. Chem., Polym. Prepr.*, 40, 375-376 (1999).

Stephen W. Bigger, Marlene J. Cran, Peter K. Fearon and Norman C. Billingham, "Use Of Chemiluminescence Techniques for Analyzing the Stability of Polymer Blends", *Proc. Additives 2002, Clearwater Beach, Florida, USA, 24th-27th March, 2002.*

Table of Contents

Chapter 3 Materials and Methods

Chapter 4 Results and Discussion

List of Tables

List of Figures

List of Abbreviations and Symbols

AO	Antioxidant
C4	Butene (comonomer)
C6	Hexene (comonomer)
C8	Octene (comonomer)
CCD	Charge coupled device
CL	Chemiluminescence
CL-OIt	CL oxidative induction time
CLI	Chemiluminescence imaging
CLI-OIt	CLI oxidative induction time
DSC	Differential scanning calorimetry
FT-IR	Fourier-transform infrared (spectroscopy)
HDPE	High-density polyethylene
iPP	Isotactic polypropylene
IR	Infrared (spectroscopy)
IS	Impact strength (Izod)
LCB	Long-chain branching
LDPE	Low-density polyethylene
LLDPE	Linear low-density polyethylene
LLPS	Liquid-liquid phase separation
LMWPE	Low molecular weight polyethylene
MD	Machine direction (film)
MFI	Melt flow index
MFR	Melt flow ratio
MI_2, MI_{21}	Melt flow index (2.1 kg, 21 kg)
mLLDPE	Metallocene-catalyzed linear low-density polyethylene
mPE	Metallocene-catalyzed polyethylene
2MPPO	2,6-dimethyl-poly(phenylene oxide)
MW	Molecular weight
MWD	Molecular weight distribution
NR	Natural rubber
OIt	Oxidative induction time
PA	Polyamide
PBD	Polybutadiene
PE	Polyethylene
PET	Polyethylene terephthalate
PP	Polypropylene
PPE	Poly(phenylene ether)
PS	Polystyrene
PVC	Polyvinyl chloride
SBR	Styrene-butadiene rubber
SCB	Short-chain branching
SCG	Slow crack growth
SSA	Successive self-nucleation and annealing
STD	Second time derivative (analysis)
TD	Transverse direction (film)
TSIA	Two-step isothermal annealing
UHMWLPE	Ultra high molecular weight linear polyethylene
UHMWPE	Ultra high molecular weight polyethylene
ULDPE	Ultra low-density polyethylene
VLDPE	Very low-density polyethylene
ΔH_{fus}	Heat of fusion of 100% crystalline PE
X	Percent crystallinity
A, A_a, A_b	IR Absorbance, at frequencies *a* and *b*
K_{1a}, K_{2a}	Absorptivities of components 1 and 2 at frequency *a*
K_{1b}, K_{2b}	Absorptivities of components 1 and 2 at frequency *b*
χ, χ_1, χ_2	Mass fraction, of components 1 and 2
ΔA	Change in *radar* plot area
G_a, G_b	Film gauge lengths
m_a, m_b	Masses of 1 m^2 film sections
ρ_1, ρ_2, ρ_3	Densities of components 1, 2 and 3
C_a, C_b	Costs of 1 m^2 film sections
c_1, c_2, c_3	Cost per unit mass of components 1, 2 and 3

Acknowledgements

Thank you to my supervisor, Associate Professor Stephen W. Bigger. I thank him for helping me to maintain focus and direction throughout the research process, and for his attention to detail. I am appreciative of his kindness and encouragement, and for valuable guidance in all aspects of scientific research.

Thank you to Dr. Peter K. Fearon and Professor Norman C. Billingham of The University of Sussex for their assistance with the development of the chemiluminescence analytical method. I am also grateful to Mettler-Toledo for the supply of the DSC-CL instrument.

Thank you to Dr. John Scheirs of ExcelPlas Australia Limited for his assistance with the development of the TSIA analytical procedure.

Thank you to Associate Professor R. John Casey and Professor John D. Orbell for providing helpful advice and for many useful discussions throughout the course of this work.

I am grateful to Qenos (formerly Kemcor Australia Limited) for providing the polymers used in the blends, for assistance with the preparation of the blends and the film, and for providing access to some of the testing equipment.

Thank you to my family for their continuous encouragement and support throughout the course of this work. I am particularly grateful for their valuable assistance in numerous trips to libraries for photocopying and for proof-reading thesis chapters.

This work was supported by an Australian Postgraduate Research Award.

Chapter 1 Introduction

This chapter provides an insight into the historical development of natural and synthetic polymers with particular attention given to the polyethylenes. The concept of polymer blends is explored and the historical development of blending polymers to form new materials is also discussed.

1.1 The History of Natural and Synthetic Polymers

The first materials that would have been classified as polymers by the current definition were derived from natural sources. References to such materials have appeared throughout history and include bitumen, amber resin, shellac, and gutta percha [1]. The use of natural rubber produced from the latex extracts of the *Hevea brasiliensis* tree [2] was possibly first discovered in the 1400s by Columbus and explorers. Natural rubber, the precursor to polyisoprene, is still widely produced commercially throughout the world. Perhaps the first instance of chemical modification of a natural material occurred in the early 1800s when natural rubber was heated with sulfur. This process was termed *vulcanization* and was first patented in 1851 [1]. The resulting product was known as *ebonite*, *vulcanite* or *hard rubber* and is recognized as one of the first thermosetting plastics materials [1]. The nitration of cellulose and subsequent production of *Parkesine* in the 1860s was arguably the first instance of a thermoplastic material [1]. The production of *celluloid* followed in the 1870s and this was produced by reacting cellulose nitrate with camphor as a plasticizer [1].

From the late 1800s to the early 1900s, the production of polymeric materials was still considerably experimental. In the late 1800s, the reaction of milk protein with formaldehyde resulted in the production of casein plastics that are still used today. Polymer resins based on phenol and formaldehyde were also produced in the late 1800s although useful products such as *Bakelite* [3] were not developed until the early 1900s [4]. Other formaldehyde resins such as those based on urea soon followed and these are still used commercially today. Cellulose acetate was developed in the 1920s as a possible replacement for the somewhat volatile *celluloid* [1]. In the early 1930s, phenolic resins were successfully commercialized and this achievement is arguably the precursor to the modern plastics industry [1].

Ethylene-based polymers such as polyolefins (*esp.* low-density- or branched-polyethylene), polyvinyl chloride and polystyrene were also first developed commercially in the 1930s. These were termed *vinyl* plastics and are among the major thermoplastics produced today. In the 1940s, significant developments included the production of polyamides (*Nylon*), polytetrafluoroethylene (*Teflon*) and melamine. High-impact polystyrene was introduced in the early 1950s and is arguably the first instance of a synthetic commercial polymer blend. The advancement of catalyst systems and polymerization techniques in the mid-1950s resulted in the production of linear polyethylene (high-density polyethylene) and crystalline polypropylene. This era also saw the commercial production of acetal resins and polycarbonates as well as acrylonitrile-butadiene-styrene that was first developed as an impact modifier for high-impact polystyrene.

The control of molecular structure during polymerization was a major achievement in the 1950s with the development of specialized catalyst systems. These systems were based on organometallic molecules and were termed *Ziegler-Natta* catalysts after the primary developers Karl Ziegler and Guilio Natta [1]. These catalysts enabled the polymerization of materials with properties different to those produced earlier using the same monomers. By the 1960s, developments in polymer technology were directed towards the production of special purpose materials rather than general commodity polymers [1]. These specialty polymers included polysulfones, aromatic polyesters and polyphenylene oxides and the trend in the development of specialty polymers continued in the 1970s. The most recent major progression in polymer science has arguably been through the pioneering work of Walter Kaminsky performed in the area of catalyst systems [5]. Advances in organometallic chemistry resulted in the production of metallocene catalysts that have been used mainly in the production of ethylene, propylene and styrene polymers. Metallocene-catalyzed polyolefins, in particular, have been produced commercially since the late 1990s [1]. Although the use of metallocene-catalysts is well established, the true potential of this technology is probably yet to be fully realized.

The growth of the plastics industry, from its early beginnings of natural polymers through to the full commercialization of sophisticated modern plastics materials, has occurred rapidly over the past 90 years or so. Table 1.1 summarizes the historical development of many of the major natural and synthetic polymers in chronological order [2,6-16]. This table illustrates many of the major achievements in polymer technology in both scientific and commercial developments. Alongside the growth of the plastics industry, the scientific study of polymers has also developed rapidly with several scientific journals dedicated to the research into polymeric materials.

1.2 The Development of Polyethylenes

Polyolefins and polyethylene (PE) in particular are highly significant polymers commercially, industrially and scientifically, and their development merits further attention. Branched PE (or low-density polyethylene, LDPE) was one of the first polyolefins produced commercially in the early 1940s by the free radical polymerization of ethylene using a high temperature and high pressure process [17]. The development of lower temperature and lower pressure processes and using highly active catalysts resulted in the production of linear PE (or high-density polyethylene, HDPE) in the mid-1950s [17].

Further developments in catalyst technology lead to the production of copolymers of ethylene with small amounts of an α-olefin [18,19]. This method of polymerization incorporates short side-chains or branches on the ethylene backbone and the resulting polymers, linear low-density polyethylene (LLDPE), were first developed commercially in the late 1970s [17]. Ultra high molecular weight polyethylene (UHMWPE) is similar in structure to HDPE [5] and is produced by the Ziegler process [17]. Due to its high melt viscosity, a result of the high molecular weight (MW) and degree of polymer chain entanglements, UHMWPE is relatively difficult to process [20-22]. The benefits of using UHMWPE arise from the superior impact properties, high abrasion resistance, low creep and good resistance to stress-cracking of this material [17].

Table 1.1. Historical development of natural and synthetic polymer materials.

Year	Polymer development/comments
1839	Vulcanized rubber was produced by heating latex or natural rubber with sulfur (Charles Goodyear, USA).
1862	Parkesine was produced by reacting modified cellulose with nitric acid to form cellulose nitrate and then mixing this polymer with a plasticizer (Alexander Parks, USA).
1869	Celluloid, cellulose nitrate plasticized with camphor was patented (John Wesley Hyatt and Isaiah Hyatt, USA).
1880	Isoprene rubber was produced (Gustave Bouchardat, France).
1898	Polycarbonates were first produced, but not fully commercialized until 1960.
1907	Bakelite, the first synthetic thermosetting polymer, was produced by reacting phenol and formaldehyde (Leo Baekeland, USA).
1912	Polyvinyl chloride was first synthesized (J. J. Ostromislensky).
1929	Styrene-butadiene rubber was first synthesized (IG Farben).
1933	Branched polyethylene was discovered accidentally (Eric William Fawcett, UK) then first produced commercially in 1939.
1935	Nylon (polyamide-6,6) was first synthesized (Wallace Hume Carothers, Du Pont).
1936	Epoxy resins were synthesized in Switzerland (Pierre Castan).
1937	Polyurethanes were first produced (Bayer, IG Farbenindustries).
1938	Polytetrafluoroethylene (*Teflon*) was discovered accidentally (Roy Plunkett, USA).
1941	Polyethylene terephthalate was first synthesized (Whinfield and Dickson).
1953	Ziegler catalyst systems (based on aluminium alkyls and titanium tetrachloride) were first developed resulting in production of linear polyethylene (Karl Ziegler, Germany) concurrent with development of Phillips catalysts (based on metal oxides) also producing linear polyethylene (Phillips Petrol. and Std. Oil).
1954	Crystalline or isotactic polypropylene was first developed using Ziegler catalysts (Guilio Natta, Italy), and produced commercially in 1957.
1960	Polyoxymethylene (polyacetal) was first synthesized (DuPont Co, USA).
1961	Aromatic polyamide fibres were introduced (DuPont Co, USA).
1968	Poly(phenylene terephthalamide) was first spun into strong, stiff fibres (Kwolek and Morgan, DuPont Co, USA).
1972	Liquid crystal polyesters were first produced commercially.
1973	Polyphenylene sulfide was first produced (Phillips Chemical Co.).
1977	Linear low-density polyethylene was first produced (Union Carbide Co., USA).
1982	Polyetherimide (amorphous engineering thermoplastic) was first introduced (General Electric Co.).
1990s	Metallocene-catalyzed polyolefins were first commercialized (Exxon, USA).
1996	Commercial production of metallocene-catalyzed polypropylenes (Exxon, USA).

More recently, advances in single-site metallocene-catalysts have resulted in the production of structurally superior PEs which were first commercially produced in the late 1990s [17]. Metallocene-catalyzed PEs (mPEs) are usually ethylene copolymers with a more uniform incorporation of the comonomer and have a narrower molecular weight distribution (MWD) than conventional LLDPEs. The terms very low-density polyethylene (VLDPE) or ultra low-density polyethylene (ULDPE) are often used to describe metallocene-catalyzed PEs [17,23-30] and due to the inherent plastic and elastomeric features, mPEs are often referred to as *plastomers* [31]. Although the mPEs are relatively new, the properties of these materials are well characterized and established in the literature [32-43].

The versatility of the polymers belonging to the PE family is further illustrated in Table 1.2 which lists the main types of PEs and their uses [2,5,17,44]. The range and diversity of the various PE grades is extended by the range of molecular weights that can be obtained by precise control of the polymerization processes [5].

Table 1.2. Types and uses of the various PE resins.

PE	Density range / g cm^{-3}	Comments and applications
LDPE	0.910-0.935	Tough and flexible polymer mainly used for packaging film, general purpose moulding of domestic products such as bottles and tubes, depending on the MW.
HDPE	0.935-0.965	Stronger and stiffer than LDPE, used mainly in blow moulding, low MW HDPEs used for general purpose moulding. Uses include pipe, tapes, films, and bottles.
LLDPE	0.910-0.925	Copolymers of ethylene and α-olefins. Structure similar to HDPE but with short-chain branching, stiffer than LDPE but different melt processability. Some films have higher impact strength, tensile strength and ductility.
UHMWPE	*ca.* 0.940	Difficult to process, can be drawn into strong fibres, used for specialized engineering applications, has superior impact properties and high abrasion resistance.
mPE	0.800-0.920	Copolymers of ethylene and α-olefins using single-site catalysts. Also known as VLDPE or ULDPE, has superior mechanical and optical properties, uses include film products, frozen food packaging.

1.3 Polymer Blends

Concurrent with the advancement of the plastics industry has been the development of the science and technology of polymer blends. Just as the first polymers of historical significance were based on natural materials, the first polymer blends were mixtures of natural polymers. Arguably the first polymer blend was a mixture of natural rubber and gutta percha developed and patented by Thomas Hancock in 1846 [45]. The term *polymer blend* can be used to describe a mixture of two or more polymers or copolymers [46] and can be interchanged with the term *polymer composite*. A *polymer alloy* describes an immiscible polymer blend with a distinct phase-morphology [46]. An *interpenetrating polymer network* is a polymer blend in which one or more components undergo polymerization in the presence of the other [47]. Other terms can be used to describe polymer blends and these primarily relate to state of miscibility of the blend.

The blending of two or more polymers to form a new material is widely established as a means to produce new materials with tailored properties. The recycling of plastic wastes often involves the reprocessing of mixtures of two or more polymer materials in various states of degradation [48-55]. Other than economical and environmental incentives, blending polymers is often aimed at improving a weak property of a component resin such as impact strength or processability [46]. The miscibility of the constituent polymers determines the compatibility of the blend on a molecular level that, in turn, determines the ultimate properties [51,56,57]. In order for structural compatibility to be achieved the polymers must ideally co-crystallize into a single phase and the resulting blend should behave like a homogeneous material [21,57]. In practice, however, polymers are often immiscible or incompatible and phase separation can occur resulting in a detriment to physical and mechanical properties [56]. The properties of the individual polymers such as density, melting temperature, degree of crystallinity and molecular weight distribution [58] also affect the miscibility and resulting properties of the blend [59].

The science and technology of polymer blends increased rapidly during the 1980s [45] and a recent survey of two largely popular journals dedicated to polymers from 1980 to the present reveals a continuation in this trend. The number of articles containing the keywords "blend", "alloy" or "composite" was expressed as a percentage of the total number of articles published per annum. A similar survey of US patents relating to polymeric materials over the same time period was conducted for comparison. Figure 1.1 illustrates the increase in the percentage of articles or patents relating to polymer blends in general and shows that the study of blends has more than doubled from an average *ca.* 15% in 1980 to an average *ca.* 40% of the published literature sampled. The relative increase in patents has been steady although not as dramatic with only a *ca.* 12% increase since 1980.

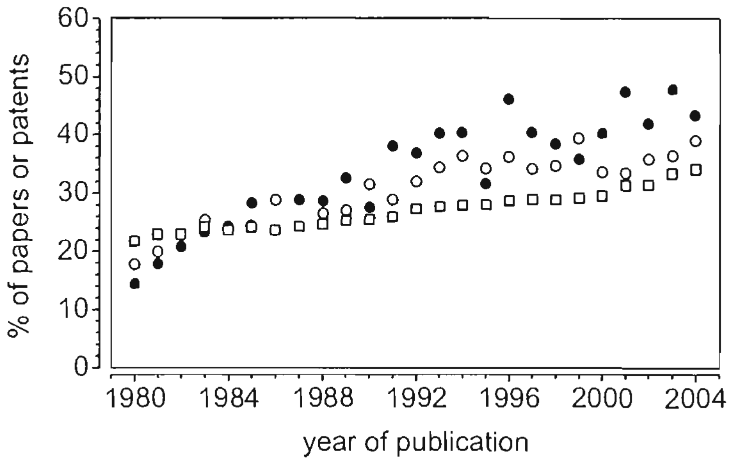

Figure 1.1. Trend in the percentage of published papers or patents relating to polymer blends from 1980 to the present for: (○) Journal of Applied Polymer Science (published by Wiley Periodicals, Inc), (●) Polymer (published by Elsevier Ltd) and (□) US Patents.

A detailed history of polymer blends from the perspective of the patent literature has been presented by Utracki in 1989 [45] and again in 1995 [60]. The author indicates that the eventual patenting or commercialization of a polymer blend has often been preceded by extensive research with a ratio of research articles to patents of 18 to 1 in 1995 [60]. From 1980 to the present, contributions to the *Journal of Applied Polymer Science* and *Polymer* pertaining to polymer blends, alloys or composites totalled more than 13000 articles. Considering the extent of published material relating to polymer blends in general, it would be virtually impossible to present a complete review of this entire area. A detailed review of the properties of blends involving polyethylene with other polyolefins is presented in Chapter 2.

1.4 Aims of this Work

In view of the continued and increasing importance of polymer blends as a means of economically developing new materials with desirable properties, the current work is aimed at the following:

- To prepare several binary PE blend systems based on conventional PEs and mPEs that are suitable for film or solid-state applications.

- To develop new analytical techniques based on differential scanning calorimetry, Fourier-transform infrared spectroscopy and chemiluminescence in order to characterize the blends.

- To test and assess the physicomechanical and optical properties (for film samples) of the blends in order to identify any blends that have optimum and desirable properties.

- To make recommendations for appropriate procedure to follow in order to identify and develop future polyolefin blends that have desirable physicomechanical and optical properties and that are commercially viable.

Chapter 2 Literature Review

The characterization of polymer blends by various techniques is particularly important as it can reveal information such as blend compatibility or incompatibility, melt behaviour, solid-state properties, oxidative stability and structural information [61-75]. Techniques for polymer and blend characterization include those based on x-ray diffraction [76-92], light scattering [59,61,68,93-110], gel permeation chromatography [111-130], neutron scattering [82,131-148], nuclear magnetic resonance [64,128,130,149-169] and various microscopic techniques [83,88,89, 96,136,170-190]. Many of these techniques are often expensive or time-consuming, however, and are not widely available in industrial situations.

For a polymer blend to be functional it must be structurally sound and have desirable physicomechanical properties that are ideally better than those of the components of the blend. Although there are almost unlimited combinations of polymers available for binary blends, the development of economical, functional, commercially important polymer blends is becoming foremost in the field of polymer blend technology. This chapter reviews various techniques that are utilized in the characterization of polymer blends with an emphasis on differential scanning calorimetry, infrared spectroscopy and chemiluminescence techniques. The solid-state properties of blends of PE with other polyolefins are also reviewed with particular attention being given to blends of PE with PE.

2.1 Blend Characterization by DSC Techniques

Differential scanning calorimetry (DSC) is widely used to identify, characterize and analyze crystalline and semi-crystalline polymers. In particular, the analysis of polymer blends by DSC is now commonplace and a number of techniques have been developed for the qualitative and quantitative analysis of blends [191-194]. Blends of LDPE and LLDPE are commercially important and the analysis of LDPE/LLDPE blends by various DSC techniques has therefore received considerable attention in the literature [65,66,68,95,195-206]. Certain types of LLDPE show two or more distinct melting temperatures when examined using DSC [207-210]. The presence of multiple peaks in DSC thermograms can be primarily explained by the presence of polymer fractions that possess different degrees of short-chain branching (SCB) [35,138,191,208,211,212]. Melting and recrystallization during heating may also contribute to multiple peaks in DSC thermograms [213]. The highest melting temperature observed in a typical DSC thermogram of LLDPE is due to the ethylene-rich or relatively linear molecules crystallizing from the melt first, whilst the peaks occurring at lower temperatures are due to the more branched species, such as octene-rich fractions, which crystallize at later stages [26,35,208,214].

The crystallinity of LLDPE is dependent upon its degree of branching where a lower proportion of SCB produce a greater degree of crystallinity [208,215]. The melting temperature of a crystal of LLDPE is determined, in part, by the lamellar thickness and so the broad endotherm typically seen in DSC traces of LLDPE is primarily attributable to the distribution of lamellar thicknesses [210,215,216]. Broad endotherms may also be a result of other factors such as the incorporation of branches into crystals, the degree of crystal perfection, lateral crystal sizes, and the heating rates used to obtain the thermograms [67,213,217]. Moreover, the temperature at any point on the DSC trace is indicative of the proportion of lamellae in the sample with that melting temperature. Thus, it is expected that the melting temperature of the polymer and the profile of the resulting endotherm will be affected by the extent to which SCB is incorporated in its crystalline structure and the resultant crystalline imperfections caused by these [209,211,215,218].

The melting behaviour of LDPE/LLDPE blends has been widely studied and such blends have been found to be miscible in the melt [63,68,95,195,196,219-227]. The miscibility of LDPE/LLDPE blends in the solid state, however, depends on the method of cooling from the melt [68,95,228-231]. The analysis of LDPE/LLDPE blends by DSC generally shows that in most cases two distinct melting peaks corresponding to constituent polymers are present on the resulting melting endotherms [68,203]. It has been suggested that the blend is volume filled by LLDPE and that LDPE crystallizes separately within the crystalline domains of the LLDPE component [68]. Prasad [195] used endotherm peak height changes to identify blends of LDPE/LLDPE and found the melting temperature of LDPE varies with density and is usually in the range of 106°C to 112°C for film-grade resins.

The DSC thermogram of LLDPE is characterized by a broad range of melting peaks with a lower melting peak around 106°C to 110°C and a higher one in the range of 120°C to 124°C [195]. In a blend with LDPE, the ratio of the two endothermic peak heights changes such that at a given weight percent of LDPE, the ratio depends on the type of comonomer present in the LLDPE [195].

It has been found that LLDPE samples having similar densities and melt flow indices can show significant differences in their molecular structure, particularly in regard to the SCB distribution [18,216,232,233]. The technique of DSC is particularly useful for identifying differences in the SCB content that exists between LLDPE samples since it enables the fractionation of the polymer on this basis [26, 197,198,218,234,235]. A limitation of the conventional DSC technique, however, is that the standard annealing procedure (i.e. heating to 180°C at the rate 10°C min^{-1}, holding at 180°C for 10 min then cooling from 180°C to room temperature at the rate of 10°C min^{-1}) yields thermograms that may have insufficient detail to enable the identification of an unknown LLDPE material [236]. Furthermore, thermograms produced using the standard DSC annealing procedure may demonstrate poor resolution of the LDPE and LLDPE components in a given blend [66,220]. Any accurate determination of the areas under the peaks of the thermogram and the subsequent quantitative analysis of the components is therefore made difficult. One method of overcoming this problem is to measure the total area under the set of unresolved peaks and to obtain the individual areas by assuming a certain distribution curve for each component [235,237].

Temperature rising elution fractionation is often employed to fractionate polyethylenes and polyethylene blends based on the level of SCB of the polymer chains, however this technique can be time-consuming and relatively expensive [18,115, 157,197,210,218,233,238-255]. Successive self-nucleation and annealing (SSA) is another technique that is widely used to promote molecular segregation in copolymers and blends [26,191,214-216,242,256] whereby components in LLDPE and LDPE/LLDPE blends are segregated based on branch distribution and branch density [161,210,239,252]. In a typical SSA procedure, however, it can take up to 20 h to perform the initial annealing step [252].

2.2 Blend Characterization by IR Techniques

The analysis of polymers and polymer blends by DSC is often accompanied by analysis techniques based on infrared (IR) spectroscopy [103,186,193,195,219,231, 257-269]. This essentially non-destructive technique is commonly used to identify polymers and can be used to determine various structural parameters of polymers and polymer blends [81,98,103,107,155,168,180,184,195,231,257-259,270-289]. This technique has the added advantage of potential integration in-line with polymer processing equipment for the purpose of quality control monitoring [290].

The investigation of structures [195,291-295], composition [289,296-301], density and crystallinity [274,293,300], degree of oxidative degradation [300,302], degree of functionalization [155], and blend compatibility [270,300,303,304] are common applications of IR spectroscopy in polymer analysis. The density of PE can be monitored using IR spectroscopy by observing the absorbance band at 730 cm^{-1} that increases in intensity with increasing crystallinity [291,305]. Furthermore, the crystallinity of PE can be calculated using the IR absorbance bands at 722 cm^{-1} and 730 cm^{-1} [274] and the extent of crystallinity can also be estimated using the absorbance band at 1894 cm^{-1} [293]. The position of the methyl deformation band usually centred at 1378 cm^{-1} can be used to identify branches in LDPE [248,306-308]. Different types of LDPE can be distinguished by taking the ratio of the Fourier-transform infrared (FT-IR) absorbance bands at 1368 cm^{-1} and 1378 cm^{-1} to give an estimate of the length of branching in the structure [309,310].

Infrared spectroscopy has been widely used to identify and analyze various structural entities of LLDPE [195,248,311-315]. Short-chain branching in LLDPE is of particular interest considering the type and distribution of SCB is responsible for the major physicomechanical properties of LLDPE [19,316-319]. The type and quantity of the comonomer used in the production of LLDPE can be determined using IR spectroscopy [316] as well as the type of LLDPE used in LDPE/LLDPE blends [195]. A summary of the major structural entities of LLDPE and their corresponding IR absorbance wavenumbers is given in Table 2.1, as well as other general structural entities associated with PE.

Table 2.1. Wavenumber of maximum absorbance for various structural entities of PE.

Absorbing species	**Wavenumber / cm^{-1}**	**Comments**	**Reference(s)**
crystalline & non-crystalline bands	720, 730	orientation of PE, linearity	[155,274,291,294,295,306,314,323]
butyl branches	745, 893	hexene comonomer	[195,312,315,316]
ethyl branches	770-780	butene comonomer	[195,248,306,312,315,316]
hexyl branches	888-890	octene comonomer	[195,312,313,324]
pendant methylene	888-890	propyl and longer / vinylidene	[314,315,325]
isobutyl branches	920	hexene comonomer	[312]
methyl branches	935	methyl SCB	[312,313,315]
vinyl end groups	909, 965, 990	terminal vinyl branching	[293,307]
amorphous methylenes	1080	methylene stretching in amorphous regions	[313]
methyl branching	1150	methyl "wagging" in crystalline phase	[313,315]
methylene "wagging"	1175	methyl "wagging" in linear PE	[313,315]
amorphous methylenes	1304, 1352, 1368	methylene "wagging"	[294,309,311,322]
methyl end groups	1378	methyl deformation band	[248,306-311,316,322,324,326]
Ethylene	1465	"scissoring" -CH_2-	[155,294,314]
carbonyl group	1712	for determination of carbonyl index	[302]
crystalline band	1894	crystallinity of PE	[293]

Infrared spectroscopic techniques have also been used to investigate other commercial copolymers and blends including the compositional analysis of styrene/isobutylene copolymer [298]. The composition of ethylene-acrylate copolymers has been examined using absorbance bands specific for CH and C=O species [296]. The structure of ethylene-propylene copolymers has been quantified by IR spectroscopy using the ratio of two absorbance peaks [299] or by deriving suitable equations [297,320]. The compatibility of 2,6-dimethyl-poly(phenylene oxide) (2MPPO) blended with polystyrene (PS) has been assessed by IR spectroscopy which showed that blending induces structural changes in 2MPPO resulting in blend compatibility [303].

Blends of polyolefins have been studied by IR in order to determine parameters such as changes in composition, structural characteristics, and compatibility [189]. For example, an IR study of the surface oxidation of LDPE and LDPE/LLDPE blends showed that LDPE is more susceptible to oxidation than the blend, presumably due to the presence of LLDPE [321]. Moreover, in blends of HDPE with LLDPE, the ratio of absorbances at 1378 cm^{-1} and 1368 cm^{-1} is a measure of methyl group content and hence the LLDPE content [322]. The composition of blends made from recycled mixed plastics such as polypropylene (PP) and HDPE can also be determined from the ratio of absorbances in FT-IR spectra of the blends [267].

Although the analysis of polymers and blends by IR spectroscopy is often qualitative, a number of useful quantitative techniques have been developed [195,267,274,297,310,323]. Non-linear relationships based on the ratio of two peaks in the same spectrum to study blends of poly(phenylene ether) (PPE) with PS and blends of PP with PE using IR spectroscopy were derived by Cole *et al.* [323]. In each of these blend systems, the non-linear equation was used to quantify the composition based on the ratio of A_{1306}/A_{757} and $A_{1306}/(A_{700} + A_{1306})$ for the PPE/PS blends, and $A_{1160}/(A_{1160} + A_{720})$ and $A_{1378}/(A_{1378} + A_{1467})$ for the PP/PE blends [323]. Each of these blend systems is comprised of two polymers with different molecular structures that facilitate the convenient selection of absorption bands that are unique to each polymer in the blend. For blends containing two different PE materials, however, the polymers have essentially the same structure and it may be more difficult to assign unique IR peaks to each component.

If one of the components in the blend is a copolymer such as LLDPE, it may be possible to identify a peak or peaks that is or are specific to the SCB in the structure of the LLDPE [248,311-316]. If a second peak is identified as common to both polymers in the blend, such that the absorptivity is equivalent, a linear relationship can be derived based on the ratio of these two absorbances and blend composition. Cole *et al.* [323] derived the following equation for the ratio of the IR absorbances of blended polymers:

$$\frac{A_a}{A_b} = \frac{K_{2a} + (K_{1a} - K_{2a})\chi_1}{K_{2b} + (K_{1b} - K_{2b})\chi_1} \qquad (2.1)$$

where A_a and A_b are the absorbencies at frequencies a and b respectively, K_{1a} and K_{2a} are the absorptivities of components 1 and 2 at frequency a respectively, K_{1b} and K_{2b} are the absorptivities of components 1 and 2 at frequency b respectively, and χ_1 is the mass fraction of component 1.

It has been noted [323] that equation (2.1) is non-linear with respect to χ_1 except for the fortuitous case where $K_{1b} = K_{2b}$. Nonetheless and with regard to the latter, polyethylene blends may be considered to be such a "fortuitous" case. Such blends contain components that are almost chemically identical and, in many cases, it should be possible to identify a frequency at which only one of the components absorbs strongly and another where both absorb.

2.3 Analysis of Polymers and Blends by Chemiluminescence

The use of DSC and IR spectroscopy for the analysis of polymers, copolymers and polymer blends is well established. Chemiluminescence (CL) is a relatively new technique that may offer new insight into the thermo-oxidative stability of polyolefins and polyolefin blends [280,327-336]. The thermo-oxidative stability of a polymer or polymer blend is an important consideration, particularly during its melt processing where excessive degradation can adversely affect its ultimate properties and thereby reduce its service life. Thus, most commercial polymer formulations contain some antioxidant (AO) to inhibit degradation during processing. At low temperatures, the thermal stability of PE is affected mainly by the presence of trace metals or acid residues that originate from the polymerization process [337]. At high temperatures, such as those required for melt processing, the stability of PE is influenced mainly by the presence of unsaturated sites in its structure that can result in chain branching and breakage [337].

The solid-state thermo-oxidative degradation of LDPE film [338-341] is believed to occur homogeneously providing the film thickness is kept constant [339]. In some cases, heterogeneous oxidation is observed where the oxidation spreads from oxidized amorphous regions to unoxidized amorphous regions in the polymer. A model has been proposed to account for the heterogeneous oxidation process and has been applied to the thermo-oxidative degradation of HDPE and LLDPE [340,341]. The difference between the oxidative stabilities of these polymers is attributed to their different crystallinities as well as the presence of less stable tertiary carbons in LLDPE [342]. In particular, HDPE has been reported to exhibit a lower rate of oxidation than LLDPE with catalyst residues influencing its rate of oxidation more than the crystallinity [342].

As metallocene-catalyzed linear low-density polyethylene (mLLDPE) has a low degree of unsaturation and a low level of metal residue, it should exhibit a high intrinsic oxidative stability [337]. Indeed, the thermo-oxidative stabilities of various types of PE have been reported to decrease in the order: HDPE > mLLDPE > LLDPE [343], which is also in agreement with the findings of Foster *et al.* [337]. However, a study [119] of the thermo-mechanical degradation of different PEs during processing suggests that conventional LLDPE is more stable than mLLDPE, a result that is contrary to the previous findings [337]. It is apparent that the current literature contains some inconsistencies with regard to the relative stabilities of the different types of PE.

The thermo-oxidative stability of polymer blends is becoming an important topic, as blending is now a widely used method of producing materials with tailored properties. It has been found that the thermo-oxidative stability of a blend may be affected by factors such as the processing conditions [344], the choice of vulcanising system [345] in the case of vulcanized blends, the extent of cross-linking [346], or the chemical nature of the components in the blend. For example, blends of ethylene vinyl acetate polymer with LDPE exhibit higher thermal stabilities than either of the pure constituents and this has been attributed to the effects of cross-linking [346]. Moreover, the blending of LDPE and isotactic polypropylene (iPP) is reported to increase the oxidative stability of the latter, presumably due to the dilution of tertiary alkyl radicals of iPP by the domains of LDPE [283].

The development of CL monitoring has resulted in a reliable technique for determining the oxidative stability of polymer formulations [73,280,329,347-350]. Chemiluminescence may be observed when a polymer such as a polyolefin is heated in the presence of oxygen [73] and CL is believed to originate from excited-state carbonyl groups formed during the termination step in the auto-oxidative process [332]. The CL oxidative induction time (CL-OIt) derived from single photon counting CL experiments is a measure of polymer stability and is obtained by monitoring the intensity of CL emission as a function of time during polymer oxidation. The CL-OIt is the time corresponding to the point of intersection between the extended baseline and the extrapolated, integrated CL signal obtained during steady-state auto-oxidation [73].

More recently, chemiluminescence imaging (CLI) [351-353] has been developed and this technique shows considerable potential as a reliable method for simultaneously collecting the CL emission from multiple samples [354]. An oxidative induction time (OIt) can also be derived from CL imaging experiments (CLI-OIt). Chemiluminescence monitoring is regarded as a highly sensitive technique that often gives greater baseline stability over long induction times than methods such as DSC [355].

A number of CL studies on a range of polyolefins report the relative thermo-oxidative stabilities of the polymers. For example, in an early study, Audouin-Jirakova and Verdu [356] found that the stability of certain polyolefins decreases in the order: HDPE > LDPE > ethylene/propylene copolymer > PP. This order was also found to correspond to an increasing degree of branching amongst the polymers. Indeed, it has been suggested [357] that the intensity of CL emission from LLDPE depends on the type and degree of SCB with longer, more frequent SCB producing a higher CL intensity than shorter, less frequent SCB. In other CL studies a decreasing order of stability of: HDPE > LLDPE > LDPE > iPP has been reported for additive-free polyolefins [327] and a decreasing order of HDPE > poly(4-methylpentene) > iPP > polybutene has also been reported [358]. In a further study, a good correlation has been found between the CL-OIt and the physico-mechanical properties of multi-extruded PP [329]. A comparison of the stabilities of PEs as assessed by different experimental methods is presented in Table 2.2.

The application of CL techniques to the study of polymer blends has received relatively little attention in the literature to date [280,330,348,359]. Nonetheless, in the study of polymer blends CL monitoring techniques have the potential to reveal important aspects such as the stability of the blend and blend miscibility that may subsequently lead to the development of more compatible blends. For example, in a study of the oxidative stability of poly(2,6-dimethyl-*p*-phenylene ether) in blends with PS and polybutadiene (PBD), CL has been successfully used to develop optimized stabilizing conditions for the system [348]. In another study, compatible mixtures of PS with poly(vinyl methyl ether) studied by CL show that at temperatures where phase separation occurs, the luminescence is stronger than that emitted from a homogeneous blend [359]. In recent studies, blends of LDPE with natural rubber (NR) or styrene-butadiene rubber (SBR) studied by CL reveal the rate of oxidation is faster in LDPE/NR blends than LDPE/SBR blends [280]. Furthermore, the technique of second time derivative analysis of CL profiles was successfully applied to a 5% (w/w) blend of PBD in PP and enabled the oxidations of the separate phases to be elucidated [330].

Table 2.2. Comparison of the stabilities of PE materials as assessed by different experimental methods.

Analysis method	Decreasing order of stability	Comments	Reference
thermo-oxidative degradation			
carbonyl	LLDPE > mLLDPE > HDPE	order in agreement with ref. [337]	[343]
thermo-gravimetric	mLLDPE > HDPE > LLDPE		[343]
hydroperoxide	mLLDPE > LLDPE > HDPE	catalyst residue in mLLDPE may decompose POOH	[343]
various	mLLDPE > LLDPE > LDPE	mLLDPE has low unsaturation and low residue levels	[337]
chemiluminescence	HDPE > LLDPE > LDPE > iPP	HDPE has low unsaturation and branching, LLDPE has higher purity and regularity than LDPE, CL increases with increased branching	[327]
	HDPE > LDPE > EP > PP	order reflects increased branching	[356]
	HDPE > P4MP > iPP > PB	order reflects increased branching	[358]
carbonyl	HDPE > LLDPE	catalyst residues affect oxidation more than crystallinity	[342]
carbonyl	HDPE/LDPE blends > HDPE, LDPE	blends less sensitive to oxidation than pure components	[360]
thermo-mechanical degradation			
various	HDPE > LDPE > LLDPE > mLLDPE	stability of LLDPE is preserved by adding AO, adding AO to mLLDPE does not retard degradation	[119]
thermo-gravimetric	stable iPP > unstable LDPE > 1:1 blend	LDPE dilutes 3 alkyl radicals of iPP in LDPE domains	[283]

2.4 The Properties of Polyolefin Blends

Polyolefins and PEs in particular have been produced commercially for nearly 80 years and their blends have been prepared for around 50 years [46,361]. This section reviews the literature relating to blends of polyolefins and PE/PE blends in particular, with an emphasis on the miscibility and physicomechanical properties of these blends. The properties of LLDPE and mLLDPE are also discussed as these polymers are often blended with other polyolefins in order to improve the physicomechanical and optical properties of conventional PEs.

2.4.1 The Properties of LLDPE and mLLDPE

Linear low-density polyethylene is produced via the copolymerization of ethylene with a small amount of an α-olefin such as but-1-ene, hex-1-ene or oct-1-ene. Short side-chains on the ethylene backbone are thus introduced [362] which causes LLDPE to have a melting temperature between that of LDPE (m.p. range 108°C to 115°C) and HDPE (m.p. range 130°C to 135°C) [82]. It is claimed that the branches in LLDPE affect its crystallinity [95,363] and crystalline melting point [18,362] and improve other properties such as stiffness [364], tensile strength [19,365], chemical resistance [95,251], tear strength [253], fracture toughness [366,367], and impact toughness [368,369].

The type and amount of comonomer are responsible, in part, for the resulting physical and mechanical properties of LLDPE [19,232,241,370]. Variations in the comonomer content, reactor conditions and catalysts used can result in improvements in tensile strength, tear resistance and melt viscosity [253]. Several studies have suggested that the impact toughness of LLDPE is due to the presence of a second rubbery phase resulting from the SCB [366,367,369], although another study [368] suggests that the improved toughness is independent of the amount of this second phase and that a rubber-toughening effect is not responsible for the observed impact behaviour.

The processability of conventional LLDPE is different to that of LDPE [364, 371,372] and therefore film blends of these materials may require different processing conditions compared to pure LDPE films [373]. For resins with the same melt flow index, LLDPE is tougher than LDPE and therefore thinner films of LLDPE can have equivalent or better mechanical properties than thicker LDPE films [17,371]. The production of films from pure LDPE presents minimal difficulties and good bubble stability is maintained throughout the extrusion process due to the long-chain branching (LCB) content of the LDPE [371]. The high melt viscosity of pure LLDPE, however, can cause melt fracture if conventional LDPE extrusion equipment is used [364,374]. Increasing the extrusion temperatures and widening the die gap can reduce the occurrence of melt fracture but this reduces the bubble stability [374].

The use of metallocene-catalysts in the production of LLDPE results in polymers with different properties compared to conventional LLDPE resins made using similar comonomers [31,375-379]. The SCB in mLLDPE is more evenly distributed along the PE chain and typical resins are produced with much lower densities than conventional LLDPE [362,378,379]. Film-grade mLLDPE has improved impact strength [380], tensile properties and optical clarity [377] compared with conventional LLDPE. It also exhibits lower melting temperatures [379] and has improved heat seal strength [31] compared with conventional LLDPE.

2.4.2 Blends of PE with Other Commodity Polymers

Blends involving PEs, including LLDPE, with other polymers have received considerable attention in the literature. In particular, the major commodity polymers such as PP, PS, polyvinyl chloride (PVC), polyethylene terephthalate (PET), and polyamide (PA) or nylon polymers have been blended with PEs for various purposes. Although these blends are outside the scope of the current work, a summary of the general properties of various PEs with some of the major commodity polymers is presented in Table 2.3.

Table 2.3. Properties of blends of PE with other commodity polymers.

Blend	**Properties of blend/comments**	**References**
LDPE/PP, HDPE/PP, LLDPE/PP	Blends are inherently immiscible with poor mechanical properties. The use of cross-linking agents during processing, the addition of ethylene-propene rubber and other copolymers can improve miscibility and mechanical properties.	LDPE/PP blends: [174,361,381-404] HDPE/PP blends: [24,183, 390,399,400,405-434] LLDPE/PP: blends: [24,28,75,383,386,400,427,435-462]
HDPE/PS, LLDPE/PS	Blends are inherently incompatible with poor mechanical properties. Addition of graft copolymers, block copolymers and other compatibilizers can improve miscibility and mechanical properties.	HDPE/PS blends: [425,463-482] LLDPE/PS blends: [125,483-490]
LLDPE/PVC	Poor miscibility, processability, and mechanical properties. Can be improved by crosslinking, addition of chlorinated PE, functionalization.	[491-501]
HDPE/PET	Blends are inherently incompatible with poor processability. Addition of nucleating agents, compatibilization, functionalization or irradiation can improve processability and ultimate properties.	[502-523]
LDPE/PA	Blends are inherently immiscible but can be improved by functionalization of LDPE, addition of compatibilizers, or by reactive compatibilization. Some mechanical properties can be improved.	[266,524-543]

2.4.3 Blends of PE and PE

As shown in Table 2.3, blends of PEs with other commodity polymers are generally inherently immiscible, due mainly to the differences in chemical structure, and often require the addition of compatibilizers or some functionalization in order to improve miscibility and mechanical properties. The development of suitable methods of compatibilization is particularly important for the recycling industry where it is impractical to completely separate polymers from waste streams prior to reprocessing [48,54,55,120,162,268,361,391,399,401,544-552]. For blends of PEs with other PEs, however, the components have essentially the same chemical structure [553] and blend compatibility issues are primarily attributable to differences in types and levels of chain branching [554].

Properties of LDPE/HDPE Blends

The melting behaviour of LDPE/HDPE blends has been extensively studied and it is widely regarded that the blend components can segregate into distinct molecular phases depending on conditions such as cooling rate and thermal treatment [71,76,82,133,171,191,200,207,220,240,301,363,555-572]. Full melt-compatibility of LDPE/HDPE blends can be achieved if the blends are crystallized rapidly from the melt [568] which may be due to miscibility of the components in the molten state [144,145,219,564,573-577]. Liquid-liquid phase separation (LLPS) can occur in LDPE/HDPE blends [564,576-580] and the extent of LLPS has been shown to be dependent on the MW of the HDPE component in particular [576]. Slow-cooled LDPE/HDPE blends can segregate on cooling [207,565] suggesting that the presence of LDPE hinders the growth of HDPE crystals and that a degree of interaction between HDPE and LDPE occurs at the molecular level [565]. Annealing LDPE/HDPE blends can result in the occurrence of three distinct endothermic peaks with the high melting peak belonging to HDPE, the low melting peak belonging to LDPE and the intermediate melting peak resulting from LDPE/HDPE co-crystals [555,556]. Similarly, LDPE/HDPE blends cooled rapidly from the melt also present three endothermic peaks [200,240,557,561], particularly when the LDPE is of low MW [557].

The incompatibility of LDPE/HDPE blends determined by thermal analysis is often supported by poor solid-state mechanical properties [207,581,582] and tensile properties of LDPE/HDPE blends are less than those predicted by the rule of mixtures [583]. For blends of waste LDPE and HDPE, the addition of 2% (w/w) dicumyl peroxide results in improved blend compatibility and subsequently improves the tensile properties of the blend [569].

Properties of HDPE/LLDPE Blends

Whereas blends of LDPE and HDPE generally form independent crystalline phases when cooled from the melt, blends of HDPE and LLDPE can co-crystallize into a single phase and are thus considered compatible [61,101,104,106,204,561,583-595]. The type and level of branching of the LLDPE component, however, is influential with regard to co-crystallization [89,145,584,586,591-593,596,597,597-601] and minimum branch contents for phase segregation have been determined for various HDPE/LLDPE blends [67,89,139,140,593,597-599,602]. Indeed, the phenomenon of LLPS can occur in HDPE/LLDPE blends or HDPE/mLLDPE blends under certain conditions [70,145,564,602-610]. Other blends of mLLDPE and HDPE are reported to be homogeneous with miscibility observed in the melt and solid states [553,597,598,611-614]. For blends of HDPE with ULDPE, however, miscibility or partial miscibility is observed only at low levels of ULDPE in the blend [27]. For blends of mLLDPE with metallocene-catalyzed HDPE, complete miscibility in the melt and crystalline states is reported [615,616]. When studied by dynamic mechanical analysis, certain HDPE/LLDPE blends show single composition-dependant peaks suggesting miscibility in both the amorphous and crystalline phases [204]. The morphology of HDPE/LLDPE (C8) blends prepared using a roll mill, a twin-screw extruder, and by solution precipitation, show that the method of melt blending results in a more morphologically uniform blend whereas the solution blended product is less homogeneous [322]. The resulting morphology of HDPE/ LLDPE blends can be revealed by a two-step etching procedure using potassium permanganate to reveal the locations of the components in the superstructures of the crystalline material [617].

The observed compatibility of HDPE/LLDPE blends determined by thermal analysis is often confirmed by invariable or superior physicomechanical properties [583,588, 594,598,618-620] and improved processability [621]. The tensile properties of HDPE/LLDPE blends are shown to vary significantly from the rule of mixtures, particularly when the ratio of levels of HDPE to LLDPE approaches 1 to 1 [589]. This is also the case for the flexural and impact properties of HDPE/LLDPE blends and is attributed to the composition of the amorphous phase of the blend [622]. The use of dynamic packing injection moulding enables the control of the molecular orientation of HDPE/LLDPE blends resulting in materials with high stiffness and high toughness [623]. The resistance to slow crack growth (SCG) of HDPE/LLDPE blends can increase significantly with levels greater than 30%-50% (w/w) LLDPE in the blend [624,625]. Furthermore, increasing the LLDPE content has a greater effect on SCG of HDPE/LLDPE blends than morphology or temperature [626]. The resulting crystallinity, crystal thickness, and the crystal network of HDPE/LLDPE blends all contribute to the resistance to SCG the blends [627]. Toughness enhancements can be achieved by the addition of *ca.* 10% LLDPE to HDPE although the tensile properties are relatively unaffected at these levels of LLDPE in the blends [628]. In blends of film-grade mLLDPE/HDPE, the addition of *ca.* 25% mLLDPE improves the tear resistance and film stiffness compared with films made entirely from HDPE [31]. The use of mLLDPE in blends with flame retardant HDPE can result in improved flow and impact resistance compared to blends using conventional LLDPE [629,630].

Properties of UHMWPE Blends

Blending other polyolefins with UHMWPE is often aimed at improving the processability of UHMWPE [631]. As a minor blend component, however, the addition of up to 10% (w/w) UHMWPE to LDPE can improve the elongation flow and birefringence of LDPE/UHMWPE blends [632]. Gel film blends of UHMWPE with a low molecular weight polyethylene (LMWPE) have improved critical draw ratio as a result of the addition of LMWPE and further improvements are observed with a LMWPE that contains shorter branches [97,633-643]. Although co-crystallization is observed over the composition range, the mechanical properties of HDPE/UHMWPE blends diminish and the rate of oxidative degradation increases with increasing UHMWPE content in the blend [22]. Other blends of UHMWPE and HDPE or medium-density polyethylene exhibit segregated crystallization and melting regardless of blend composition [644-649] although miscibility or partial miscibility in the molten state can be occur in some blends with HDPE [94,650,651]. The addition of UHMWPE to HDPE is shown to increase the resistance to SCG [648] although the yield strength is shown to decrease [22]. Melt miscibility can occur between blends of UHMWPE and LLDPE providing the blends are prepared by sequential loading [59]. Blending UHMWPE with LLDPE can increase the crystallization rate of LLDPE and such blends show high interfacial adhesion between the blend components [652]. Ultra high molecular weight linear polyethylene (UHMWLPE) is also inherently difficult to process due to its high melt viscosity. Blending UHMWLPE and conventional linear PE can result in superior mechanical properties, improved processability and enhanced crystallinity [21].

2.4.4 Blends Involving LDPE, LLDPE and mLLDPE

Blending conventional LLDPE with LDPE can result in the production of materials that have significantly better properties than those made of LDPE alone [59,68,95, 198,224,228,364,365,374,653-657]. Such blends are commonly produced in order to obtain film products with high impact strength, optical clarity, good "shrinkability" or a combination of these attributes. The ability of LLDPE to enhance the properties of film blends is arguably a result of the SCB and SCB distribution of the LLDPE component.

Properties of mLLDPE/LLDPE Blends

Although conventional LLDPE is often used as a component in LDPE film blends, films made entirely from LLDPE are becoming increasingly popular [17,84, 370,658-665]. The production of LLDPE film using conventional film blowing equipment, however, is often difficult due to the processability of LLDPE [380,666-668] and can result in poor optical properties rendering such films unsuitable for certain applications [17]. Film-grade mLLDPEs are generally easier to process than typical LLDPEs in conventional equipment with the added benefit of some improved physicomechanical and optical properties in the resulting films [380,667]. Blending mLLDPE and LLDPE with different comonomer types and contents can sometimes result in phase separation [669,670] and a subsequent detriment to some of the mechanical properties [671]. Indeed, binary blends of mLLDPEs can exhibit

LLPS that is affected primarily by branch content and to a lesser extent, branch type [672].

Properties of LDPE/LLDPE and LDPE/mLLDPE Blends

Blending conventional LLDPE with LDPE is widely established as a means to significantly improve various properties of LDPE [225,226,365,374,618,656,657, 666,673-680] and the commercial importance of LDPE/LLDPE film blends is well recognized [59,68,95,228,364,365,374,653-655,666]. The melt behaviour of LDPE/ LLDPE blends, in particular, has received significant attention in the literature [63, 64,68,95,195,196,198-201,203,204,221-224,227,229,231,368,681-695]. The phenomenon of LLPS is observed for some LDPE/LLDPE blends with two crystal populations observed by DSC and transmission electron microscopy for most blend compositions [202]. Other LDPE/LLDPE blends have been found to be miscible in the melt and do not segregate into separate phases provided they are cooled quickly from the melt [228-230]. The slow cooling of molten LDPE/LLDPE blends, however, can result in the formation of independent crystalline phases that can be associated with the two constituent polymers [68,95,231]. It has been suggested that the addition of HDPE to immiscible LDPE/LLDPE blends can induce full miscibility in the resulting ternary blend [696].

Due to the inherent difficulties encountered during the processing of conventional LLDPE [364,371,372,680], LDPE/LLDPE blends typically require modified processing or extrusion conditions [373]. The elongational viscosity of LDPE/ LLDPE blends has been shown to vary in proportion to the LDPE content and this is an important factor when modelling processes such as blow moulding and film blowing [654]. The melt tension and subsequent film bubble stability during tubular extrusion blowing of LDPE are significantly improved by the addition of LLDPE [59,95,225,374,655,677,686, 697-699]. Furthermore, blending LLDPE with LDPE can result in significant improvements in toughness, impact strength, optical clarity, environmental stress-cracking resistance as well as resistance to thermal embrittlement and increased tear resistance [365,679].

If mLLDPE is used as a replacement for conventional LLDPE in a blend with LDPE, the improvements in the final film product are often more pronounced [380,612,615,700-702] which may be a result of the improved miscibility of the blend components [684]. In addition to the improved physicomechanical properties, the processability of mLLDPE blends with LDPE is significantly better than that of conventional LLDPE blends with LDPE [380,700,703,704]. The resulting miscibility of certain LDPE/mLLDPE blends, however, depends on the molecular weight of the mLLDPE component and is apparently not affected by the length of the SCB [230,705] although the distribution of SCB is reported to influence miscibility to some extent [706].

Downgauging LDPE/mLLDPE Film Blends

Reducing the gauge or thickness of a polymer film while maintaining or improving key performance properties can be both environmentally and economically beneficial [364]. For LLDPE and LDPE resins with the same melt flow index, LLDPE is inherently tougher than LDPE and therefore thinner films of LLDPE can have equivalent mechanical properties to thicker LDPE films [17,371]. A study of blends of mLLDPE with a typical film-grade HDPE [707] has shown that downgauged films can be formulated with properties similar to conventional films where film toughness and stiffness is maintained. In a commercial example of downgauging, the addition of up to 30% (w/w) mLLDPE to LDPE in the production of plastic bags can result in thinner film gauges and stronger final products [708].

The Future of Polymer Blends

Clearly there is extensive literature available relating to polyolefin blends and PE blends in particular. Due to the relatively new development of mPEs and other metallocene-catalyzed polymers, there exists a wide-ranging scope for the study of blends involving these polymers. The possibilities of developing new polymer materials based on blends of mPEs with other polymers, new or recycled, are extensive and relatively unexplored at present.

Chapter 3 Materials and Methods

3.1 Polymers Used for Blending

The resins used to prepare the blends studied are commercially available PE resins provided by Qenos (formerly Kemcor Australia Limited) and ExxonMobil. The blend systems studied are designated B1 through B6. The characteristics of the polymers used in the B1 blends are shown in Table 3.1 and those of the polymers used in the B2 through B6 blends are shown in Table 3.2. The specific systems of blends that were studied are defined in Table 3.3.

3.2 Blend Preparation or Extrusion

3.2.1 Blends Involving LDPE1 and LLDPE1 through LLDPE5 (B1 Blends)

Blends of LLDPE1 through LLDPE5 with LDPE1 were prepared by melt mixing the polymers in a Brabender Plasticorder mixer (model PLV151) at a temperature of 160°C for 5 min using a mixing speed of 60 rpm.

3.2.2 Blends Involving LDPE2, LDPE3 and mLLDPE1 (B2 Blends)

Blends containing 10%, 20%, 50%, 75% and 90% (w/w) mLLDPE1 with LDPE2 or LDPE3 were prepared by dry blending the polymers for 15 min. Each blend was then compounded in a Gonninan twin-screw extruder using an average screw speed of 75 rpm. The average extruder temperature profile was 180°C, 190°C, 210°C, and 240°C for the feed zone, compression zone, metering zone, and die zone respectively. The extrudate was immediately cooled to room temperature in a water bath, dried and pelletized. A sample of each compounded blend was collected for film extrusion and physical property measurements. Each of the compounded blends, as well as each of the respective resins, was blown into a film using a Glouchester film extruder. The screw speed used in the production of each film was 90 rpm except for those comprising 50%, 75%, 90% and 100% (w/w) mLLDPE1, where the speed was 50 rpm to account for the increased viscosity of these melts.

The die gap for each film was 1 mm except for the 50%, 75%, 90% and 100% (w/w) mLLDPE1 films, which was 2 mm.

3.2.3 Blends Involving LDPE2, LLDPE6 and mLLDPE2 (B3 Blends)

Blends of LLDPE6 or mLLDPE2 with LDPE2 were prepared by dry blending the polymers for 15 min. A sample of each of the dry blends was collected for physical property measurements and processed by melt compounding in a Werner and Pfliederer twin-screw extruder using an average screw speed of 120 rpm. The average extruder temperature profile was 170°C, 180°C, 190°C, and 200°C for the feed zone, compression zone, metering zone, and die zone respectively. The extrudate was immediately cooled to room temperature in a water bath, dried and pelletized. Each of the blends containing 5%, 10%, 15%, 20%, 30%, 40%, 70% and 85% (w/w), as well as each of the respective resins, was blown into film of 80 μm thickness using a Glouchester film extruder. The blends comprising 20%, 30% and 40% (w/w) LLDPE6 or mLLDPE2 with LDPE2 were also blown into film of 60 μm and 100 μm thickness using the same Glouchester film extruder. The screw speed used in the production of each film was 90 rpm except for those comprising 70%, 85% and 100% (w/w) mLLDPE2, where the speed was reduced to 50 rpm to accommodate the increased viscosity of the melts. The die gap for each film was 1 mm except for the 70%, 85% and 100% (w/w) mLLDPE2 films, which was 2 mm.

3.2.4 Blends Involving LLDPE6 and mLLDPE2 (B4 Blends)

Blends containing 10%, 20%, 30%, 40%, 50%, 60%, 70%, 80% and 90% (w/w) mLLDPE2 with LLDPE6 were prepared by dry blending the polymers for 15 min. A sample of each of the dry blends was collected for physical property measurements and processed by melt compounding in a Werner and Pfliederer twin-screw extruder using an average screw speed of 120 rpm. The average extruder temperature profile was 150°C, 160°C, 180°C, and 190°C for the feed zone, compression zone, metering zone, and die zone respectively. The extrudate was immediately cooled to room temperature in a water bath, dried and pelletized. Each of the blends containing 10%, 30%, 50%, 70% and 90% (w/w) mLLDPE2 with LLDPE6, as well as each of the respective resins, was blown into film of 80 μm thickness using a Glouchester film extruder. The screw speed used in the production of each film was 90 rpm except for those comprising 50%, 70%, 90% and 100% (w/w) mLLDPE2, where the speed was reduced to 50 rpm to accommodate the increased viscosity of the melts. The die gap for each film was 1 mm except for the 50%, 70%, 90% and 100% (w/w) mLLDPE2 films, which was 2 mm.

3.2.5 Blends Involving LDPE4, mLLDPE3 and mLLDPE4 (B5 Blends)

Blends of LDPE4 with mLLDPE3 or mLLDPE4 were dry blended for 5 min prior to processing by melt compounding the polymers in a Werner and Pfliederer twin-screw extruder using an average screw speed of 140 rpm. The average extruder temperature profile was 100°C, 110°C, 120°C, and 130°C for the feed zone, compression zone, metering zone, and die zone respectively. The extrudate was cooled to room temperature in a water bath, dried and pelletized. Each blend was compression moulded to a thickness of 2 mm in accordance with ASTM Method D 1928 at a temperature of 150°C and then cooled to room temperature at a rate of 15°C min^{-1}.

3.2.6 Blends Involving HDPE1, HDPE2 and mLLDPE5 (B6 Blends)

Blends of mLLDPE5 with HDPE1 or HDPE2 were dry blended for 5 min prior to processing by melt compounding the polymers in a Werner and Pfliederer twin-screw extruder using an average screw speed of 120 rpm. The average extruder temperature profile was 150°C, 170°C, 180°C, and 190°C for the feed zone, compression zone, metering zone, and die zone respectively. The extrudate was cooled to room temperature in a water bath, dried and pelletized. Each blend was compression moulded to a thickness of 2 mm in accordance with ASTM Method D 1928 at a temperature of 180°C. The blends were either quench-cooled or cooled to room temperature at a rate of 15°C min^{-1}.

Table 3.1. Characteristics of the polymers used in the B1 blends.

PE	Comonomer	MI_2[a] / dg min^{-1}	Density / g cm^{-3}	T_m[b] / °C	X[c] / %	T_1 / °C[d]	T_2 / °C[d]
LDPE1[e]		0.7	0.921	111.4	33	-	-
LLDPE1[f]	butene (C4)	1.0	0.918	121.3	31	117	112
LLDPE2[f]	hexene (C6)	0.8	0.926	126.2	39	121	116
LLDPE3[f]	hexene (C6)	0.8	0.921	125.5	32	119	113
LLDPE4[f]	hexene (C6)	0.9	0.918	123.8	34	122	116
LLDPE5[f]	octene (C8)	1.0	0.920	120.5	32	119	113

Notes:
[a] Melt flow index (MI_2) measured using a load of 2.1 kg.
[b] Peak melting temperature (T_m).
[c] Percent crystallinity (X) calculated from the ratio of the heat of fusion to that of a 100% crystalline PE (using $\Delta H_{fus} = 288$ J g^{-1}) [709].
[d] T_1 and T_2 are the temperatures used for the TSIA treatment.
[e] In each case, the 100% LDPE reference material was subjected to the same thermal treatment as the blended materials.
[f] Each of the LLDPE resins was produced by gas-phase polymerization using conventional Ziegler-Natta catalysts.

Table 3.2. Characteristics of the polymers used in the B2 through B6 blends.

PE	Comonomer	MI_2[a] / dg min^{-1}	Density / g cm^{-3}	T_m[b] / °C	X[c] / %	M_n / Dalton	M_w/M_n	AO / ppm
HDPE1[d]		0.1	0.954	135.3	55	28000	8.2	300
HDPE2[d]		0.9	0.956	136.4	55	13500	11	500
LDPE2		0.2	0.921	112.4	33	23400	8.0	0
LDPE3		0.9	0.921	106.2	37	14100	11	0
LDPE4		73	0.918	110.1	19	9100	4.3	0
LLDPE6[e]	hexene (C6)	0.7	0.921	122.9	35	33000	3.4	500
mLLDPE1[e]	butene (C4)	0.6	0.901	92.4	25	30100	2.3	1000
mLLDPE2[e]	hexene (C6)	1.1	0.917	115.4	35	62400	2.8	1000
mLLDPE3[e]	butene (C4)	28	0.901	93.2	13	24500	2.2	250
mLLDPE4[e]	butene (C4)	34	0.882	78.1	3	21500	2.2	250
mLLDPE5[e]	octene (C8)	1.1	0.897	101.7	16	49300	2.4	1000

Notes:
[a] Melt flow index (MI_2) measured using a load of 2.1 kg.
[b] Peak melting temperature (T_m).
[c] Percent crystallinity (X) calculated from the ratio of the heat of fusion to that of a 100% crystalline PE (using $\Delta H_{fus} = 288$ J g^{-1}) [709].
[d] HDPE1 produced by slurry polymerization; HDPE2 produced by gas-phase polymerization.
[e] LLDPE6 produced by gas-phase polymerization using conventional Ziegler-Natta catalysts; mLLDPE1 through mLLDPE5 produced by gas-phase polymerization using metallocene catalysts.

Table 3.3. Systems of blends that were studied.

System	Components		% (w/w) of component #2 in blend																	
	#1	#2	0	5	10	15	20	25	30	35	40	50	60	65	70	75	80	85	90	100
B1	LDPE1	LLDPE1	✓	✓	✓	✓	✓	✓	✓	✓		✓	✓			✓				✓
	LDPE1	LLDPE2	✓	✓	✓	✓	✓	✓	✓	✓		✓	✓			✓				✓
	LDPE1	LLDPE3	✓	✓	✓	✓	✓	✓	✓	✓		✓	✓			✓				✓
	LDPE1	LLDPE4	✓	✓	✓	✓	✓	✓	✓	✓		✓	✓			✓				✓
	LDPE1	LLDPE5	✓	✓	✓	✓	✓	✓	✓	✓		✓	✓			✓				✓
B2	LDPE2	mLLDPE1	✓		✓		✓					✓				✓			✓	✓
	LDPE3	mLLDPE1	✓		✓		✓					✓				✓			✓	✓
B3	LDPE2	LLDPE6	✓	✓	✓	✓	✓		✓		✓	✓			✓			✓		✓
	LDPE2	mLLDPE2	✓	✓	✓	✓	✓		✓		✓	✓			✓			✓		✓
B4	LLDPE6	mLLDPE2	✓		✓		✓		✓		✓		✓		✓		✓		✓	✓
B5	LDPE4	mLLDPE3	✓	✓	✓	✓		✓		✓		✓				✓			✓	✓
	LDPE4	mLLDPE4	✓	✓	✓	✓		✓		✓		✓				✓			✓	✓
B6	HDPE1	mLLDPE5	✓	✓	✓		✓			✓		✓		✓				✓		✓
	HDPE2	mLLDPE5	✓	✓	✓		✓			✓		✓		✓				✓		✓

3.3 Polymer and Blend Characterization

A list of the ASTM Methods used in the tests is given in Appendix 1.

3.3.1 Melt Flow Index and Density

The melt flow index (MFI) of each polymer or blend was measured using a Davenport melt rheometer in accordance with ASTM Method D 1238 using a load of 2.16 kg or 21.6 kg, at a melt temperature of 190°C. The density of each polymer and blend was measured in accordance with ASTM Method D 1505 or ASTM Method D 792.

3.3.2 Gel Permeation Chromatography

The molecular weight distribution of each polymer used in the B2 through B6 blend systems was obtained using a Waters Alliance GPCV 2000 Series gel permeation chromatography system which was connected to a differential refractive index detector and a multi-capillary viscometry detector. A series of three Styragel columns were used and the instrument was calibrated using polystyrene standards. The elution solvent was 1,2,4-trichlorobenzene and a column temperature of 140°C and flow rate of 1.0 cm^3 min^{-1} were used.

3.3.3 Level of Phenolic Antioxidants

With the exception of the LDPE materials, the resins contain chemically equivalent, commercial phenolic AOs. None of the resins contain any other additives. The concentration of phenolic AO in the polymer resins used in the B3 through B6 blend systems was measured using ASTM Methods D 5815, D 1996 and D 5524.

3.3.4 Standard Thermal Analysis by DSC

The melting behaviour of the B2 through B6 blend systems was investigated using DSC. For all DSC measurements, nitrogen was used as the purge gas and an empty aluminium pan was used as a reference. The instrument was calibrated using indium and zinc standards.

Sample Preparation for Standard Thermal Analysis

Plaques (100 μm thickness) of each of the blends were prepared by compression moulding at 180°C and 0.5 MPa and were immediately quench-cooled to room temperature.

Melting Temperature and Percent Crystallinity

The percentage of crystallinity and peak melting temperature of each polymer resin used in each blend system was determined using a Perkin-Elmer DSC-7 differential scanning calorimeter in accordance with ASTM Method D3417. A sample of the polymer (*ca.* 15 mg) was sealed in an aluminium pan and heated in the instrument at a rate of 10°C min^{-1} over the temperature range of 50°C to 180°C.

Melting and Crystallization Behaviour of the Blends

The melting and crystallization behaviour of each blend was determined using DSC. A sample (*ca.* 15 mg) of each blend was sealed in an aluminium pan and heated or cooled in the instrument at a rate of 10°C min^{-1} over the temperature range of 50°C to 180°C to record the melting or crystallization thermogram.

3.3.5 Thermal Characterization by DSC

A two-step isothermal annealing (TSIA) procedure was developed for the thermal characterization of the B1 blends.

Sample Preparation for TSIA Experiments

Plaques (400 μm thickness) of the blends were prepared by compression moulding at 180°C and 150 MPa and were immediately quench-cooled to room temperature.

Samples (*ca.* 5 mg) were punched from the plaques and sealed in aluminium pans in preparation for heat treatment and/or thermal analysis. Prior to the determination of its crystalline melting temperature, each sample was annealed for 1 min at 180°C and cooled to room temperature at 10°C min^{-1} on a Mettler FP2 hot stage.

Measurement of Melting Temperatures for TSIA

Thermograms of the B1 blends were obtained using DSC on a Perkin-Elmer DSC-7 instrument. Nitrogen was used as the purge gas and an empty aluminium pan was used as a reference. The instrument was calibrated using an indium standard. During each run the samples were heated from 50°C to 150°C at the rate of 10°C min^{-1}. The crystalline melting temperature of each polymer was determined from the temperature axis on its thermogram and these temperatures were used in programming the TSIA processes for the blends.

Two-Step Isothermal Annealing

The optimized TSIA process for the B1 blends involved heating each blend to 180°C on a Mettler FP2 hot stage, maintaining this temperature for approximately 1 min, and then cooling at the rate of 2°C min^{-1} to the temperature of the first crystallization minimum. The sample was held at this temperature for 2 h, after which it was cooled at the rate of 2°C min^{-1} to the second minimum where it was held for 4 h and then cooled to 20°C at the rate of 10°C min^{-1}.

3.3.6 Fourier-Transform Infrared Spectroscopy Measurement

Plaques (100 μm thickness) of the B2, B3, B5 and B6 blends were prepared by compression moulding at 180°C and 0.5 MPa and were immediately quench-cooled to room temperature. The FT-IR spectra were recorded using a Bruker model Vector 22 FT-IR spectrophotometer (32 scans at a resolution of 2.0 cm^{-1}).

3.3.7 Chemiluminescence Measurements

Chemiluminescence data were obtained for each of the B3 through B6 blends.

Sample Preparation for CL Experiments

Plaques (100 μm thickness) of each of the blends were prepared by compression moulding at 180°C and 0.5 MPa and were immediately quench-cooled to room temperature.

Chemiluminescence Recorded by Photon Counting

Two different photon-counting apparatus were used to collect the CL data. Each instrument contained a quartz-fronted bialkali cathode photomultiplier tube (Thorn-EMI, model 9813-QB) coupled to a single-gated photon counter (Stanford Research Systems, model SR400). The signal-to-noise ratio was maintained at a high level by cooling the photocathode to -20°C during the experiments. In one of the instruments (CL instrument #1) a Eurotherm model 2416 controller was used to maintain the sample at a constant temperature. In the other instrument (CL instrument #2) the specimen was contained in the sample compartment of a Mettler model 821^e DSC. All CL experiments were carried out at 170°C in an oxygen atmosphere (1 bar, flow rate of 100 mL min^{-1}).

Chemiluminescence Recorded by Imaging

The CL of the oxidizing polymer was recorded using a charge coupled device (CCD) camera (Astrocam, TE3/W/S) and the sample was oxidized on the temperature controlled hot-stage of a DSC instrument (Mettler, DSC821^e) that could be connected to either oxygen or a nitrogen supply. The CCD chip of the camera was maintained at -40°C during the experiments.

Second Time Derivative Analysis of CL Data

All raw CL data obtained were subjected to second time derivative (STD) analysis [330] in order to derive accurate values of the CL-OIt and CLI-OIt.

3.4 Physicomechanical Property Measurement

The mechanical properties of the B2 through B4 blends were measured on film samples whereas those of the B5 and B6 blends were determined using pressed plaques. Tensile strength and tear strength tests were performed in both the machine direction (MD) and transverse direction (TD) for each sample of film.

3.4.1 Mechanical Properties of Plaqued Blends

Tensile testing of the B5 and B6 blends was performed in accordance with ASTM Method D 638 using a crosshead speed of 500 mm min^{-1} or 50 mm min^{-1} and a sampling rate of 10 points s^{-1}. The impact properties of the B5 blends were measured using an instrumented impact tester in accordance with ASTM Method D 3763 at room temperature and at -20°C. The Izod pendulum impact strength testing of the B6 blends was performed in accordance with ASTM Method D 256.

3.4.2 Mechanical and Optical Properties of Film Samples

Tensile testing of the B2 through B4 film samples was performed using an Instron tensile testing machine in accordance with ASTM Method D 882. A crosshead speed of 500 mm min^{-1} and a sampling rate of 10 points s^{-1} were used. The dart impact resistance was determined using a free-falling dart impact tester in accordance with ASTM Method D 1709. The tear resistance measurements were conducted using an Elmendorf tear strength tester in accordance with ASTM Method D 1922. The percent haze of each film sample was measured in accordance with ASTM Method D 1003 using a Gardner haze meter and the percent gloss of each sample was measured in accordance with ASTM Method D 2457 using a Pacific Scientific Glossgard II 45° gloss meter.

Chapter 4 Results and Discussion

This chapter examines the results of the analyses of various polymer blends containing conventional and metallocene-catalyzed PEs. The use of new DSC, FT-IR spectroscopic and CL analytical techniques for the characterization of the blends is explored. The physicomechanical and optical properties (for film samples) of the blends involving metallocene-catalyzed PEs are investigated in order to identify any blends that have optimum and desirable properties.

4.1 Blend Characterization by DSC

In this section, the use of a relatively quick and simplified form of multi-step crystallization-fractionation, namely a two-step isothermal annealing (TSIA) procedure is developed and investigated. The ability of this method to resolve the LDPE and LLDPE exothermic peaks satisfactorily is examined and the profile of the LLDPE component is characterized.

4.1.1 Thermal Analysis Before and After TSIA Treatment

Figure 4.1 shows DSC thermograms for blends of LDPE1 with ethyl-branched C4 LLDPE1 over the composition range of 0%, 5%, 25%, 30%, 60%, and 100% (w/w) LLDPE1, prior to the TSIA treatment. For the 100% LDPE1 and the blend containing 5% (w/w) LLDPE1, each DSC trace is comprised of a single, broad thermogram with a peak melting temperature *ca.* 110°C. The DSC traces of the remaining blends comprise two main peaks with the peak at the lower melting temperature due to the LDPE1 component whilst the peak at the higher melting temperature is associated with LLDPE1. Blends containing 25% and 30% (w/w) show the presence of a shoulder on the LLDPE1 peak that suggests the presence of a third crystalline phase [207,220]. The position of the LLDPE peak on the temperature axis increases with increasing LLDPE content in the blend whereas the position of the LDPE1 peak remains relatively constant for each blend. This increase in the peak melting temperature of LLDPE1 may be due to increased disruption of the LLDPE crystalline structure caused by the presence of the

LDPE1 component [68,198]. The peak melting temperature for 100% LLDPE1 was found to be 121.5°C which is in good agreement with the literature value of 121°C obtained by Haghighat and Birley [220].

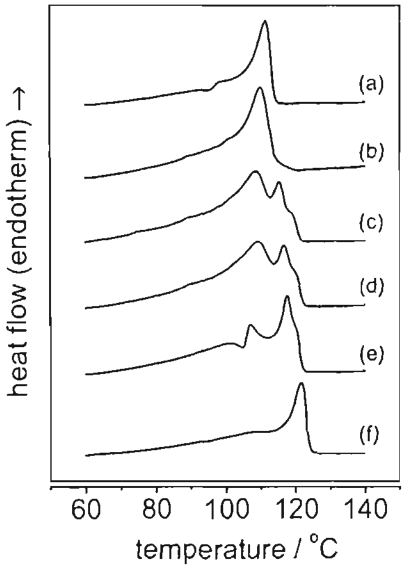

Figure 4.1. DSC melting thermograms of LDPE1/LLDPE1 blends containing: (a) 0%, (b) 5%, (c) 25%, (d) 30%, (e) 60% and (f) 100% LLDPE1 prior to the TSIA procedure. Blend compositions are (w/w).

The DSC thermograms for blends of LDPE1 with LLDPE1 after TSIA treatment and over the same composition range as in Figure 4.1 are shown in Figure 4.2. The thermogram of the 100% LDPE1 is comprised of a single peak, as expected, with a peak melting temperature *ca.* 110°C while the blend containing 5% (w/w) LLDPE1 shows an additional small peak. The thermograms of the remaining blends and the 100% LLDPE1 are each comprised of three main peaks. In each case, the peaks associated with the LDPE1 and LLDPE1 components are better resolved than the corresponding peaks in Figure 4.1. The higher melting peak in Figure 4.2 occurs at *ca.* 127°C which is about 5°C higher than the peak melting temperature of 100% LLDPE1 prior to the TSIA treatment. This temperature is also approximately 10°C less than a typical unbranched HDPE suggesting that the TSIA treatment results in the segregation of a phase that has a lower branch density than the corresponding material in Figure 4.1 that produced the highest melting range peak [209,216].

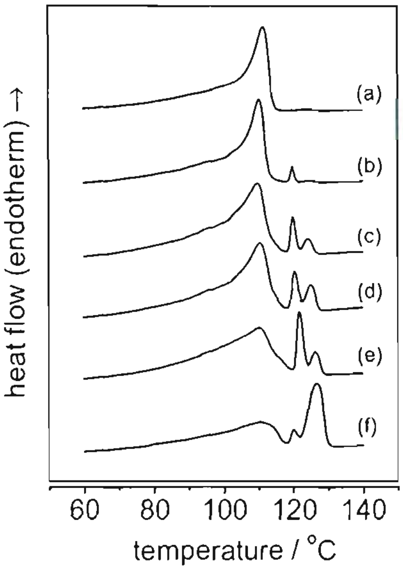

Figure 4.2. DSC melting thermograms of LDPE1/LLDPE1 blends containing: (a) 0%, (b) 5%, (c) 25%, (d) 30%, (e) 60% and (f) 100% LLDPE1 after the TSIA procedure. Blend compositions are (w/w).

The DSC thermograms for blends of LDPE1 with butyl-branched C6 LLDPE2 over the composition range of 0%, 5%, 25%, 30%, 60%, and 100% (w/w) LLDPE2, prior to the TSIA treatment, are shown in Figure 4.3. The blends containing 25% and 30% (w/w) LLDPE2 are comprised of two peaks whereas each of the other thermograms is comprised of a single peak. Figure 4.4 shows the DSC thermograms for the same blends after the TSIA treatment at the same compositions as shown in Figure 4.3. The thermogram of the 100% LDPE1 is comprised of a single peak while the blend containing 5% (w/w) LLDPE2 is comprised of two peaks. The thermograms of the remaining blends and the 100% LLDPE2 are also comprised of three peaks. The lower melting peak corresponds to the 100% LDPE1 component with a relatively consistent peak temperature of *ca.* 110°C. The second melting peak corresponds to the 100% LLDPE2 component with a peak temperature ranging between 122°C and 124°C. The higher melting peak ranges between 128°C and 131°C, which is approximately 5°C higher than that of the 100% LLDPE2 after standard annealing. This may be attributed to an enhanced crystalline perfection at the lamellar surface resulting from a lower branch density [208,214,216]. Thermograms before and after the TSIA procedure for the remaining C6 LLDPE3 and C6 LLDPE4 blends behave similarly to the blends shown in Figure 4.3 and Figure 4.4 (see Appendix 2).

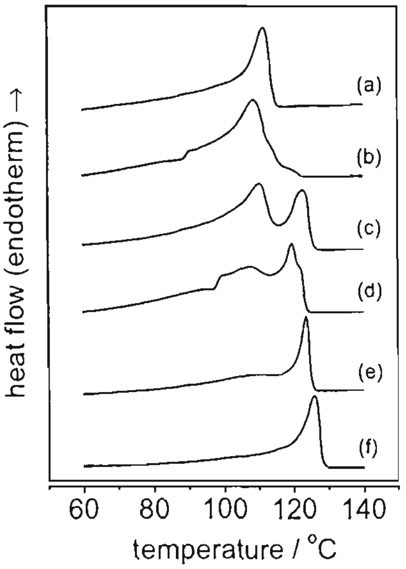

Figure 4.3. DSC melting thermograms of LDPE1/LLDPE2 blends containing: (a) 0%, (b) 5%, (c) 25%, (d) 30%, (e) 60% and (f) 100% LLDPE2 prior to the TSIA procedure. Blend compositions are (w/w).

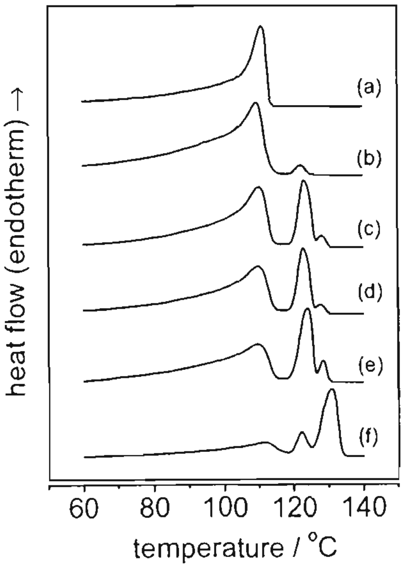

Figure 4.4. DSC melting thermograms of LDPE1/LLDPE2 blends containing: (a) 0%, (b) 5%, (c) 25%, (d) 30%, (e) 60% and (f) 100% LLDPE2 after the TSIA procedure. Blend compositions are (w/w).

Figure 4.5 shows DSC thermograms for blends of LDPE1 with hexyl-branched C8 LLDPE5 over the composition range of 0%, 5%, 25%, 30%, 60%, and 100% (w/w) LLDPE5, prior to the TSIA treatment. Other than the 100% LDPE1 and the blend containing 5% (w/w) LLDPE5, the thermogram of each blend is broad and comprised of two or more peaks that are poorly resolved. The thermograms of the same blends after the TSIA treatment are shown in Figure 4.6. It appears that the LDPE component is effectively segregated from the LLDPE component as a result of the TSIA process. The peak melting temperature for 100% LLDPE5 was found to be 121.8°C before TSIA and 122.6°C and 124.6°C after TSIA, which is in good agreement with the value of 124.3°C obtained by Starck [210].

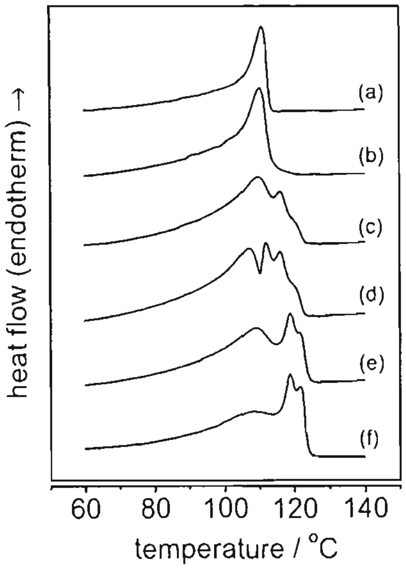

Figure 4.5. DSC melting thermograms of LDPE1/LLDPE5 blends containing: (a) 0%, (b) 5%, (c) 25%, (d) 30%, (e) 60% and (f) 100% LLDPE5 prior to the TSIA procedure. Blend compositions are (w/w).

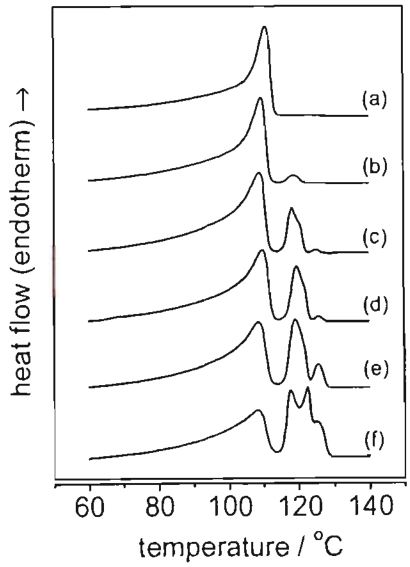

Figure 4.6. DSC melting thermograms of LDPE1/LLDPE5 blends containing: (a) 0%, (b) 5%, (c) 25%, (d) 30%, (e) 60% and (f) 100% LLDPE5 after the TSIA procedure. Blend compositions are (w/w).

4.1.2 Crystallization and Melting Temperatures

The DSC crystallization thermograms of LDPE1/LLDPE1 blends over the composition range of 0%, 5%, 25%, 30%, 60%, and 100% (w/w) LLDPE1 are presented in Figure 4.7. In each case, a single crystallization peak is observed suggesting that the LDPE and LLDPE crystal species are either co-crystallizing or crystallizing separately but over a similar temperature range. The crystallization thermograms for the remaining blends are presented in Appendix 2. The peak crystallization temperature as a function of composition for each blend is shown in Figure 4.8. For each of the three systems of C6 LLDPE blends, two crystallization peaks are observed whereas the C4 and C8 LLDPE blends show only a single peak. This suggests that during the crystallization process, the blends containing C6 LLDPE exclude the LDPE component during crystallization [68,95,202,228].

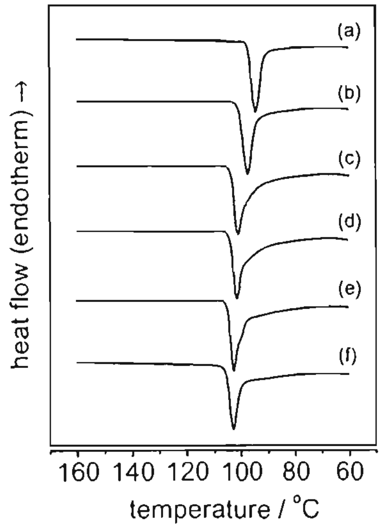

Figure 4.7. DSC crystallization thermograms of LDPE1/LLDPE1 blends containing: (a) 0%, (b) 5%, (c) 25%, (d) 30%, (e) 60% and (f) 100% LLDPE1. Blend compositions are (w/w).

The peak melting temperatures as a function of composition for the C4 LLDPE1 and C6 LLDPE2 blends before and after the TSIA treatment are shown respectively in Figure 4.9 and Figure 4.10. Similar plots for the remaining C6 LLDPE3 and LLDPE4 blends were obtained (see Appendix 2). In all cases, only two melting peaks are evident before the TSIA treatment, whereas three peaks are observed after the TSIA treatment. This suggests that the TSIA procedure can be used to deconvolute the LDPE1 and LLDPE peaks in blends where there is a significant overlap or a single peak is present. The trend in the peak melting temperatures for the C6 LLDPE blends reflects the trend in the densities of these resins with the resin of highest density and concomitantly the highest crystallinity, having the highest peak melting temperature in the composition range.

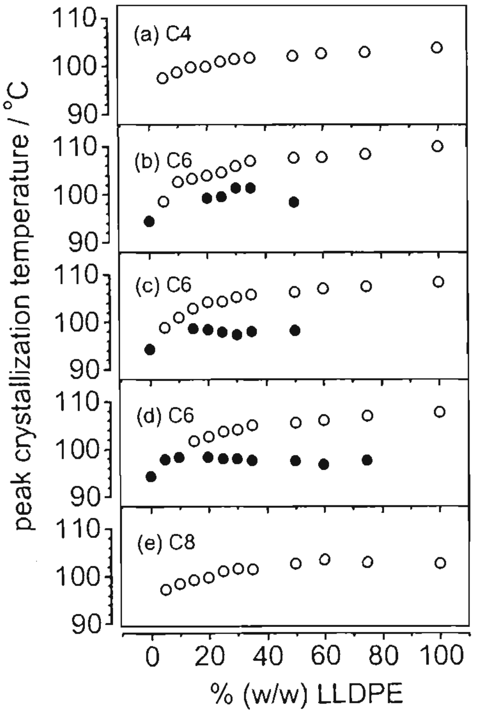

Figure 4.8. Peak crystallization temperature versus composition for: (a) LDPE1/LLDPE1 blends, (b) LDPE1/LLDPE2 blends, (c) LDPE1/LLDPE3 blends, (d) LDPE1/LLDPE4 blends and (e) LDPE1/LLDPE5 blends where: (o) LLDPE and (•) LDPE1.

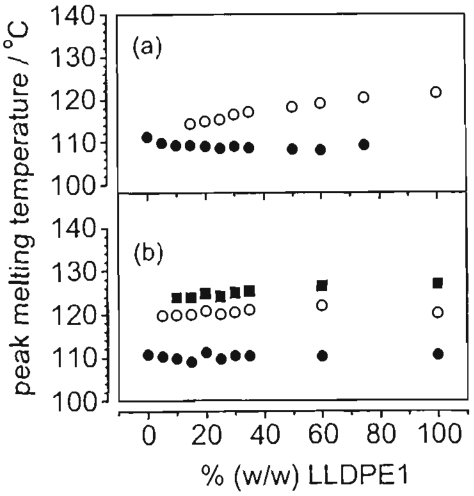

Figure 4.9. Peak melting temperature versus composition for the LDPE1/LLDPE1 blends: (a) before the TSIA treatment and (b) after the TSIA treatment: (•) LDPE1, (o) LLDPE1 peak 1 and (■) LLDPE1 peak 2.

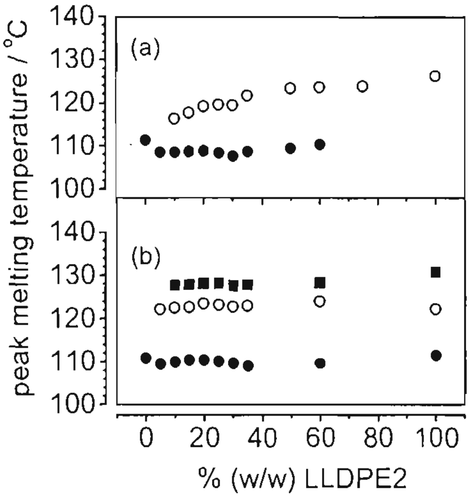

Figure 4.10. Peak melting temperature versus composition for the LDPE1/LLDPE2 blends: (a) before the TSIA treatment and (b) after the TSIA treatment: (•) LDPE1, (○) LLDPE2 peak 1 and (■) LLDPE2 peak 2.

Figure 4.11 shows the peak melting temperature as a function of composition for the C8 LLDPE5 blends before and after the TSIA treatment. The C8 LLDPE and C4 LLDPE blends show consistently lower peak melting temperatures than those of the C6 LLDPE blends over the range of blends examined. These observations suggest that the peak melting temperature of LLDPE is a maximum when the polymer contains butyl branching which is consistent with the notion that the C6 LLDPE blends contain thicker lamellae [214,235,256].

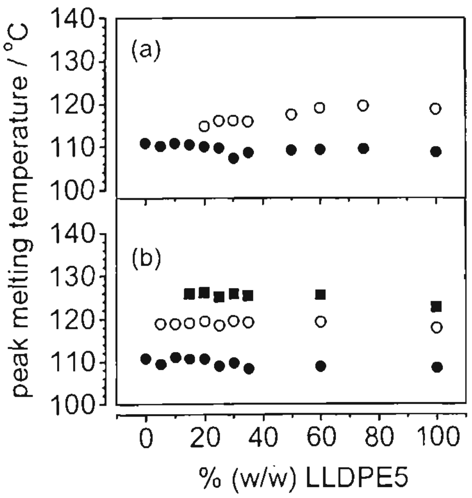

Figure 4.11. Peak melting temperature versus composition for the LDPE1/LLDPE5 blends: (a) before the TSIA treatment and (b) after the TSIA treatment: (•) LDPE1, (○) LLDPE5 peak 1 and (■) LLDPE5 peak 2.

4.1.3 Integrated Area Analysis

Figure 4.12 shows the integrated area of the LLDPE component versus composition for the C4 LLDPE1 blends before and after the TSIA treatment. Plots of the integrated area versus composition before and after the TSIA treatment for the C6 LLDPE2 and C8 LLDPE5 blends are shown in Figure 4.13 and Figure 4.14 respectively. Similar plots were obtained for the remaining C6 LLDPE3 and C6 LLDPE4 blends (see Appendix 2).

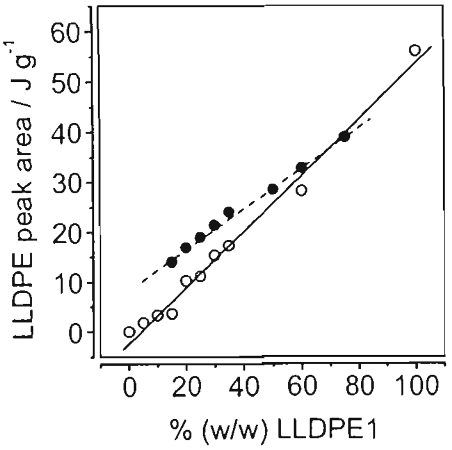

Figure 4.12. Integrated area under the LLDPE peak versus composition for the LDPE1/LLDPE1 blends: (•) before the TSIA treatment and (o) after the TSIA treatment.

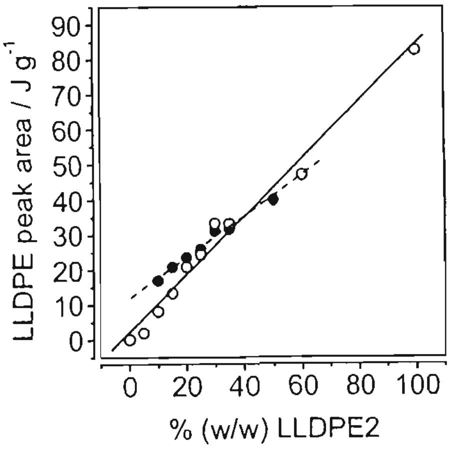

Figure 4.13. Integrated area under the LLDPE peak versus composition for the LDPE1/LLDPE2 blends: (•) before the TSIA treatment and (o) after the TSIA treatment.

Linear regression analyses were performed for all blends and gradients, intercepts and correlation coefficients are reported in Table 4.1. Generally good linear relationships were obtained for each blend system both before and after TSIA as revealed by the regression coefficients obtained in these analyses.

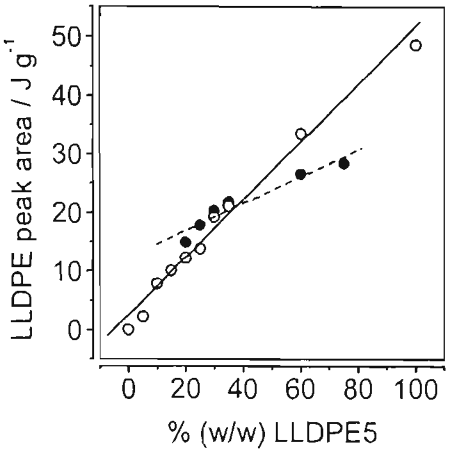

Figure 4.14. Integrated area under the LLDPE peak versus composition for the LDPE1/LLDPE5 blends: (•) before the TSIA treatment and (o) after the TSIA treatment.

It is evident from Figure 4.12 to Figure 4.14 and the data in Table 4.1 that the TSIA procedure effectively increases the gradient of the plot in each case. This thereby increases the analytical sensitivity if such a plot were to be used as a calibration for an analytical method to determine the composition of a blend. The sensitivity as reflected by the gradients is increased by a factor of between 18% and 114%. Furthermore, it is interesting to note that the intercepts are reduced by a factor between 30% and 124% as a result of TSIA. This confirms that the thermal treatment is effective at segregating the components of the blend and further suggests that a time of annealing between 2 and 4 h is sufficient to obtain satisfactory resolution. This result contrasts with the longer annealing times suggested by other workers [191,215,242,252].

Table 4.1. Regression coefficients for peak area line of best fit calculations before and after TSIA treatment.

	Before TSIA treatment			After TSIA treatment		
Blend	**gradient**	**intercept**	r^2	**gradient**	**intercept**	r^2
LDPE1/LLDPE1	0.4035	8.8116	0.995	0.5601	-2.1157	0.988
LDPE1/LLDPE2	0.5774	11.83	0.9922	0.8159	1.9022	0.9809
LDPE1/LLDPE3	0.5567	9.2074	0.9914	0.7711	6.3567	0.9775
LDPE1/LLDPE4	0.4835	8.8849	0.9773	0.5691	1.3742	0.9833
LDPE1/LLDPE5	0.2278	12.364	0.9304	0.4885	2.2044	0.9842

4.2 Blend Characterization by FT-IR Spectroscopy

A more rapid technique of polymer or blend characterization which often accompanies DSC is the analysis by IR spectroscopy which can be qualitative, quantitative or both. The quantitative analysis of polymer blends by IR spectroscopy usually involves non-linear relationships based on the ratio of two peaks in the same spectrum and is ideally suited to the analysis of polymers that have fundamental structural differences. In Section 2.2, equation (2.1) was introduced which relates the ratio of the IR absorbances to the mass fractions of the blend components.

Although this equation is clearly non-linear, for a PE blend system where component 1 absorbs strongly at frequency *a*, and both components absorb at frequency *b*, $K_{1b} = K_{2b}$ and equation (2.1) becomes:

$$\frac{A_a}{A_b} = \frac{K_{2a} + (K_{1a} - K_{2a})\chi_1}{K_{2b}} \qquad (4.1)$$

Here the ratio A_a/A_b is a linear function of χ_1. Clearly, *b* is a frequency that is common to both polymers in the blend and not a particular moiety related to one of the components only, such as a SCB.

It is apparent that the merit of the derived equation (4.1) lies in its propensity to be applied to the analysis of polymer blends whose absorption properties have been previously calibrated. In order to establish equation (4.1) as one that can be used in routine polymer analysis, a number of polyethylene blends were analyzed by FT-IR spectroscopy and the applicability of this equation investigated. The results of the investigation are reported in this section.

4.2.1 Optimizing Spectral Analysis Parameters

Table 4.2 shows the linear regression coefficients obtained by plotting, for various combinations of wavenumbers *a* and *b*, the absorbance ratio A_a/A_b (where A_a and A_b are the absorbances at wavenumbers *a* and *b* respectively) versus the blend composition. Clearly, in Table 4.2 the value of A_a remains constant for each given blend system and corresponds to that of the comonomer in the system.

Table 4.2. Regression coefficients for various peak selections of Ab.

	mLLDPE1 blended with		LDPE2 blended with		LDPE4 blended with		mLLDPE5 blended with	
	LDPE2	LDPE3	LLDPE6	mLLDPE2	mLLDPE3	mLLDPE4	HDPE1	HDPE2
	A_{771}	A_{771}	A_{893}	A_{893}	A_{771}	A_{771}	A_{888}	A_{888}
A_{888}	0.9562	0.9898	**0.9924***	**0.9816***	0.9852	0.9898		
A_{908}	0.9148	0.9492	0.9830	0.9450	0.9508	0.9755	0.9265	0.9060
A_{965}	0.5042	0.6905	0.8921	0.9269	0.8833	0.9481	0.8599	0.5282
A_{990}	0.7797	0.8277	0.1547	0.7965	0.8762	0.9260	0.9752	0.9784
A_{1017}	0.5832	0.4352	0.7146	0.9372	0.8416	0.9192	0.8922	0.7328
A_{1050}	0.9549	0.9770	0.9751	0.9088	0.9485	0.9744	0.9795	0.9830
A_{1080}	**0.9838***	**0.9937***	0.9275	0.9566	**0.9874***	**0.9915***	0.9615	0.9348
A_{1176}	0.9369	0.9688	0.9754	0.9752	0.9731	0.9816	**0.9898***	**0.9852***
A_{1896}	0.9651	0.9809	0.5026	0.7894	0.9109	0.9616	0.9873	0.9765
A_{2018}	0.9859	0.9850	0.6145	0.8067	0.9454	0.9723	0.9890	0.9842

The regression coefficients can be used to identify optimum wavenumbers such that there is a high degree of linearity between the ratio A_a/A_b and the composition of the blend. It is also apparent from the data that certain combinations of wavenumbers are more appropriate for the analysis of particular blend systems. For example, the absorbance peak A_{990} (terminal vinyl branching) [293] is suitable for use as the A_b peak for the HDPE blends but not for any of the LDPE blends. Some peaks are also less suitable for selection within blend systems, such as the A_{965} absorbance peak, which is much less suitable for the HDPE1/mLLDPE5 blends than the HDPE2/ mLLDPE5 blends. This is possibly due to the different processes used to polymerize HDPE1 and HDPE2 (see Table 3.2) [293,307].

4.2.2 FT-IR Analysis of Blends Involving LDPE

The FT-IR absorbance spectra for each of the LDPE2, LDPE3 and mLLDPE1 film samples in the regions between 1095-1050 cm^{-1} and 800-755 cm^{-1} are shown in Figure 4.15. The mLLDPE1 polymer is an ethylene-butene copolymer containing ethyl branches that absorb at 772 cm^{-1}, whereas the LDPE samples do not absorb significantly at 772 cm^{-1} [312]. Each of the LDPE2, LDPE3 and mLLDPE1 samples absorbs at 1080 cm^{-1} with a similar absorptivity due to the skeletal C-C stretching of methylene in the amorphous regions [313]. As confirmed by the data

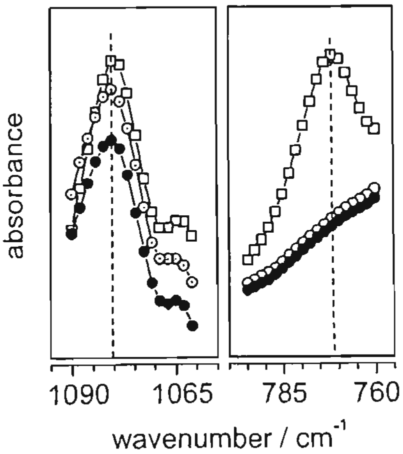

Figure 4.15. FT-IR absorbance spectra of the: (○) LDPE2, (●) LDPE3 and (□) mLLDPE1 film samples in the regions between 1095-1050 cm^{-1} and 800-755 cm^{-1}.

in Table 4.2, the ratio of absorbances at wavenumbers 772 cm^{-1} and 1080 cm^{-1} is therefore suitable for use in equation (4.1) for the LDPE2/mLLDPE1 and LDPE3/mLLDPE1 blends. Figure 4.16 shows a plot of the absorbance ratio, A_{772}/A_{1080}, versus χ_1 for the LDPE2/mLLDPE1 and LDPE3/mLLDPE1 blends. Both the LDPE2/mLLDPE1 and LDPE3/mLLDPE1 data demonstrate good agreement with equation (4.1) with high regression coefficients (see Table 4.2).

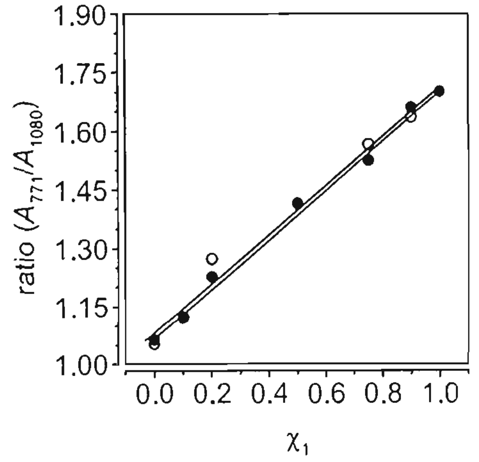

Figure 4.16. Absorbance ratio, A_{772}/A_{1080}, versus χ_1 for the: (o) LDPE2/mLLDPE1 blends and (•) LDPE3/mLLDPE1 blends.

Figure 4.17 shows the FT-IR absorbance spectra for the LDPE2, LLDPE6 and mLLDPE2 film samples in the region between 905-875 cm^{-1}. The LLDPE6 and mLLDPE2 polymers are ethylene-hexene copolymers and these contain butyl branches that absorb at 894 cm^{-1} [195,312,315,316], but do not contain any significant hexyl branching. The LDPE2 polymer exhibits both LCB and SCB including pendant methylene branches that absorb at 888 cm^{-1} as well as some butyl branching [314,315,710]. For the LDPE2/LLDPE6 and LDPE2/mLLDPE2 blends, the ratio A_{894}/A_{888}, is therefore suitable for use in equation (4.1) as confirmed by the data in Table 4.2. Although these peaks overlap in the blends to some extent, the fact that peak ratios are measured rather than integrated areas [292,323] effectively minimizes possible effects of the overlap. A plot of A_{894}/A_{888} versus χ_1 for the LDPE2/LLDPE6 and LDPE2/mLLDPE2 blends is shown in Figure 4.18. The data for both the LDPE2/LLDPE6 and LDPE2/mLLDPE2 blends show good agreement with equation (4.1) with linear regression coefficients close to unity (see Table 4.2), which also suggests that any overlap is negligible.

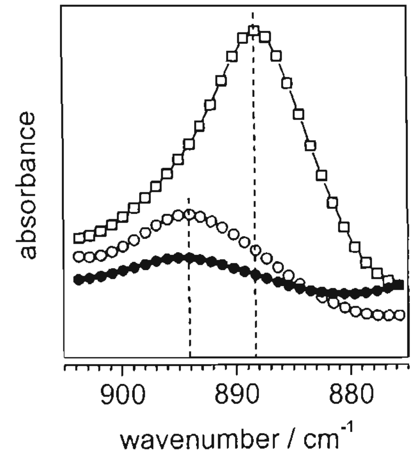

Figure 4.17. FT-IR absorbance spectra of the: (□) LDPE2, (○) LLDPE6 and (●) mLLDPE2 film samples in the region between 905-875 cm^{-1}.

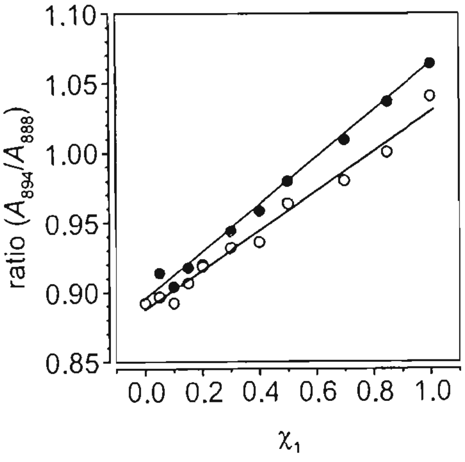

Figure 4.18. Absorbance ratio, A_{894}/A_{888}, versus χ_1 for the: (●) LDPE2/LLDPE6 blends and (○) LDPE2/mLLDPE2 blends.

The FT-IR absorbance spectrum for each of the LDPE4, mLLDPE3 and mLLDPE4 film samples in the regions between 1100-1050 cm^{-1} and 795-745 cm^{-1} are shown in Figure 4.19. Both the mLLDPE3 and mLLDPE4 polymers are ethylene-butene copolymers with significant ethyl SCBs that absorb at 771 cm^{-1} [312]. Each of the LDPE4, mLLDPE3 and mLLDPE4 polymers absorb at 1080 cm^{-1}, which can again be attributed to the skeletal C-C stretching of methylene in the amorphous regions [313]. In the case of the LDPE4/mLLDPE3 and LDPE4/mLLDPE4 blends, the ratio of absorbances at wavenumbers 771 cm^{-1} and 1080 cm^{-1} is therefore suitable for use in equation (4.1) as confirmed by the data in Table 4.2. Figure 4.20 shows a plot of the absorbance ratio A_{771}/A_{1080} versus χ_1 for the LDPE4/mLLDPE3 and LDPE4/mLLDPE4 blends. Both the LDPE4/mLLDPE3 and LDPE4/mLLDPE4 systems show good agreement with equation (4.1) with high regression coefficients.

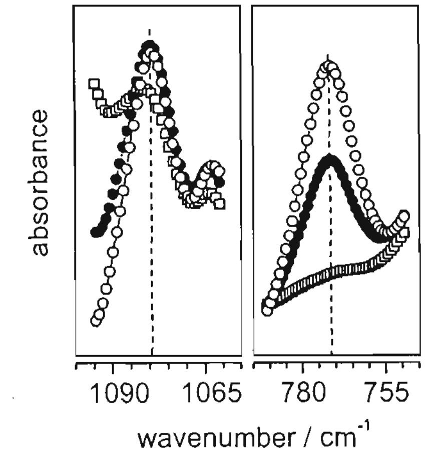

Figure 4.19. FT-IR absorbance spectra of the: (□) LDPE4, (●) mLLDPE3 and (○) mLLDPE4 film samples in the regions between 1100-1050 cm^{-1} and 795-745 cm^{-1}.

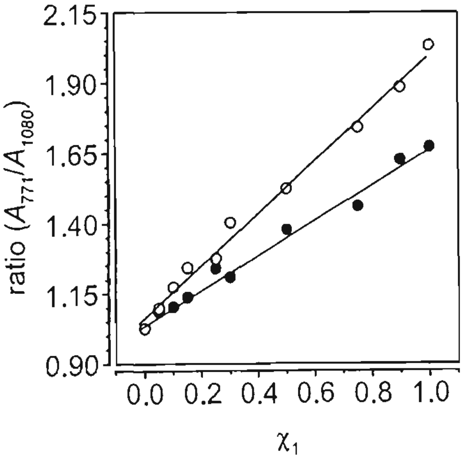

Figure 4.20. Absorbance ratio, A_{771}/A_{1080}, versus χ_1 for the: (●) LDPE4/mLLDPE3 blends and (○) LDPE4/mLLDPE4 blends.

4.2.3 FT-IR Analysis of Blends Involving HDPE

Figure 4.21 shows the absorbance spectra of the HDPE1, HDPE2, and mLLDPE5 film samples in the regions between 1195-1145 cm^{-1} and 800-755 cm^{-1}. The polymer mLLDPE5 is an ethylene-octene copolymer that has significant hexyl SCB with an intense peak at 889 cm^{-1} [195,312, 313,324]. Although the HDPE1 and HDPE2 polymers also absorb at 889 cm^{-1}, these peaks are not attributable to SCB. The peak at 1176 cm^{-1} is associated with the methylene "wagging" mode of PE [315] and appears in all three PE samples studied. In the case of the HDPE1/mLLDPE5 and HDPE2/mLLDPE5 blends, and as confirmed by the data in Table 4.2, the ratio of absorbances at wavenumbers 889 cm^{-1} and 1176 cm^{-1} is suitable for use in equation (4.1). A plot of the absorbance ratio A_{889}/A_{1176} versus χ_1 for the HDPE1/ mLLDPE5 and HDPE2/mLLDPE5 blends is given in Figure 4.22. Both the HDPE1/mLLDPE5 and HDPE2/mLLDPE5 systems show good agreement with equation (4.1) with regression coefficients close to unity (see Table 4.2).

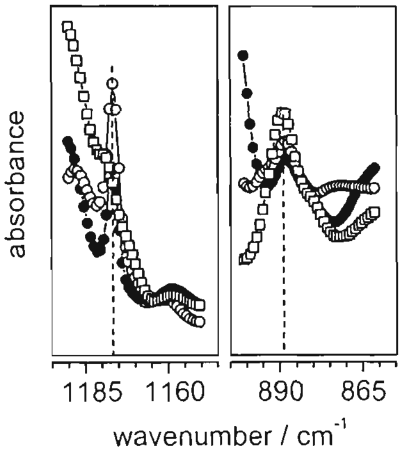

Figure 4.21. FT-IR absorbance spectra of the: (○) HDPE1, (●) HDPE2 and (□) mLLDPE5 film samples in the regions between 1195-1145 cm^{-1} and 905-855 cm^{-1}.

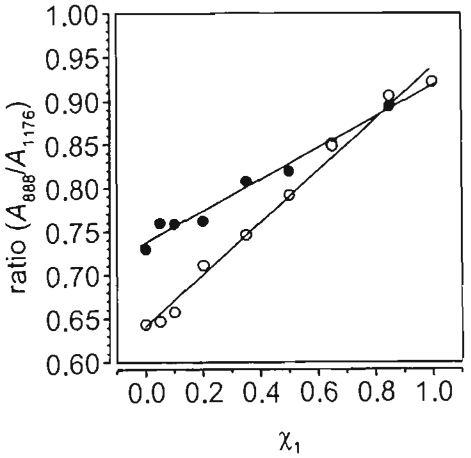

Figure 4.22. Absorbance ratio, A_{889}/A_{1176}, versus χ_1 for the: (○) HDPE1/mLLDPE5 blends and (●) HDPE2/mLLDPE5 blends.

4.3 Blend Miscibility by CL and DSC Techniques

Differential scanning calorimetry and IR spectroscopy are reliable techniques often used for the analysis of polymers and polymer blends. Chemiluminescence is a relatively new technique that may offer new insight into the thermo-oxidative stability of polyolefins and polyolefin blends [280,327-336]. In this section the application of CL monitoring techniques to PE blends is examined in order to identify any possible relationship between CL-OIt data and blend miscibility. An emphasis is placed on mPEs in order to address, in part, the current lack of published information on such systems. In addition to this, particular attention is directed to the assertion that any incompatibility reflected in the melt miscibility of a given blend system is also reflected in the CL behaviour of that system. The relative stabilities of the pure components as well as the performance of commercial stabilizers in the blends are also reported along with data obtained from CLI experiments that enable a preliminary assessment to be made of the reproducibility of the CL technique.

4.3.1 Idealized Blend Systems

Figure 4.23 shows typical DSC traces for selected blends belonging to the LDPE2/mLLDPE2 blends on the first heating after quench-cooling. In each case, a single endotherm is observed which suggests that the blends are melt miscible and are compatible on a molecular level [202,579,711]. Similar behaviour is also observed for blends within the LDPE2/LLDPE6 system (see Appendix 3). As a result, one may expect that the oxidative stability of the LDPE2/LLDPE6 and LDPE2/mLLDPE2 blend systems will exhibit idealized behaviour. In each of the LDPE2/LLDPE6 and LDPE2/mLLDPE2 blend systems, the LDPE2 component is unstabilized whereas the LLDPE6 and mLLDPE2 components each contain a certain level of a phenolic AO (see Table 3.2). Thus the level of AO in these systems decreases linearly with increasing LDPE2 content. It has been shown that the OIt varies linearly with phenolic AO content [327] and so in the absence of any adverse effects caused by blend incompatibility, the stability of the LDPE2/LLDPE6 and LDPE2/mLLDPE2 systems is expected to vary linearly with composition. Figure 4.24 shows a plot of the CL-OIt versus composition for each of the LDPE2/LLDPE6 and LDPE2/mLLDPE2 systems. In both cases, the CL-OIt decreases linearly with increasing LDPE2 in the blend, confirming idealized behaviour and suggesting blend compatibility. The data also suggest the oxidative stability of pure mLLDPE2 is more than six times greater than that of pure LLDPE6, although the level of AO in mLLDPE2 is only twice that in LLDPE6. Notwithstanding the fact that the efficiency of a given stabilizer is dependent on the polymer matrix in which it is placed, the apparent greater inherent stability of mLLDPE2 may be partly attributable to its more uniform distribution of SCB compared with that in LLDPE6.

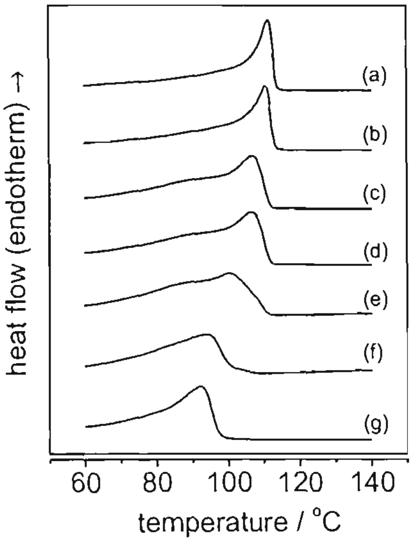

Figure 4.23. DSC endotherms of selected LDPE2/mLLDPE2 blends containing: (a) 0%, (b) 10%, (c) 20%, (d) 30%, (e) 50%, (f) 70% and (g) 100% mLLDPE2. Blend compositions are (w/w).

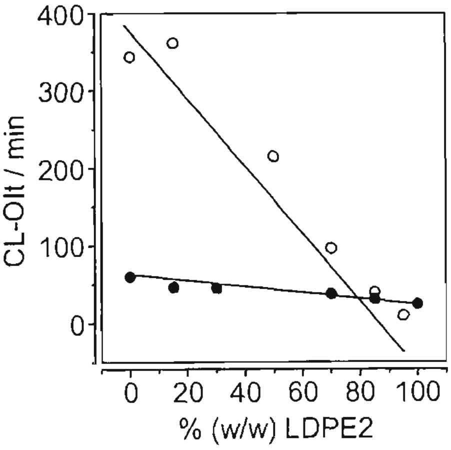

Figure 4.24. CL-OIt versus composition for the: (●) LDPE2/LLDPE6 blends and (○) LDPE2/mLLDPE2 blends where the data were obtained from CL instrument #1.

The stability of commercial LLDPEs is very much affected by the content of the catalyst residue and the chemical structure of the residue. These are, in turn, determined by post-polymerization treatment processes such as de-ashing, neutralization, or the "killing" process. The superior oxidative stability of mLLDPE2 observed in this study, can be attributed in part to the "clean" synthesis involved in its production, which leaves little catalyst residue behind in the polymer [337]. In polymers produced by the more standard Ziegler-Natta and Phillips processes these metal residues have been shown to decompose polymer hydroperoxides catalytically during the low-temperature oxidation of the polyolefin [337]. Furthermore, it has been shown that in the absence of AOs, LLDPE is much more stable than LDPE [327]. The inferior oxidative stability of the LDPE has been attributed to its irregular, branched structure which gives rise to labile tertiary hydrogen atoms on its backbone [327]. These have been identified as the premier site for oxygen addition to polymers leading to hydroperoxide formation and the subsequent degradation of the polymer [150].

The melting behaviour of each of the quench-cooled LDPE2/LLDPE6 and LDPE2/mLLDPE2 systems is similar to that observed for the quench-cooled LDPE4/mLLDPE3 and LDPE4/mLLDPE4 systems in so far as a single melting endotherm is obtained on the first heat cycle (see Figure 4.25 and Appendix 3). In these systems, the LDPE4 component is unstabilized whereas the mLLDPE3 and mLLDPE4 polymers contain phenolic AOs (see Table 3.2). The level of AO in the LDPE4/mLLDPE3 and LDPE4/mLLDPE4 blends therefore decreases linearly with increasing levels of LDPE4. Figure 4.26 shows a plot of the CL-OIt versus the blend composition for each of the LDPE4/mLLDPE3 and LDPE4/mLLDPE4 systems. In both cases, the CL-OIt decreases linearly with increasing concentration of LDPE4 in the blend, suggesting that the systems exhibit idealized behaviour and that each blend is compatible across all compositions. The oxidative stability of pure mLLDPE3 is approximately twice that of the pure mLLDPE4, although these materials contain the same level of AO. A distinguishable difference between the pure resins however is the MW, with the lower MW resin (mLLDPE4) exhibiting a lower CL-OIt than the higher MW resin (mLLDPE3). Similarly, the pure LDPE2 and LDPE4 resins have different MWs with the lower MW resin (LDPE4) exhibiting a slightly lower CL-OIt than LDPE2.

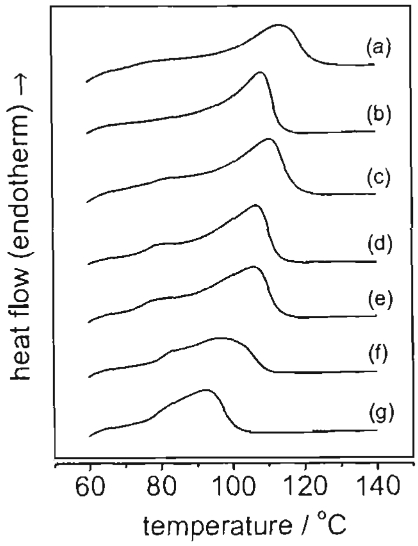

Figure 4.25. DSC endotherms of selected LDPE4/mLLDPE3 blends containing: (a) 0%, (b) 10%, (c) 25%, (d) 35%, (e) 50%, (f) 75% and (g) 100% mLLDPE3. Blend compositions are (w/w).

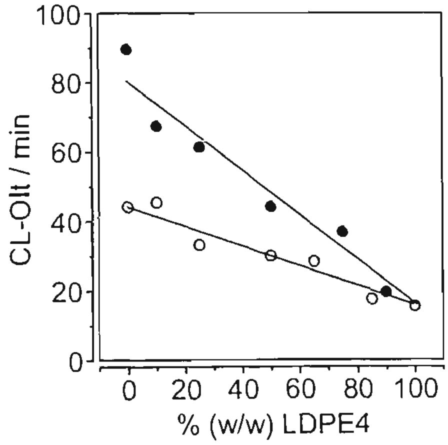

Figure 4.26. CL-OIt versus composition for the: (●) LDPE4/ mLLDPE3 blends and (o) LDPE4/mLLDPE4 blends where the data were obtained from CL instrument #1.

The LLDPE6/mLLDPE2 system is comprised of polymers that are structurally similar to each other and should therefore be compatible. Melt compatibility for the components of the LLDPE6/mLLDPE2 system is reflected by a single DSC melting endotherm that is observed for each blend as shown in Figure 4.27. Each of the resins that comprise the LLDPE6/mLLDPE2 system is stabilized with a phenolic AO and the mLLDPE2 resin contains twice the level of AO as the LLDPE6 resin. The total AO level in the blends therefore increases linearly with an increasing concentration of LLDPE6. Figure 4.28 shows a plot of the CL-OIt versus composition for the LLDPE6/mLLDPE2 system wherein the CL-OIt is observed to increase linearly with increasing concentration of mLLDPE2. The linearity of this plot supports the notion that the blend compatibility suggested by the DSC data (see Figure 4.27) is also reflected in the idealized behaviour of the thermo-oxidative stability data.

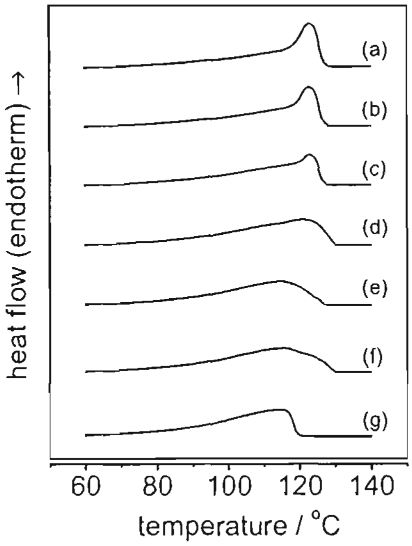

Figure 4.27. DSC endotherms of selected LLDPE6/mLLDPE2 blends containing: (a) 0%, (b) 10%, (c) 30%, (d) 50%, (e) 70%, (f) 90% and (g) 100% mLLDPE2. Blend compositions are (w/w).

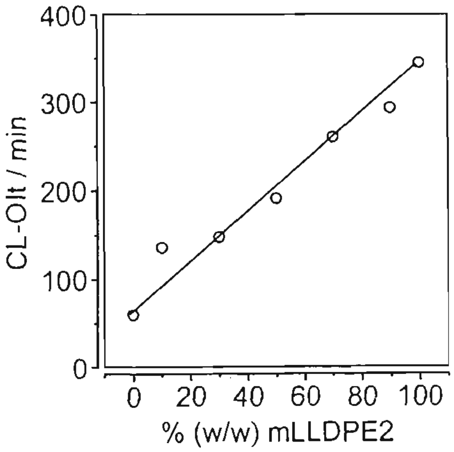

Figure 4.28. CL-OIt versus composition for the LLDPE6/mLLD-PE2 blends where the data were obtained from CL instrument #1.

4.3.2 Non-Idealized Blend Systems

The systems where mLLDPE5 is blended with either HDPE1 or HDPE2 are less ideal. Figure 4.29 shows the DSC melting endotherms for selected blends belonging to the HDPE1/mLLDPE5 system where two peaks covering a wide melting range are evident in some cases and correspond to the blend components. Indeed, the endothermic curves for all blend systems studied in this work cover a notably wide melting range. However, endothermic curves showing a significantly wider melting range and multiple peaks when compared with those of the individual polymers have been interpreted as being indicative of immiscibility or partial immiscibility in the blend [592]. This may be attributable to the chain branching of the mLLDPE component resulting from the octene comonomer [712].

The behaviour of the HDPE2/mLLDPE5 system is similar to that of the HDPE1/mLLDPE5 system with two peaks distinguishable in many endotherms (see Appendix 3). The presence of two peaks in the endotherms suggests that some degree of immiscibility exists in the melt and that the components in these systems are incompatible. The second peak corresponding to the mLLDPE component becomes more apparent when the data are subjected to a first time derivative analysis and are presented at higher resolution (see Appendix 3).

Each of the components of the HDPE1/mLLDPE5 and HDPE2/mLLDPE5 systems contain phenolic AOs such that the mLLDPE5 is stabilized at a relatively higher level than either the HDPE1 or HDPE2 (see Table 3.2). The overall level of AO in each system therefore increases linearly with an increasing mLLDPE5 level. A plot of the CL-OIt versus composition for each of the HDPE1/mLLDPE5 and HDPE2/mLLDPE5 systems is shown in Figure 4.30. In contrast to the other systems studied in this work the CL-OIt of each of the HDPE1/mLLDPE5 and HDPE2/mLLDPE5 systems does not increase linearly with an increasing level of the more stable component in the blend. The CL-OIt values of the HDPE1/mLLDPE5 system deviate negatively from the theoretical straight line drawn between the OITs of the pure components (i.e. the theoretical line that represents the situation where the observed stability is additive).

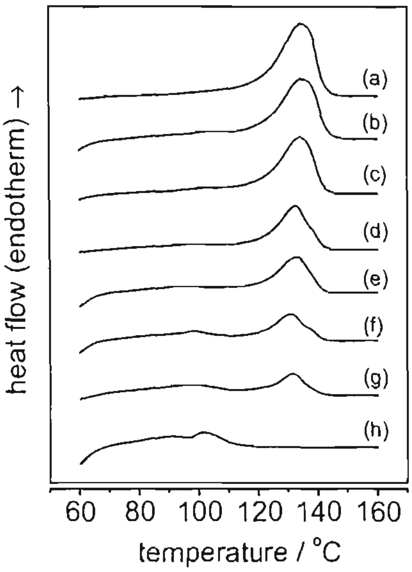

Figure 4.29. DSC endotherms of selected HDPE1/mLLDPE5 blends containing: (a) 0%, (b) 10%, (c) 20%, (d) 35%, (e) 50%, (f) 65%, (g) 85% and (h) 100% mLLDPE5. Blend compositions are (w/w).

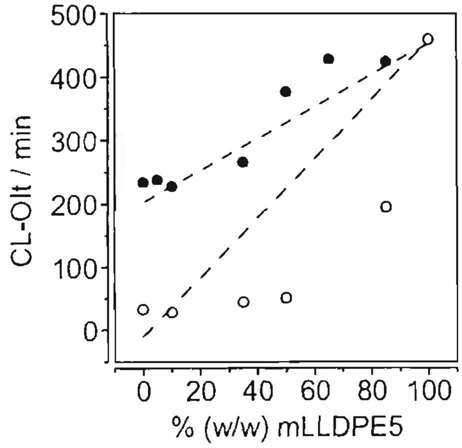

Figure 4.30. CL-OIt versus composition for the: (○) HDPE1/ mLLDPE5 blends and (●) HDPE2/mLLDPE5 blends where the data were obtained from CL instrument #1. Dotted lines show expected trends for idealized behaviour.

It is important to note that since the activation energy for thermal oxidation is typically high for stabilized samples then small differences in temperature will give rise to large deviations in the observed OIt. However, the consistent trends exhibited by the OIt values obtained in the current work suggest that such temperature fluctuation effects are not responsible for the observed deviations from idealized behaviour. Indeed, the deviation of the HDPE1/mLLDPE5 system is negative for all compositions in the entire range. In the case of the HDPE2/mLLDPE5 system, the deviation is negative only up to a composition of about 40% (w/w) mLLDPE5 after which the CL approaches that of the 100% mLLDPE5. The persistence of a negative deviation for the HDPE1/mLLDPE5 system across all compositions suggests that this system is less compatible than the HDPE2/mLLDPE5 system. In either case the CL-OIt behaviour is non-ideal and this is a reflection of the behaviour previously observed in the DSC analysis (see Figure 4.29). Furthermore, similar non-linear OIt behaviour with blend composition has been observed in the case of incompatible blends of EPR and PP [713]. In the HDPE1/mLLDPE5 and HDPE2/ mLLDPE5 systems studied in the present work, the similarly observed effects may be due to a decrease in stabilizer efficiency that occurs when the solid-state incompatibility of the blend components persists to produce a melt that is heterogeneous. The heterogeneity of the resultant melt may therefore play a key role in the decreased stabilizer efficiency that is observed.

4.3.3 Consistency between CL Instruments and Techniques

In order to assess the consistency of CL-OIt data obtained from two different instruments, each of the nine commercial PE formulations that were used to make the blend systems were oxidized in CL instrument #2 under the same conditions used previously in CL instrument #1 (i.e. 170°C, oxygen atmosphere, 1 bar, flow rate 100 mL min^{-1}). Shown in Figure 4.31 are the integrated CL profiles obtained from CL instrument #2 for each of the PE resins. The metallocene-catalyzed mLLDPE2 and mLLDPE5 resins are the most stable presumably due to the high level of AO in each. The low stabilities of mLLDPE3 and mLLDPE4 may be partly attributed to their relatively low MW (see Table 3.2).

The structural uniformity [327] and the absence of catalyst residues in metallocene-catalyzed PE resins [337] are believed to contribute to the stability of these materials. The relative order of inherent stability of PE resins has been reported by other workers as mLLDPE > HDPE > LDPE [327,337]. However, in the present study it is unlikely that the effects of structural differences between the metallocene-

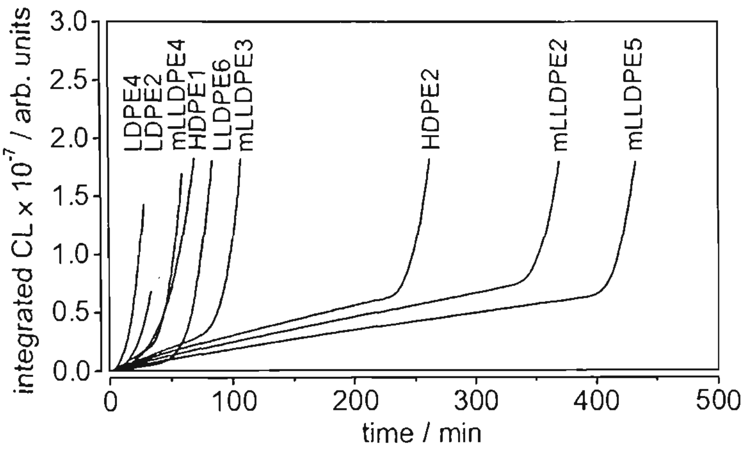

Figure 4.31. Integrated CL profiles obtained from CL instrument #2 for each of the commercial PE resins used to make the blends.

catalyzed resins outweigh those due to the respective stabilizer levels and so the relative order of stability observed amongst the resins is most likely to have been determined by the level of AO in each resin. In particular, the AO content of HDPE2 lies between that of mLLDPE2 and mLLDPE4 and this is reflected by its intermediate stability, however the inherent stability of HDPE2 is also determined to some extent by its high degree of crystallinity that inhibits oxygen access during oxidation [327]. The LDPE resins exhibit the lowest stability and this is presumably due to the absence of stabilizer in these and, to some extent, their low crystallinities. Similarly, the lower stability of HDPE1 compared with HDPE2 is also attributable to the relative AO levels in these materials.

An indication of the consistency of typical CL-OIt data can be achieved by plotting the CL-OIt data that were obtained using CL instrument #1 against the corresponding data that were obtained using CL instrument #2. Figure 4.32 shows such a plot where the CL-OIt values plotted on the abscissa and ordinate axes were derived from the integrated CL profiles by means of the STD analysis protocol described previously [330]. The linearity of the plot suggests that there is a high degree of consistency between the results obtained from the two instruments and the favourable gradient and intercept values, which are close to unity and zero respectively, further suggest that a high degree of reproducibility has been attained.

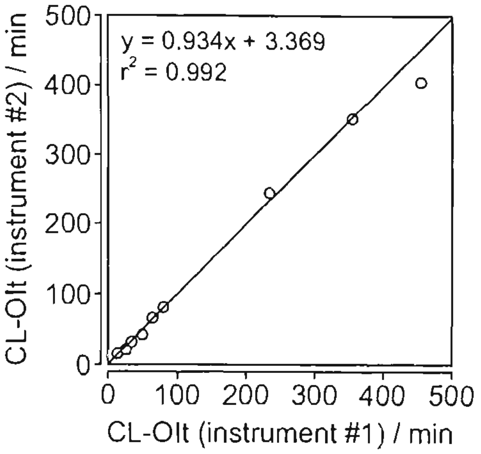

Figure 4.32. CL-OIt values obtained from CL instrument #2 versus the corresponding CL-OIt values obtained from CL instrument #1 for each of the commercial PE resins used to make the blends.

A preliminary investigation of the extent to which results obtained from CLI experiments correlate with those obtained from photon-counting CL experiments was conducted using four of the resins that were used to make the blends. These resins were individually subjected to oxidation in a CLI apparatus under the same conditions used for the single-photon counting CL studies (i.e. 170°C, oxygen atmosphere, 1 bar, flow rate 100 mL min^{-1}). Figure 4.33 shows the integrated CLI profiles for these resins together with the indicated CLI-OIt values that were obtained using STD analysis [330]. The CLI experiments were conducted using single samples to avoid the possible inter-sample "infection" that has been observed previously during multiple sample CL imaging experiments [335,714]. The order of stability that is revealed by the results of the CLI experiments is the same as that observed previously in the single photon counting experiments, although the CLI-OIt values are significantly greater than the corresponding CL-OIt values. A more quantitative assessment of the correlation between the two techniques can be made by plotting the CL-OIt values obtained from the single photon counting experiments against the CLI-OIt values obtained from the CLI experiments. Such plots are presented in Figure 4.34 for CL-OIt data derived from both CL instrument #1 and CL instrument #2. The plots show that, for each single photon counting instrument, there is good correlation between the OIt values obtained using it and those obtained using the CLI instrument. However, there is an offset of approximately 100 min with respect to the CLI data that is attributable to a discrepancy in the temperature calibration of the CLI instrument during these preliminary trials. This highlights the importance of accurate temperature calibration in CL work.

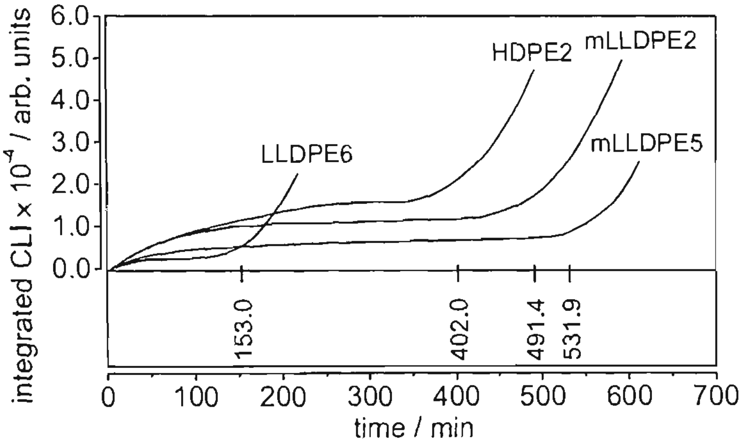

Figure 4.33. Integrated CLI profiles for selected PE resins oxidized at 170°C in an oxygen atmosphere (1 bar, flow rate 100 mL min^{-1}).

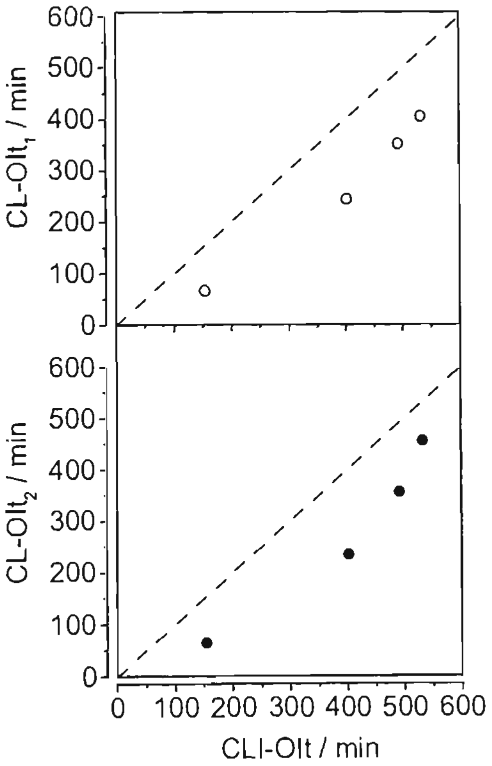

Figure 4.34. A comparison of CL-OIt data obtained from single photon counting CL experiments with CLI-OIt data obtained from CLI experiments. CL-OIt data were obtained using two different instruments: (●) CL instrument #1, (○) CL instrument #2. Broken lines indicate the desirable situation where total correlation exists.

4.4 Physicomechanical Properties of Polyethylene Blends

In this section, the physicomechanical properties of various polyethylene blends are investigated in order to identify blends that have superior or optimal properties. An emphasis is placed on blends with mPEs as these materials are relatively new and are therefore not represented in the literature as extensively as blends of conventional PEs to date.

4.4.1 Effect of Blending mLLPDE with HDPE

Blending HDPE with conventional LLDPE is primarily aimed at improving the processability of the HDPE [621] but may also result in improvements in other properties such as resistance to slow crack growth [715]. The physicomechanical properties of blends of two HDPEs with one mLLDPE are examined in this section in order to identify properties that may be improved by blending.

Physical Properties of HDPE1/mLLDPE5 and HDPE2/mLLDPE5 Blends

The density of PE is a function of the type and level of LCB and SCB within the polymer [565]. A plot of density versus composition for blends of HDPE1 with mLLDPE5 is shown in Figure 4.35. The plot shows that the density of the blend is additive with respect to the blend composition. A similar plot was obtained for blends of HDPE2 with mLLDPE5 (data not shown). Such linearity has been shown to be the case for a number of polyethylene blends [21,373,547,584] and suggests that the presence of one type of crystal in the blend has little effect on the ability of the other species to crystallize from the melt [373]. The density of the mLLDPE resin is considerably lower than that of the HDPEs which is another characteristic property of mPE resins [31,378,379].

The MFI of a polymer or polymer blend is related to its relative molecular weight and is often used to characterize processability [17,58,372]. A plot of MFI versus composition for HDPE1/mLLDPE5 or HDPE2/mLLDPE5 blends is shown in Figure 4.36(a). For the HDPE1/mLLDPE5 blends, this plot shows an upward trend in the MFI that is slightly less than being additive over the range of compositions investigated. For the HDPE2/mLLDPE5 blends, however, the variation in MFI with composition is approximately linear. A corresponding plot of the melt flow ratio (MFR, MI_{21}/MI_2) versus composition is shown in Figure 4.36(b). From this plot it is evident that the MFR for each of the blends is less than additive and that the MFR of 100% mLLDPE5 is significantly lower than that of 100% HDPE1 or 100% HDPE2. These data are consistent with the notion that mPE resins have narrow molecular weight ranges which is reflected by their low MFR values [31,377,379]. Furthermore, the data in Figure 4.36(b) suggest that the polydispersity of HDPE1 is greater than that of HDPE2.

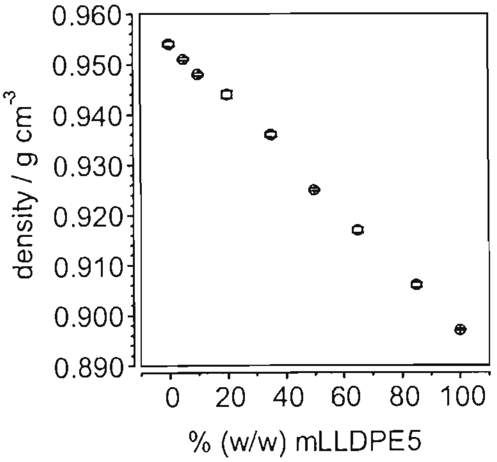

Figure 4.35. Density versus composition for HDPE1/mLLDPE5 blends.

Tensile Properties of HDPE1/mLLDPE5 and HDPE2/mLLDPE5 Blends

A plot of yield strength versus composition for blends of HDPE1 or HDPE2 with mLLDPE5 is shown in Figure 4.37. From this plot it is evident that the addition of mLLDPE5 decreases the yield strength of each blend from *ca.* 33 MPa (for HDPE1) and 25 MPa (for HDPE2) to *ca.* 12 MPa (for mLLDPE5) in a non-linear manner. This reduction in yield strength may be a result of the lower crystallinities of the mLLDPE components [365,655]. Although this trend is clearly non-linear, the variation in yield strength with blend composition is similar to that reported elsewhere [589,594].

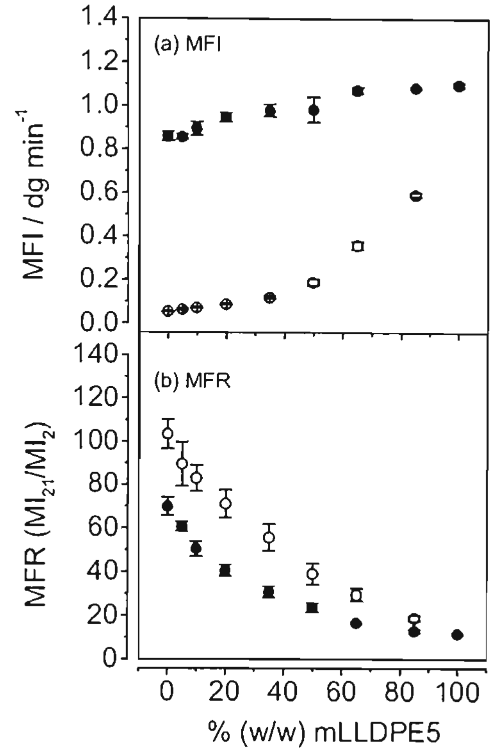

Figure 4.36. Plots of: (a) MFI and (b) MFR versus composition for: (o) HDPE1/mLLDPE5 blends and (•) HDPE2/mLLDPE5 blends.

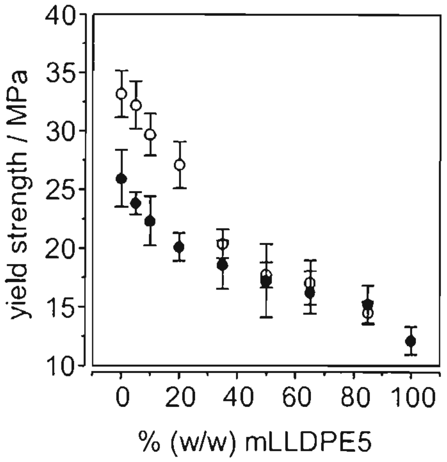

Figure 4.37. Yield strength versus composition for: (o) HDPE1/ mLLDPE5 blends and (•) HDPE2/mLLDPE5 blends.

A plot of break strength versus composition for blends of HDPE1 or HDPE2 with mLLDPE5 is shown in Figure 4.38. The break strength of HDPE1/mLLDPE5 blends was observed to vary between *ca.* 20 and 24 MPa and the break strength of HDPE2/mLLDPE5 blends was observed to vary between *ca.* 18 and 24 MPa. These observations are in accordance with those made for blends of HDPE with conventional LLDPE where the break strength was found to increase with increasing levels of LLDPE in the blend [207].

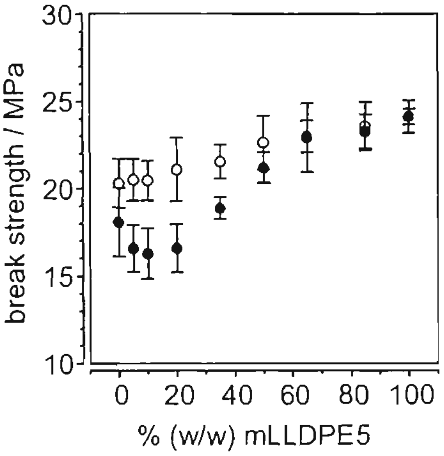

Figure 4.38. Break strength versus composition for: (o) HDPE1/ mLLDPE5 blends and (•) HDPE2/mLLDPE5 blends.

The percent elongation at break versus composition for blends of HDPE1 or HDPE2 with mLLDPE5 is shown in Figure 4.39. From this plot it is evident that increases in percent elongation from a minimum of *ca.* 400% (for HDPE2) to *ca.* 700% occur upon the addition of mLLDPE. Increases of this magnitude have also been reported in the case of film blends [654]. This increase may be a function of the homogeneous molecular structure of the mLLDPE component [377].

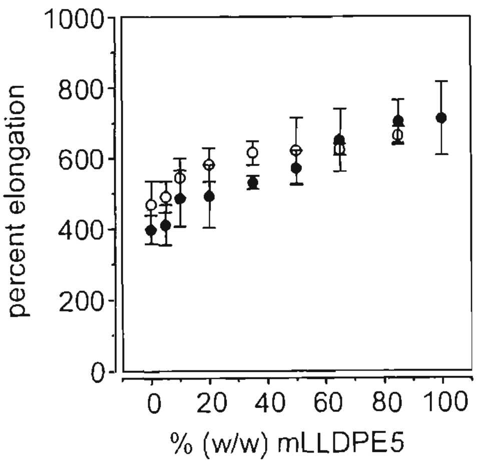

Figure 4.39. Percent elongation at break versus composition for: (o) HDPE1/mLLDPE5 blends and (•) HDPE2/mLLDPE5 blends.

Izod Impact Properties of HDPE1/mLLDPE5 and HDPE2/mLLDPE5 Blends

The Izod impact strength (IS) versus composition for blends of HDPE1 or HDPE2 with mLLDPE5 is shown in Figure 4.40(a). For blends containing greater than 50% (w/w) mLLDPE5, up to and including 100% mLLDPE5, no break was observed under the test conditions. This suggests that the mLLDPE5 has superior impact properties which are imparted as a result of blending with HDPE. It is also evident from this plot that HDPE1 has much better resistance to impact than HDPE2 (*ca.* 90% greater). The individual effects of blending mLLDPE5 with HDPE1 or HDPE2 are reflected in Figure 4.40(b) which shows the percentage increase in IS with blend composition. This plot shows that the IS of HDPE2/mLLDPE5 blends are improved dramatically with increases between *ca.* 27% and 92% whereas HDPE1/mLLDPE5 blends are improved on average by only *ca.* 10%. The tensile and impact properties presented here are clearly non-linear and this is consistent with the notion of an immiscible or partially immiscible blend reflected by the DSC and CL data (see Figure 4.29 and Figure 4.30 respectively).

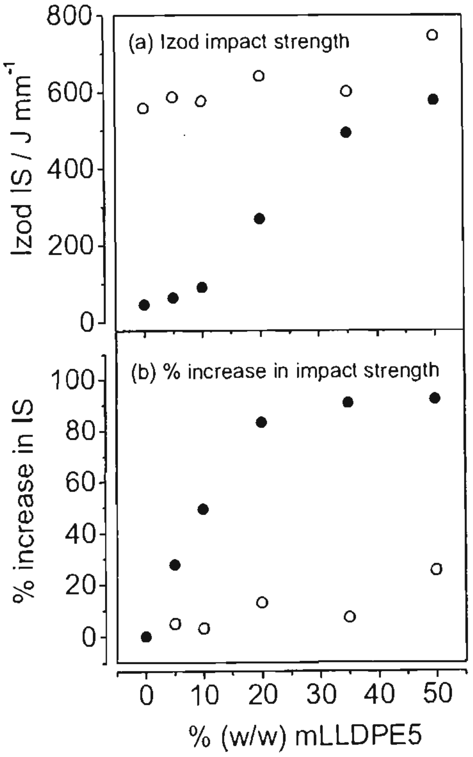

Figure 4.40. Plots of: (a) Izod impact strength and (b) % increase in impact strength versus composition for: (○) HDPE1/mLLDPE5 blends and (●) HDPE2/mLLDPE5 blends.

4.4.2 Effect of Blending Low MW mLLPDE with Low MW LDPE

This section examines the physicomechanical properties of blends of a low MW LDPE with two low MW mLLDPEs in order to identify properties that may be improved by blending.

Physical Properties of LDPE4/mLLDPE3 and LDPE4/mLLDPE4 Blends

Figure 4.41(a) shows plots of density versus composition for blends of LDPE4 with mLLDPE3 or mLLDPE4. These plots show that the density of the blend is additive with respect to the blend composition. The densities of the mLLDPE resins are much lower than conventional PEs which is another characteristic property of mPE resins [31,378,379]. A plot of MFI versus composition for blends of LDPE4 with mLLDPE3 or mLLDPE4 is shown in Figure 4.41(b). The MFI for each of the blends shows a downward trend over the range of compositions.

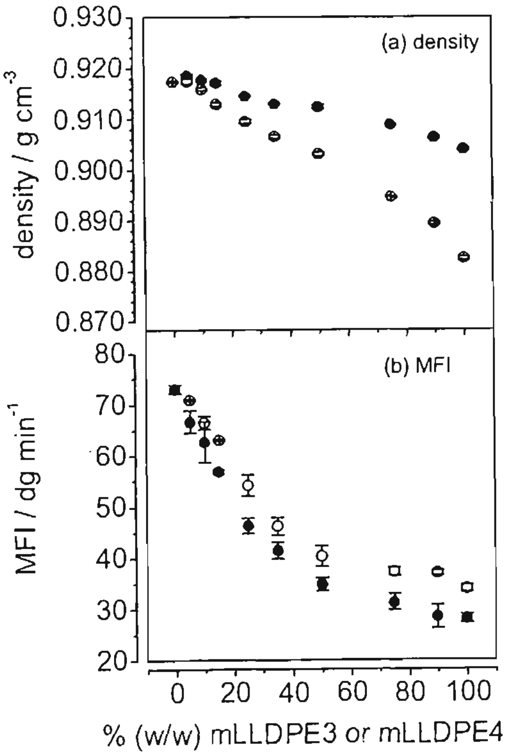

Figure 4.41. Plots of: (a) density and (b) MFI versus composition for: (•) LDPE4/mLLDPE3 blends and (o) LDPE4/mLLDPE4 blends.

Tensile Properties of LDPE4/mLLDPE3 and LDPE4/mLLDPE4 Blends

A plot of yield strength versus composition for blends of LDPE4 with mLLDPE3 or mLLPDE4 is shown in Figure 4.42. From this plot it is evident that the addition of mLLDPE decreases the yield strength of each blend from *ca.* 9.5 to less than 6 MPa in a non-linear but uniform manner. This reduction in yield strength may be a result of the lower crystallinities of the mLLDPE components [365,655]. There was no yield strength determined for the 100% mLLDPE4 which has the overall lowest density and crystallinity of all materials used in the blends (see Table 3.2). For blends of conventional LLDPE with LDPE, it has been shown that LLDPE increases the yield strength of the blend as a result of the distribution of SCB in the LLDPE matrix [365].

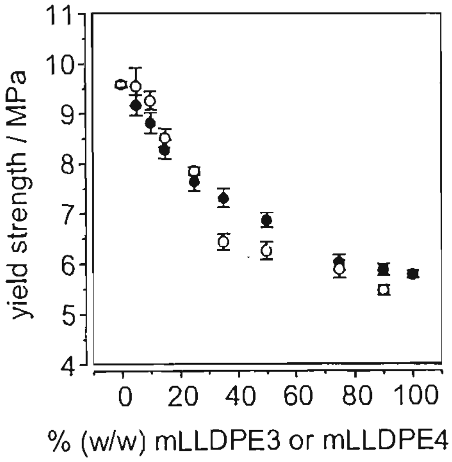

Figure 4.42. Yield strength versus composition for: (•) LDPE4/ mLLDPE3 blends and (o) LDPE4/mLLDPE4 blends.

A plot of break strength versus composition for blends of LDPE4 with mLLDPE3 or mLLPDE4 is shown in Figure 4.43. The break strength of blends with mLLDPE was observed to vary between 6 and 8 MPa with the 100% mLLDPE3 having and break strength of *ca.* 9 MPa. For blends involving mLLDPE4, the break strength varies between *ca.* 5.5 and 6.5 MPa over the entire composition range. In contrast, the break strength of LDPE is generally improved with the addition of conventional LLDPE [95,655]. In blends of HDPE with conventional LLDPE both the break strength and percent elongation at break improve with increasing levels of LLDPE in the blend [207].

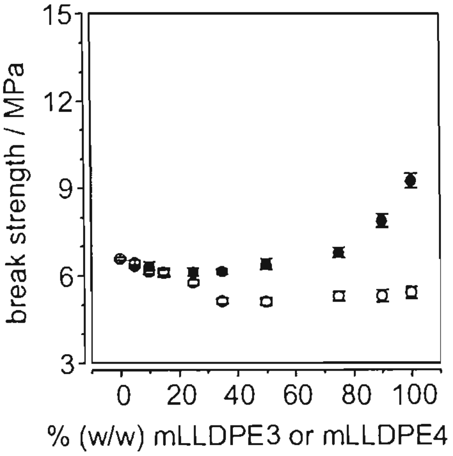

Figure 4.43. Break strength versus composition for: (•) LDPE4/mLLDPE3 blends and (o) LDPE4/mLLDPE4 blends.

The percent elongation at break versus composition for LDPE4/mLLDPE3 and LDPE4/mLLDPE4 blends is shown in Figure 4.44. From this plot it is evident that increases in percent elongation from *ca.* 100% to *ca.* 900% occur upon the addition of mLLDPE and this is also shown to be the case for film blends [654]. This increase may be a function of the homogeneous molecular structure of the mLLDPE component [377] or as a result of the lower density of the blend [17]. Although the tensile properties are clearly non-linear, there are no apparent discontinuities in the data and this is consistent with there being blend compatibility [553,583,716]. This supports the notion of blend compatibility suggested previously by the DSC data and the CL data (see Figure 4.25 and Figure 4.26 respectively).

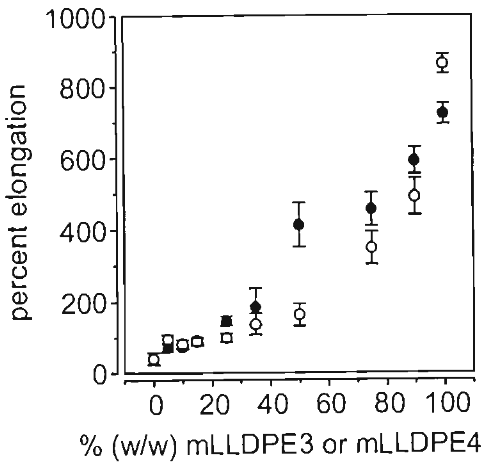

Figure 4.44. Percent elongation at break versus composition for: (•) LDPE4/mLLDPE3 blends and (o) LDPE4/mLLDPE4 blends.

Impact Properties of LDPE4/mLLDPE3 and LDPE4/mLLDPE4 Blends

Instrumented impact testing of the LDPE4/mLLDPE3 and LDPE4/mLLDPE4 blends was conducted at room temperature and at -20°C. The resulting force-displacement curves were analyzed for a number of characteristic features. Typical force-displacement curves for selected blends of LDPE4 with mLLDPE3 at room temperature and at -20°C are shown in Figure 4.45. With the exception of 100% LDPE4, there was no significant variation in the force-displacement curve for these blends. Blends of LDPE4 with mLLDPE4 (see Figure 4.46), however, show changes in the shape and the initial gradient of the curve.

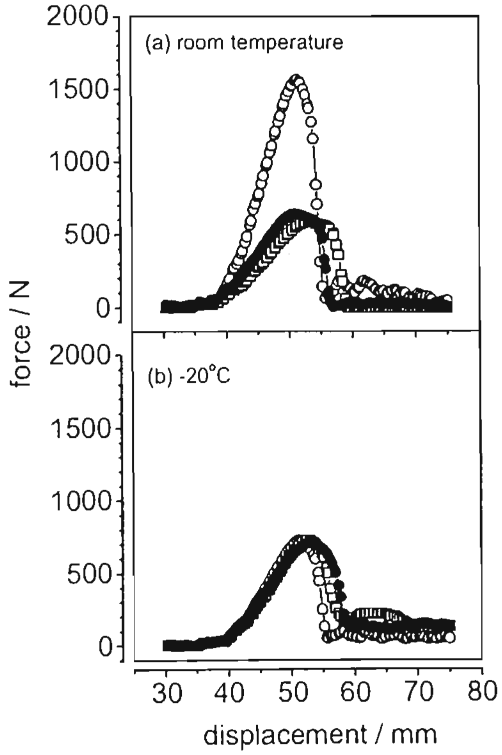

Figure 4.45. Force versus displacement at: (a) room temperature and (b) -20°C for: (○) 100% LDPE4, (●) 50% (w/w) mLLDPE3 and (□) 100% mLLDPE3.

The integrated area under the force-displacement curve is representative of the energy required by the sample to cause it to yield and then fail [369]. The "energy-to-peak" is the area under the curve enclosed by the baseline and the force trace up to the peak and is representative of the energy absorbed by the sample when it yields [369]. A plot of energy-to-peak for blends of LDPE4 with mLLDPE3 or mLLDPE4 is shown in Figure 4.47. The energy-to-peak for each of the blends is similar ranging between *ca.* 0.7 J and 0.8 J when measured at -20°C. At room temperature, the energy-to-peak is also similar and remains between 0.6 J and 0.8 J for levels up to 50% (w/w) mLLDPE. Above this level, the energy-to-peak increases up to maximima of *ca.* 4.7 J and *ca.* 11 J for 100% mLLDPE3 and mLLDPE4 respectively. The greater energies absorbed by the 100% mLLDPE samples may be due to the greater ductility of these materials that result from the homogeneity of the SCB [19,232,253,370].

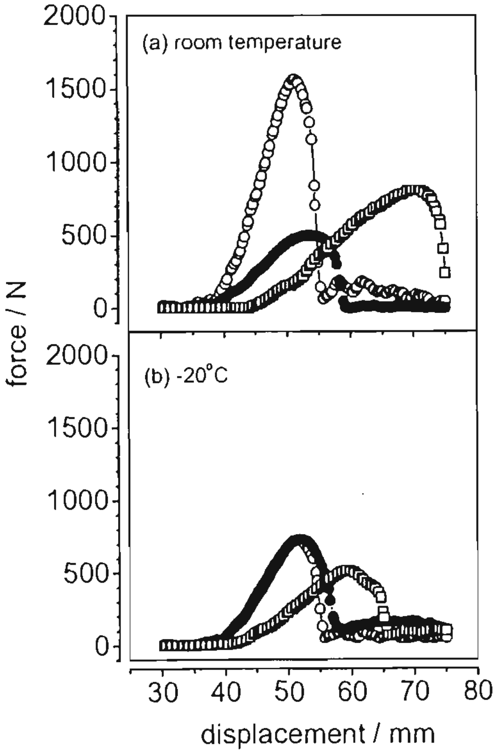

Figure 4.46. Force versus displacement at: (a) room temperature and (b) -20°C for: (o) 100% LDPE4, (•) 50% (w/w) mLLDPE4 and (□) 100% mLLDPE4.

The "energy-to-break" is the total area under the curve up to the nominal break point and this area is representative of the total energy required to break the test specimen [369]. A plot of energy-to-break versus composition for blends of LDPE4 with mLLDPE3 or mLLDPE4 is shown in Figure 4.48. For each blend, the total energy-to-break was again found to be relatively consistent between 7 J and 11 J at room temperature as well as at -20°C for LDPE4/mLLDPE3 and LDPE4/mLLDPE4 blends. The highest energy-to-break was found to be *ca.* 16.7 J for 100% LDPE4 measured at room temperature which may be a result of the low MW of this particular LDPE [369].

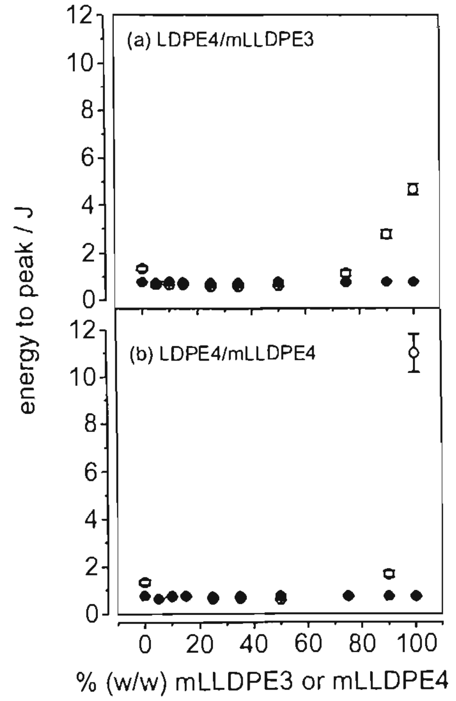

Figure 4.47. Energy-to-peak versus composition at: (○) room temperature and (●) -20°C for: (a) LDPE4/mLLDPE3 blends and (b) LDPE4/mLLDPE4 blends.

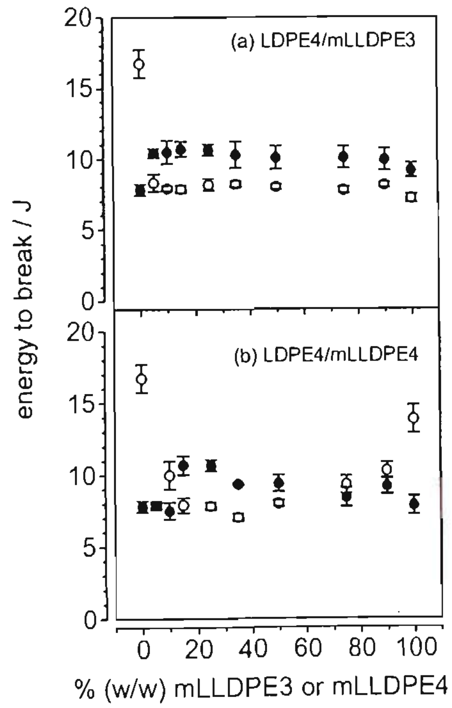

Figure 4.48. Energy-to-break versus composition at: (○) room temperature and (●) -20°C for: (a) LDPE4/mLLDPE3 blends and (b) LDPE4/mLLDPE4 blends.

The ratio of the energy-to-peak to the energy-to-break is an indication of the relative ductility of the test samples [369]. A plot of this ratio of energies versus composition is shown in Figure 4.49. From this plot it is evident that there is little difference in the relative ductility of each of the blends at either test temperature with the ratio of energies being relatively consistent between *ca.* 0.07 and 0.10. Low values such as these suggest a brittle material, which is characteristic of branched LDPE [369]. The ratio of energies for 100% mLLDPE3 and 100% mLLDPE4 at room temperature, however, are much higher and are 0.65 and 0.79 respectively. This is indicative of these particular materials being more elastic and is consistent with the properties of mPE materials in general [366-369]. Conventional LLDPE is reported to be a highly ductile material as a result of the SCB and SCB distribution [369]. Freezing the 100% mLLDPE samples at -20°C, however, reduces the relative elasticity of the mLLDPE and causes the samples to be more brittle.

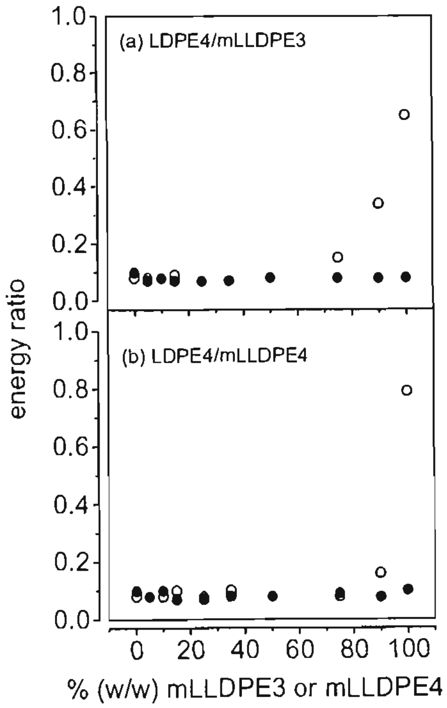

Figure 4.49. Ratio of energies versus composition at: (○) room temperature and (●) -20°C for: (a) LDPE4/mLLDPE3 blends and (b) LDPE4/mLLDPE4 blends.

The initial gradient of the force-displacement curve is an indication of the relative stiffness, or modulus, of the material [369]. A plot of the modulus versus composition is given in Figure 4.50. For the blends tested at room temperature, the modulus of the each of the samples decreases from *ca.* 80 to 10 N mm^{-1}. This suggests that with increasing levels of mLLDPE, the ductility of the material increases [369]. For the blends tested at -20°C, the modulus of the LDPE4/mLLDPE3 blends remains relatively unchanged and is comparatively higher than the modulus measured at room temperature. Blends of mLLDPE4 tested at -20°C show an increase in modulus from *ca.* 50 to 130 N mm^{-1}, followed by a decrease to *ca.* 50 N mm^{-1}. This suggests that the ductility of mLLDPE at -20°C is lower than the ductility at room temperature and this has been shown to be the case for conventional LLDPE [369].

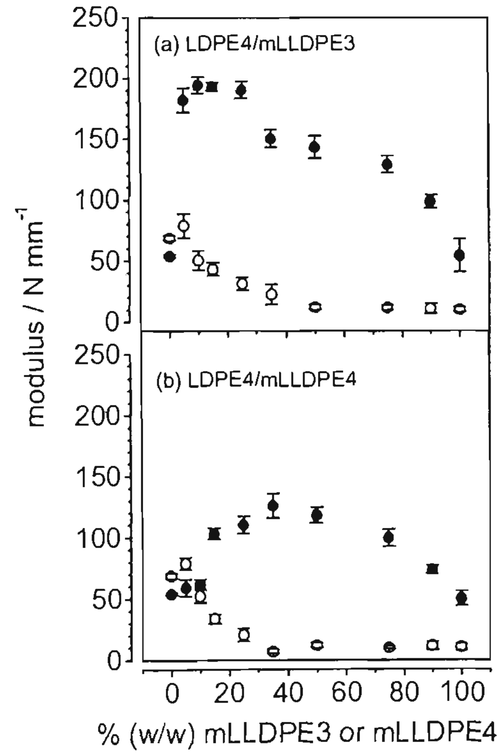

Figure 4.50. Modulus versus composition for: (a) LDPE4/mLLDPE3 blends and (b) LDPE4/mLLDPE4 blends at: (○) room temperature and (●) -20°C.

4.4.3 Effect of Blending mLLPDE with LLDPE for Film Applications

This section investigates the effect of blending mLLDPE with conventional LLDPE on the physicomechanical and optical properties of blown films.

Physical Properties of LLDPE6/mLLDPE2 Blends

Figure 4.51 shows a plot of density versus composition for blends of mLLDPE2 with LLDPE6. This plot indicates that the density of the blend is additive with respect to the blend composition. The density of 100% mLLDPE2 is slightly lower than the conventional LLDPE6 resin which is a characteristic property of mPE resins [31,378,379].

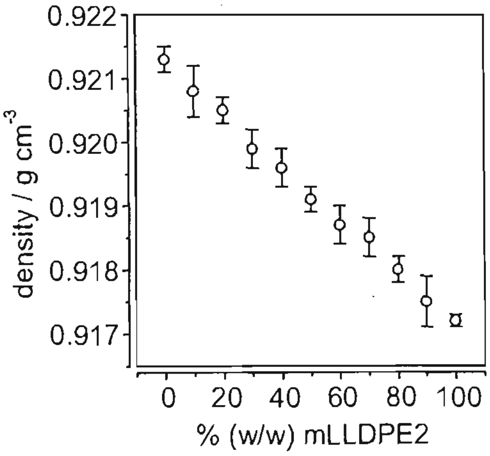

Figure 4.51. Density versus composition for LLDPE6/mLLDPE2 blends.

A plot of MFI versus composition for LLDPE6/mLLDPE2 blends is shown in Figure 4.52(a) and a plot of the corresponding MFR versus composition is shown in Figure 4.52(b). The MFI increases from *ca.* 0.7 to *ca.* 1.0 dg min^{-1} with increasing levels of mLLDPE2 in the blend. The MFR decreases from *ca.* 16 to a minimum of *ca.* 14 at a level of 60% (w/w) mLLDPE2 followed by an increase to *ca.* 16 for 100% mLLDPE2. This unusual variation in MFR is indicative of blending a material with a relatively narrow molecular weight range with a material having a broader MWD [31,377].

Mechanical Properties of LLDPE6/mLLDPE2 Blends

The yield strength versus composition of the LLDPE6/mLLDPE2 blends is shown in Figure 4.53. In the TD of the film the yield strength decreases from *ca.* 13 MPa to a minimum of 10.4 MPa at 70% (w/w) mLLDPE2. Whereas conventional LDPE/ LLDPE film blends show no observable yield strength in the MD [228,555], yield strengths between *ca.* 12.5 MPa to 11 MPa are measured in the MD of the film blends of LLDPE6 with mLLDPE2.

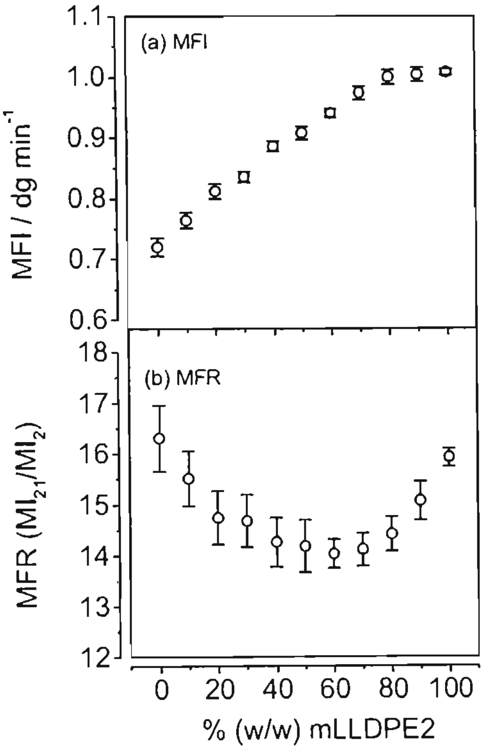

Figure 4.52. Plots of: (a) MFI and (b) MFR versus composition for LLDPE6/mLLDPE2 blends.

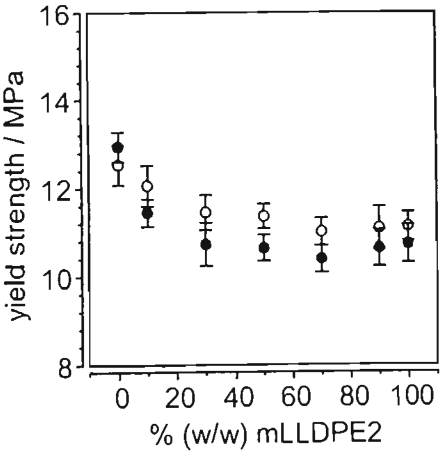

Figure 4.53. Yield strength versus composition for LLDPE6/ mLLDPE2 blends in the: (o) MD and (•) TD of the film.

A plot of the break strength versus composition is shown in Figure 4.54(a). The break strength increases approximately linearly from *ca.* 44 MPa to 54 MPa in the

MD of the film and from *ca.* 45 MPa to 54 MPa in the TD of the film. These data suggest that there is little change in the break strength in the TD of the film up to and including levels of *ca.* 50% (w/w) mLLDPE2 in the blends. Furthermore, the break strength values for the 100% mLLDPE2 and 100% LLDPE6 are similar in both the MD and TD of the film. The percent elongation at break versus composition is shown in Figure 4.54(b). In both the MD and TD of the film, the percent elongation decreases with increasing mLLDPE2 in the blend. The variation in percent elongation is more significant in the TD of the film as expected [717].

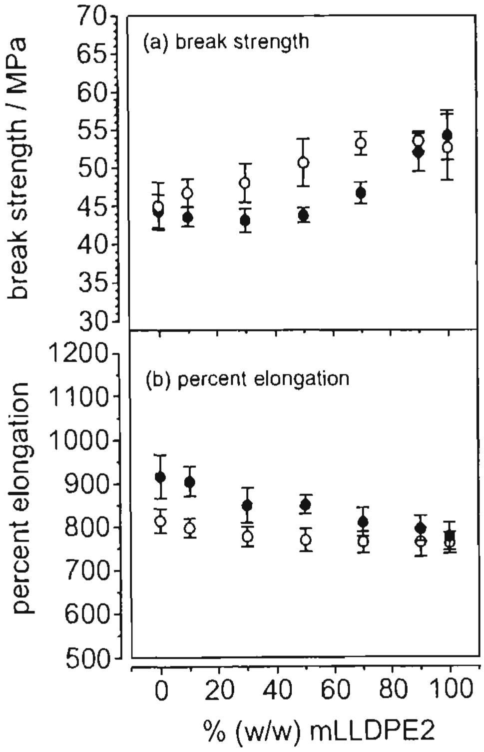

Figure 4.54. Plots of: (a) break strength and (b) percent elongation versus composition for LLDPE6/mLLDPE2 blends in the: (○) MD and (●) TD of the film.

A plot of dart impact strength versus composition is shown in Figure 4.55(a). The 100% mLLDPE2 film has more than twice the dart impact strength than 100% LLDPE6. The increase in dart impact strength with increasing levels of mLLDPE2 is approximately linear suggesting an additive relationship with composition. This observed behaviour supports the notion of blend compatibility suggested by the DSC data (see Figure 4.27) and the CL data (see Figure 4.28) shown previously. A plot of tear resistance versus composition is shown in Figure 4.55(b). In both the

MD and the TD of the film the tear resistance shows little variation with increasing levels of mLLDPE2. In each case, the tear resistance in the TD is consistently greater than that in the MD at the same composition possibly due to orientation effects that originate from the film blowing process [663,679,718].

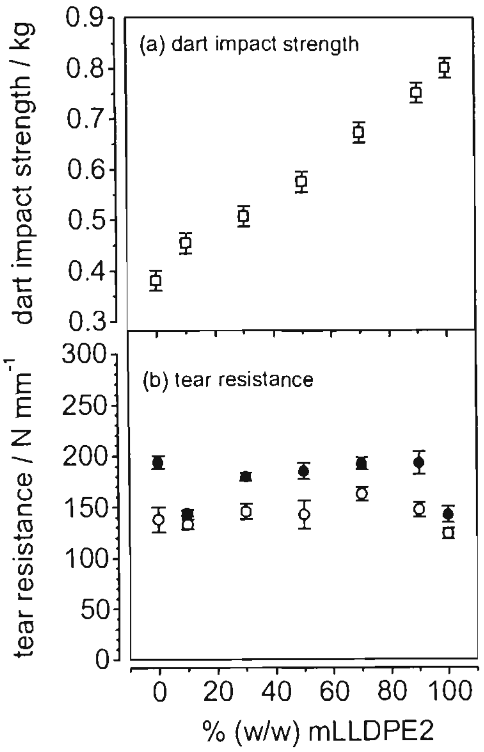

Figure 4.55. Plots of: (a) dart impact strength and (b) tear resistance versus composition for LLDPE6/mLLDPE2 blends. Tear resistance measured in the: (o) MD and (•) TD of the film.

Optical Properties of LLDPE6/mLLDPE2 Blends

Figure 4.56 shows plots of the percent haze and the percent gloss versus composition for blends of mLLDPE2 and LLDPE6. From this plot it can be seen that the percent haze varies between *ca.* 12% and 18% for compositions up to and including 90% (w/w) mLLDPE2. A maximum of *ca.* 30% haze is observed for 100% mLLDPE2 with a minimum of *ca.* 12% at a level of 70% (w/w) mLLDPE2. In contrast, the percent gloss varies between *ca.* 60% and 70%. A minimum of *ca.* 33% gloss is observed for 100% mLLDPE2 and a maximum of *ca.* 70% gloss is observed for a blend containing 50% (w/w) mLLDPE2. These data suggest that the addition of mLLDPE2 to LLDPE6 has little effect on the overall clarity and optical properties of the film. Conversely, the data can also be interpreted in a way that suggests the addition of a small amount (*ca.* 10% (w/w)) of LLDPE6 to mLLDPE2 dramatically improves the optical properties of the latter. This is consistent with findings reported for blends of conventional LLDPE with LDPE [226,374,655].

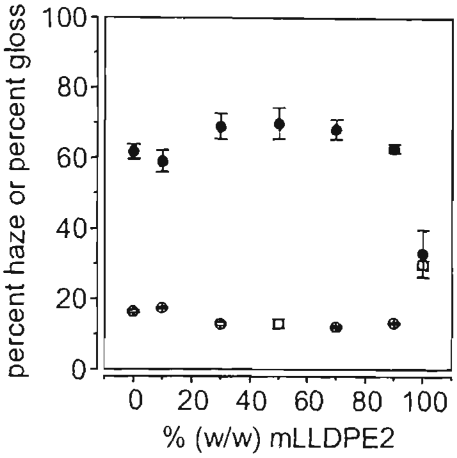

Figure 4.56. Plots of: (o) percent haze versus and (•) percent gloss versus composition for LLDPE6/mLLDPE2 blends.

4.4.4 Effect of Blending mLLPDE with LDPE for Film Applications

Blending mLLDPE with LDPE can result in the production of films that have improved properties compared with films made entirely from LDPE [380,612, 615,700,701] and such blends can also be processed significantly better than blends of conventional LLDPE with LDPE [226,374,380]. In view of the potential of mLLDPE to enhance the physicomechanical properties of LDPE, this section examines certain binary blends of mLLDPE with LDPE in order to identify any blends that have optimal and desirable characteristics.

Melting Behaviour of LDPE2/mLLDPE1 and LDPE3/mLLDPE1 Blends

The melting behaviour of the crystalline phase of a polymer is a function of the density and crystallinity of the polymer [59]. Figure 4.57 shows the DSC melting endotherms for the LDPE2/mLLDPE1 blends. In each case, a single crystalline melting peak is observed suggesting the presence of a homogeneous crystalline phase [61,207,220,585]. Single crystalline melting peaks are also observed for the melting endotherms of the LDPE3/mLLDPE1 blends (see Appendix 3).

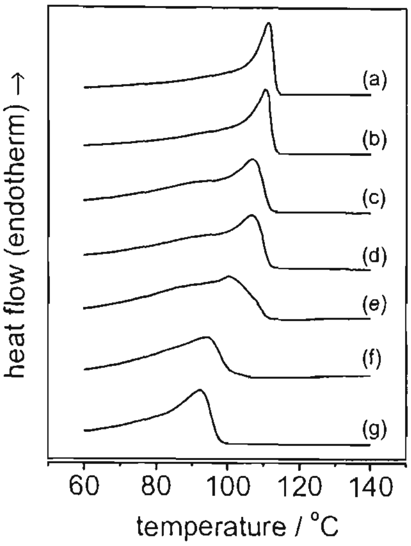

Figure 4.57. DSC endotherms of selected LDPE2/mLLDPE1 blends containing: (a) 0%, (b) 10%, (c) 20%, (d) 50%, (e) 75%, (f) 90% and (g) 100% mLLDPE1. Blend compositions are (w/w).

Physical Properties of LDPE2/mLLDPE1 and LDPE3/mLLDPE1 Blends

Figure 4.58 shows plots of density versus composition for blends of mLLDPE1 with LDPE2 or LDPE3. From these plots it can be seen that the density of the blend is additive with respect to the blend composition. The density of the mLLDPE is considerably lower than conventional LLDPE resins which is characteristic of mPE resins [31,378,379]. A plot of MFI versus composition for LDPE2/mLLDPE1 and LDPE3/mLLDPE1 blends is shown in Figure 4.59(a). The MFI for blends of mLLDPE1 with LDPE2 increases approximately linearly whereas the MFI for blends with LDPE3 show a downward trend over the range of compositions. A plot of the corresponding MFR versus composition for each of these blends is shown in Figure 4.59(b). From this plot it is evident that the MFR for each of the blends is less than additive and that the MFR of pure mLLDPE1 is significantly lower than that of pure LDPE2 or LDPE3. These data are consistent with the notion that mPE resins have narrow molecular weight ranges which is reflected by their low MFR values [31,377,379]. Furthermore, the data in Figure 4.59(b) suggest that the polydispersity of LDPE2 is greater than that of LDPE3.

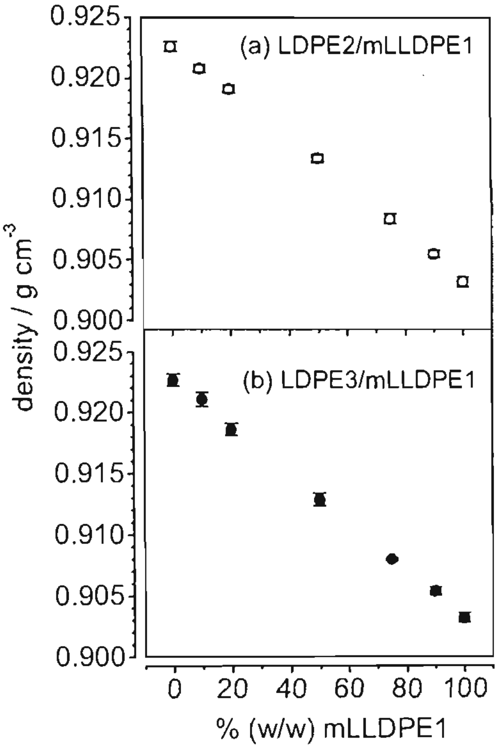

Figure 4.58. Density versus composition for: (o) LDPE2/mLLDPE1 blends and (•) LDPE3/mLLDPE1 blends.

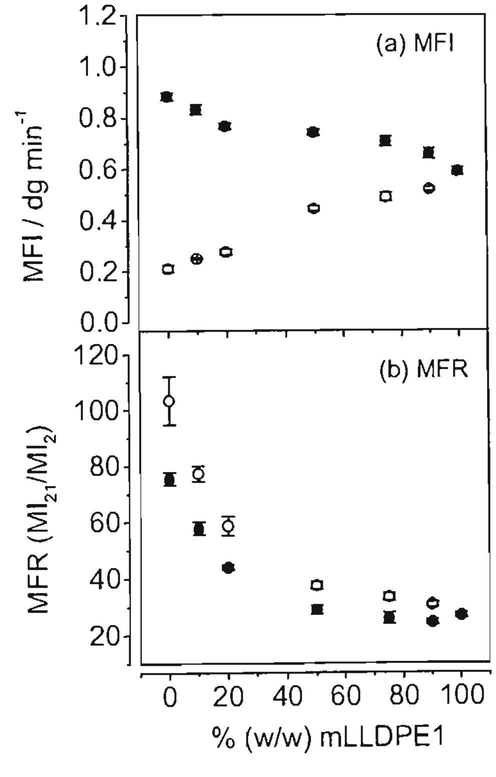

Figure 4.59. Plots of: (a) MFI and (b) MFR versus composition for: (o) LDPE2/mLLDPE1 blends and (•) LDPE3/mLLDPE1 blends.

Mechanical Properties of LDPE2/mLLDPE1 and LDPE3/mLLDPE1 Blends

The yield strength in the TD as a function of composition for the blends of mLLDPE1 with LDPE2 or LDPE3 is shown in Figure 4.60. From this plot it is evident that the yield strength decreases with increasing levels of mLLDPE1 from *ca.* 11 to 7 MPa, and that this decrease is non-linear. In contrast, the yield strength of the film blends of conventional LLDPE with LDPE generally increases with the addition of LLDPE [655], which may be due to the heterogeneous SCB distribution of LLDPE [365]. In the current work, there was no yield strength measurable in the MD of any of the 100% films or, indeed, the blends. This is also reported for some conventional LLDPE/LDPE film blends [228,365,555].

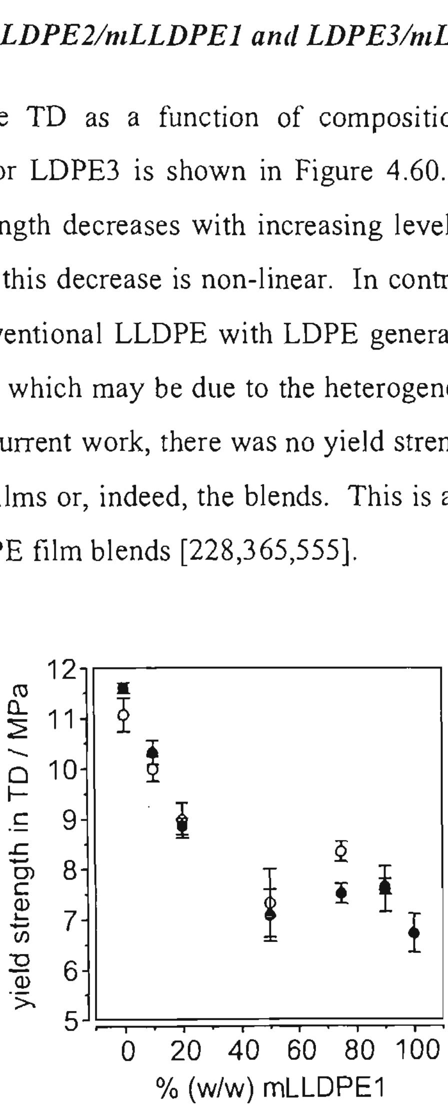

Figure 4.60. Yield strength in the film TD versus composition for:
(o) LDPE2/mLLDPE1 blends and (•) LDPE3/mLLDPE1 blends.

Plots of the break strength versus composition for each blend in the MD and TD of the film are shown in Figure 4.61. In the MD (Figure 4.61(a)), there is no significant variation in the break strength up to and including levels of *ca.* 50% (w/w) mLLDPE1 in either of the film blends. Furthermore, the values of the MD break strength in this range are similar for both of the blends, which may be attributable to a similar extent of alignment of the chains in each blend. For levels above 50% (w/w) mLLDPE1, it is not clear whether this trend continues. However, in the TD (Figure 4.61(b)) the variation in break strength appears to follow an upward trend across the entire composition range. There is also a significant increase (*ca.* 25%) in break strength in the TD after the addition of *ca.* 10% (w/w) mLLDPE1. For film blends of conventional LLDPE with LDPE, the break strength is shown to decrease with increasing levels of LLDPE [374].

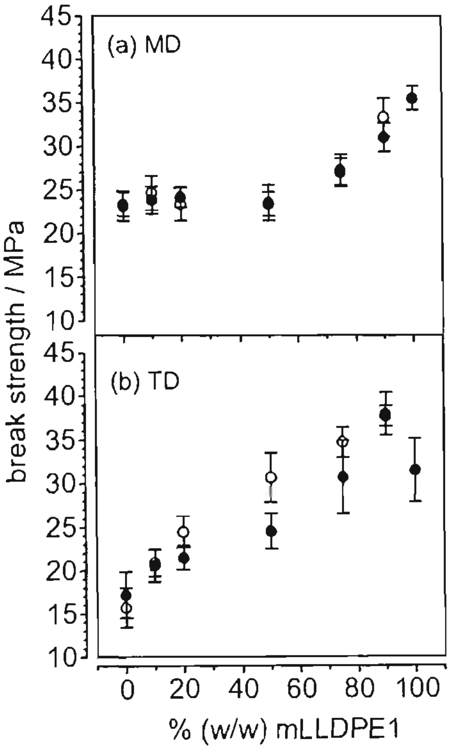

Figure 4.61. Break strength versus composition for: (○) LDPE2/mLLDPE1 blends and (●) LDPE3/mLLDPE1 blends in: (a) MD and (b) TD of the film.

The percent elongation at break versus composition in the film blends is shown in Figure 4.62. In the MD of the film (Figure 4.62(a)), the elongation at break increases with increasing mLLDPE1 in the blend with the most significant increase occurring above levels of *ca.* 20% (w/w) mLLDPE1. In the TD of the film (see Figure 4.62(b)), the elongation values are numerically much greater than those corresponding to the MD and the increase in these values follows an immediate upward trend similarly to the case of the break strength data. In contrast, the elongation values for conventional LDPE/LLDPE blends have been shown to either decrease or increase only slightly with blend composition [374].

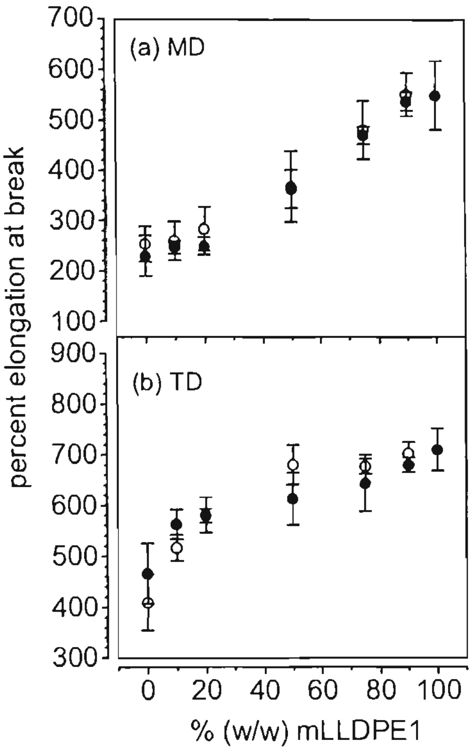

Figure 4.62. Percent elongation at break versus composition for: (o) LDPE2/mLLDPE1 blends and (•) LDPE3/mLLDPE1 blends in: (a) MD and (b) TD of the film.

The dart impact test is a measure of the relative shock resistance of a polymer film sample [374,377,379]. A plot of the dart impact strength versus composition for the film blends is shown in Figure 4.63. The 100% mLLDPE1 film has *ca.* 90% higher dart impact strength than either 100% LDPE2 or 100% LDPE3. The increase in dart impact strength with increased levels of mLLDPE1 is non-linear and there is a significant improvement in this property at levels above *ca.* 10% (w/w) mLLDPE1 [377]. The increase observed beyond this level may be due to the homogeneity of the molecular structure of the mLLDPE1 [377,379]. Studies of conventional LLDPE/LDPE blends [374] do not show as significant an increase in dart impact strength over the range of compositions as that observed in the present work. It is interesting to note that this fast-rate technique is capable of differentiating between the two LDPE materials insofar as there is a significant difference between both of the blends that can be detected at each of the compositions studied. The ability of this technique to differentiate between the two LDPE materials may be explained on the basis that dart impact strength is relatively independent of film orientation [663] and thus this test will reflect molecular structural properties without being influenced by the manner in which the sample has been produced.

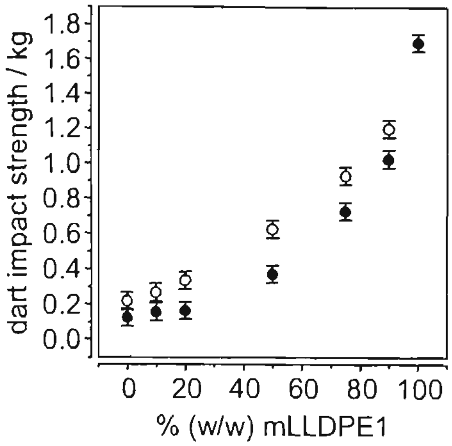

Figure 4.63. Dart impact strength versus composition for: (○) LDPE2/mLLDPE1 blends and (•) LDPE3/mLLDPE1 blends.

A plot of tear resistance versus composition for both blends is shown in Figure 4.64. In the MD (Figure 4.64(a)), the tear resistance of both blends shows a similar upward trend with increasing mLLDPE1 content. In all cases, the tear resistance of the LDPE3 blend in the MD remains greater than that of the LDPE2 blend across the entire composition range which is expected due to higher polydispersity of the LDPE3 [718]. In the TD (Figure 4.64(b)) the scatter in the data makes it difficult to identify any trend. Nonetheless, the observation can be made that the overall tear strength in the TD is greater than the corresponding tear strength in the MD at all compositions. Clearly, this is expected due to orientation effects resulting from the film blowing process [663,679,718]. Furthermore, the superior tear strength of the LDPE3 compared with the LDPE2 is more apparent from the 100% LDPE data obtained from TD experiments (Figure 4.64(a)), than from the MD experiments (Figure 4.64(b)). In contrast, blends of conventional LLDPE with LDPE are reported to show a less than additive decrease in the MD tear resistance with increasing LLDPE content [364,365,374]. The structural differences between conventional LLDPE and mLLDPE are a possible reason for the behaviour observed elsewhere [31,379] and that observed in the current work.

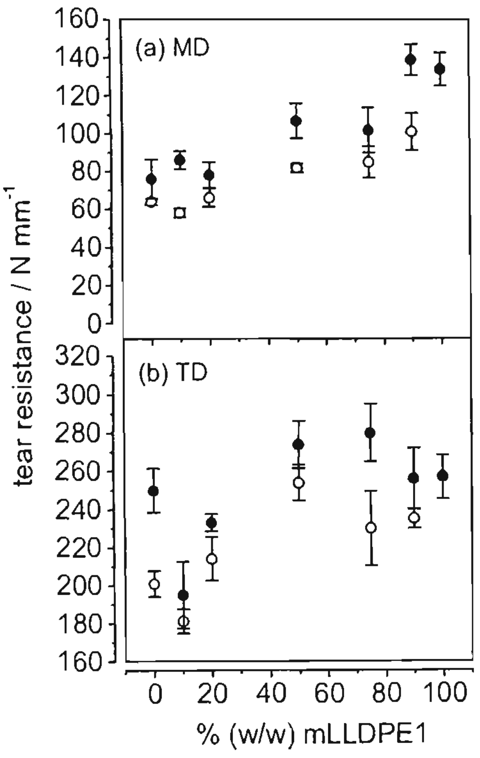

Figure 4.64. Tear resistance versus composition for: (o) LDPE2/ mLLDPE1 blends and (•) LDPE3/mLLDPE1 blends in: (a) MD and (b) TD of the film.

Optical Properties of LDPE2/mLLDPE1 and LDPE3/mLLDPE1 Blends

Figure 4.65 shows plots of the percent haze and the percent gloss versus composition for both of the blends. From this plot it can be seen that the percent haze (Figure 4.65(a)) increases to a maximum of *ca.* 9% at a blend composition of *ca.* 50% (w/w) LDPE2. This cloudiness may be due to melt fracture on the surface of the film that occurs in the blend as a result of some partial miscibility or processing conditions [374,719]. The blends of mLLDPE1 with LDPE3 have overall less haze than the blends involving LDPE2, and have a maximum of *ca.* 6% haze. The blend containing LDPE3 shows a dramatic decrease in percent haze to *ca.* 3% at levels of mLLDPE1 greater than *ca.* 30% (w/w) whereas the blend containing LDPE2 persists at a high level of haze beyond that composition.

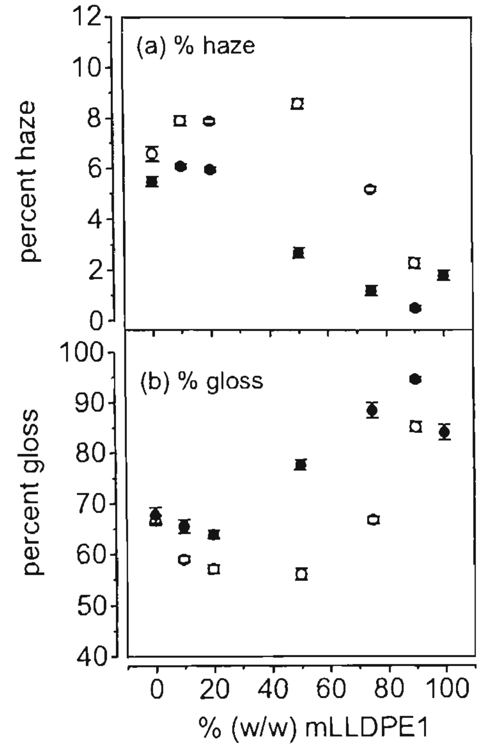

Figure 4.65. Plots of: (a) percent haze and (b) percent gloss versus composition for: (○) LDPE2/mLLDPE1 blends and (●) LDPE3/ mLLDPE1 blends.

The behaviour of the blend containing LDPE3 is comparable to that exhibited in blends of conventional LLDPE with LDPE which show a significant reduction in haze [374] and improved film clarity [364] with increased levels of LLDPE. The 100% mLLDPE1 film exhibits the lowest haze and this reflects a characteristic property of mPE films resulting from their low crystallinity [377,379]. The plots of the percent gloss data (Figure 4.65(b)) complement those data obtained for the percent haze insofar as blends that possess a high percent haze have a correspondingly low percent gloss and the optimal blend composition appears close to 30% (w/w) mLLDPE1 as previously indicated. The 100% mLLDPE1 film has a gloss of *ca.* 95% that indicates its superior optical properties [377,379].

Theoretical Manipulation of Data – "Radar" Plots

The physicomechanical and optical data can be most conveniently handled simultaneously by means of a *radar* plot. These parameters are plotted on a percentage scale on separate radial axes that issue outwards from an origin and the axes are equiangular with respect to each other. In the current work the radials on each *radar* plot are calibrated in 20% increments with zero being at the centre of the plot and 100% at the outermost limit. Standardization of each quantity appearing on the plot was achieved by, firstly, identifying the maximum value of that quantity that was observed over all experiments, and secondly, expressing the corresponding datum as a percentage of that value. The haze data are represented on the *radar* plots as the difference between the maximum percent haze value and the particular percent haze value, in order to provide a quantity whose value increases as the haze decreases. Thus, an improvement in the overall properties of a material will be indicated on the *radar* plot by dilation of the resultant polygon towards the outer extremities of the plot and a concomitant increase of the area of the polygon. The total area of a polygon on a *radar* plot is the sum of the areas of its triangular segments.

The area, A_i, of the i^{th} triangular segment defined by the ordinate (r_i, r_{i+1}, 0) on a *radar* plot having n such segments is given by equation (4.2):

$$A_i = \sum_{i}^{n-1} \tfrac{1}{2} r_i r_{i+1} \sin(2\pi/n) \qquad (4.2)$$

Since $r_n = r_1$, then the total area, A_T of the polygon is given by:

$$A_T = A_n + \sum_{i=1}^{n-1} A_i$$

$$= \tfrac{1}{2} r_{n-1} r_1 \sin(2\pi/n) + \sum_{i=1}^{n-1} \tfrac{1}{2} r_i r_{i+1} \sin(2\pi/n) \qquad (4.3)$$

The MFR parameter is derived from MFI thus reflecting blend processability [17,58,372], was not included on the *radar* plots. This parameter can be plotted as a function of the blend composition and superimposed on a graph of the *radar* plot area versus composition in order to identify an optimal blend composition. Such a blend would presumably have optimal physicomechanical and optical properties along with optimal processability.

Figure 4.66 and Figure 4.67 show *radar* plots for the LDPE2/mLLDPE1 and LDPE3/mLLDPE1 systems at 10% and 20% (w/w) mLLDPE1 respectively. The plots reveal that these systems have in general good haze, gloss, TD yield, and tear strength, but have relatively low dart impact strengths. The latter arises as a result of the normalization process used to obtain the dart impact data where the maximum dart impact observed corresponds to 100% mLLDPE1. At blend compositions in the range appropriate for, say, possible commercial films the level of mLLDPE1 would be much lower than this. Thus an arbitrary value of the maximum dart impact would be considerably lower and so the percent dart impact strengths would be correspondingly higher. In any case, the arbitrary nature of the choice in will not affect the overall comparisons between the blends so long as this value remains constant within the analyses.

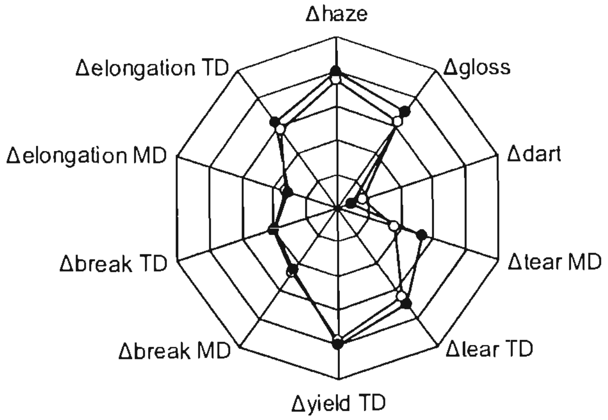

Figure 4.66. *Radar* plots of blends containing 10% (w/w) mLLD-PE1 with: (o) LDPE2 and (•) LDPE3.

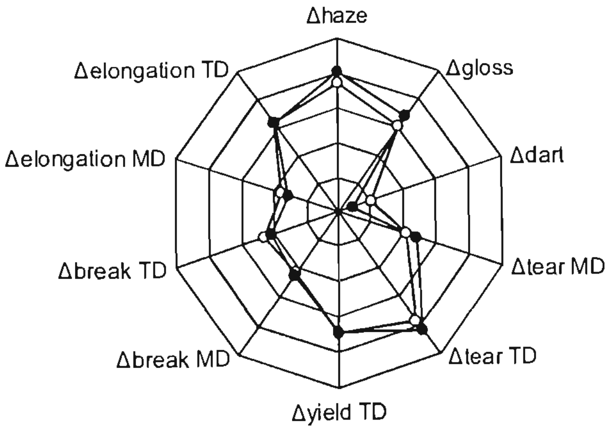

Figure 4.67. *Radar* plots of blends containing 20% (w/w) mLLD-PE1 with: (o) LDPE2 and (•) LDPE3.

The differences between the LDPE2 and LDPE3 constituents are relatively small across most properties represented on the *radar* plot at 10% (w/w) mLLDPE1 (see Figure 4.66). On the other hand, more noticeable differences between these two materials can be seen at the higher level of 20% (w/w) mLLDPE1 (see Figure 4.67). On the basis of the *radar* plot areas associated with these figures, it can be shown that blends containing the LDPE3 material have overall superior properties than those containing the LDPE2. However, it should be noted that with regard to dart impact strength (i.e. the high-rate deformation test) the *radar* plots reveal the blends containing LDPE2 are superior compared to those containing LDPE3. As expected, this observation supports the data previously presented in Figure 4.63 where LDPE2 is consistently superior to LDPE3 in this regard.

Blend Optimization

The normalized areas associated with the *radar* plots for all blend compositions studied have been calculated and are presented in Figure 4.68(a) and Figure 4.68(b) for the LDPE2/mLLDPE1 and LDPE3/mLLDPE1 systems respectively. As expected, the normalized area increases with increasing mLLDPE1 content in each of the blends. The normalized MFR values for each of the blends have been superimposed on these plots and, as expected, the values decrease with increasing mLLDPE1 content in the blend (see Figure 4.68(b)). Since a relative decrease in the normalized MFR parameter reflects a reduction in processability [17,58,372] and an increase in the normalized *radar* area indicates an improvement in the overall film properties, then the point at which these two plots intersect will be indicative of a blend with optimal physicomechanical and optical properties as well as optimal processability. For blends of mLLDPE1 with LDPE2 (see Figure 4.68(a)), the optimal blend composition is *ca.* 30% (w/w) mLLDPE1 whereas for blends of mLLDPE1 with LDPE3 (see Figure 4.68(b)), the optimal blend composition is *ca.* 20% (w/w) mLLDPE1.

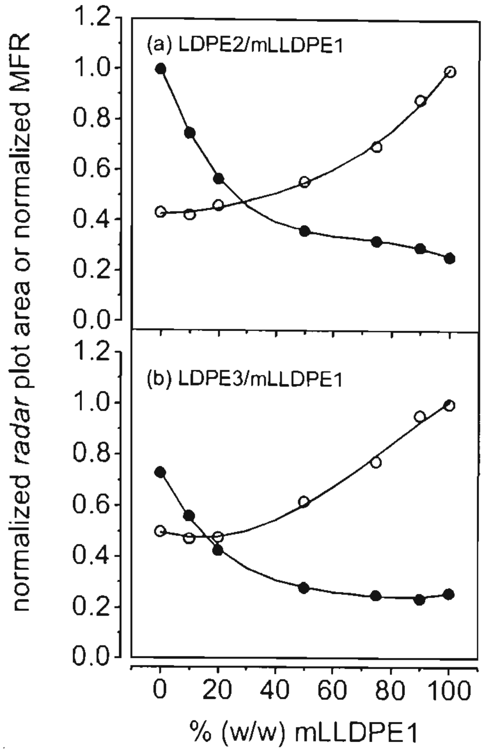

Figure 4.68. Plots of: (o) normalized *radar* plot area and (•) normalized MFR versus composition for: (a) LDPE2/mLLDPE1 blends and (b) LDPE3/mLLDPE1 blends.

4.4.5 Effect of Downgauging on the Properties of LDPE Film Blends

In view of the potential benefits that may be gained from downgauging film blends, this section examines certain binary blends of LDPE with mLLDPE or LLDPE in order to identify any blends that have optimal and desirable characteristics at constant gauge length. Based on these findings, an optimal composition range is sought at various gauge lengths in order to assess the effects of downgauging.

Physical Properties of LDPE2/LLDPE6 and LDPE2/mLLDPE2 Blends

Figure 4.69 shows that the density of each blend was confirmed to be additive with respect to the blend composition with the density of pure mLLDPE2 being slightly lower than the conventional LLDPE6 resin even though these materials were produced with the same comonomer. Such behaviour is characteristic of mLLDPE2 resins [31,378,379].

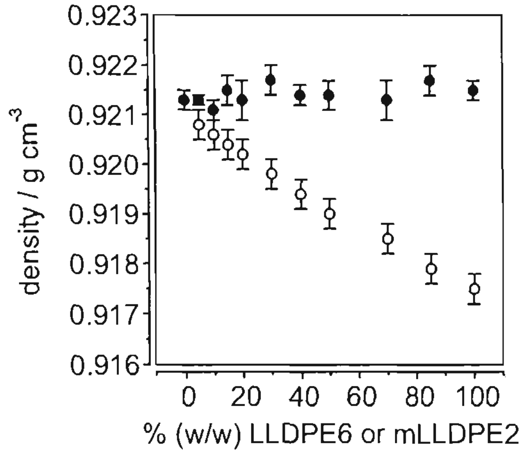

Figure 4.69. Density versus composition for: (•) LDPE2/LLDPE6 blends and (o) LDPE2/mLLDPE2 blends.

A plot of MFI versus composition for LDPE2/mLLDPE2 and LDPE2/LLDPE6 blends is shown in Figure 4.70(a) with a corresponding plot of MFR versus composition for each of these blends shown in Figure 4.70(b). The MFI for each of the LDPE2/mLLDPE2 and LDPE2/LLDPE6 blends increases over the composition range whereas the MFR decreases over the same composition range. This reflects the difference in the molecular weights of each of the resins and is consistent with there being a reduction in the polydispersity of the blend with increasing amount of mLLDPE2 or LLDPE6. It is also evident that the MFR for each of the blends is less than additive and that the MFR of pure mLLDPE2 or pure LLDPE6 is significantly lower than that of pure LDPE2.

Mechanical Properties of LDPE2/LLDPE6 and LDPE2/mLLDPE2 Blends

With the exception of the 100% mLLDPE2 and LLDPE6 films, there was no measurable yield strength found in the MD of the film blends. The yield strengths in the MD of the 100% mLLDPE2 and LLDPE6 film samples were found to be 11.13 MPa and 12.53 MPa respectively. Conversely, the yield strength in the TD for all of the blends was measurable and this quantity for the blends of mLLDPE2 or LLDPE6 with LDPE2 is plotted as a function of composition in Figure 4.71. From this plot it is evident that the yield strength decreases with increasing levels of mLLDPE2 whereas the yield strength of the film blends of LLDPE6 with LDPE2 increases with the addition of LLDPE6 [655]. The latter observation may be due to the heterogeneous SCB distribution of LLDPE6 [365] and has also been shown to be the case for other conventional LLDPE/LDPE film blends [228,555].

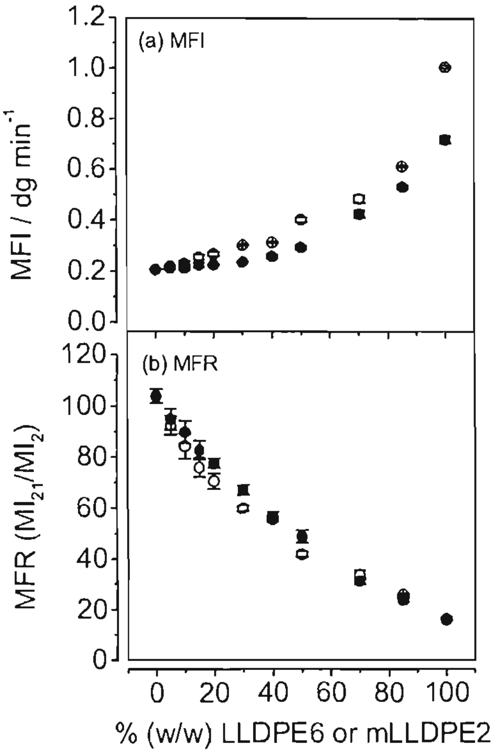

Figure 4.70. Plots of: (a) MFI and (b) MFR versus composition for: (•) LDPE2/LLDPE6 blends and (o) LDPE2/mLLDPE2 blends.

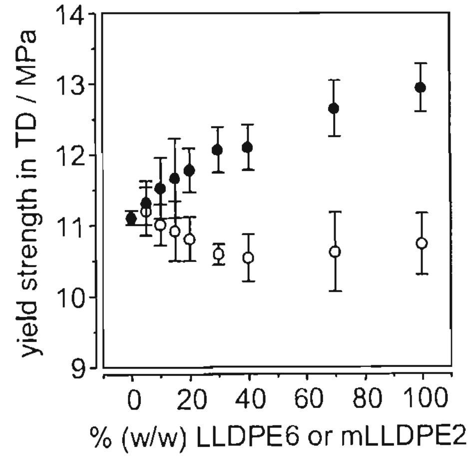

Figure 4.71. Yield strength in the film TD versus composition for: (•) LDPE2/LLDPE6 blends and (o) LDPE2/mLLDPE2 blends.

Plots of the break strength versus composition for each blend in the MD and TD of the film are shown in Figure 4.72. In the MD of the film (Figure 4.72(a)), there is no significant variation in the break strength up to and including levels of *ca.* 40% (w/w) mLLDPE2 or LLDPE6 in either of the film blends. Furthermore, the values of the MD break strength in this range are similar for both of the blends, which may be attributable to a similar extent of alignment of the chains in each blend [661,720]. For levels above 50% (w/w) mLLDPE2 or LLDPE6 the break strength continues an upward trend with the ultimate break strength of 100% mLLDPE2 being *ca.* 22% greater than that of 100% LLDPE. In the TD of the film (Figure 4.72(b)), the variation in break strength appears to follow an upward trend across the entire composition range for each of the blends. Furthermore, there is only slight variation in the break strength values in the MD compared to the TD which suggests that that the molecular orientation is similar in each direction [661,721]. The percent elongation at break versus composition in the film blends is shown in Figure 4.73. The elongation at break increases with increasing mLLDPE2 or LLDPE6 in the blend in both the MD and TD of the film. In each case, the elongation values for 100% LLDPE6 are greater than those for the 100% mLLDPE2 reflecting the more heterogeneous nature of LLDPE6 [19,211,233,248,249].

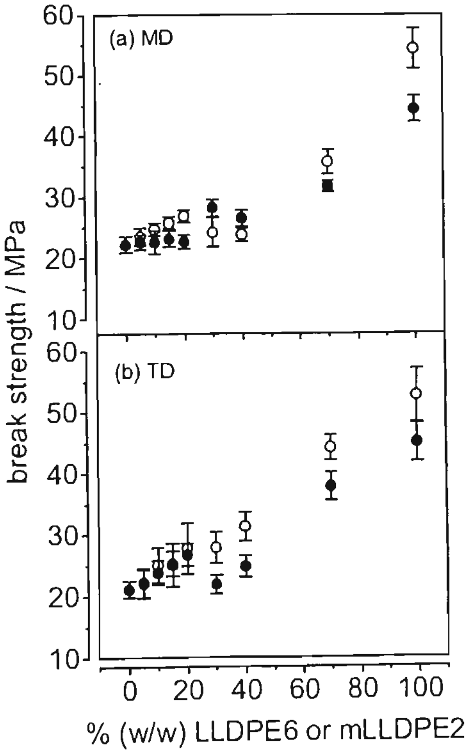

Figure 4.72. Break strength versus composition for: (•) LDPE2/LLDPE6 blends and (o) LDPE2/mLLDPE2 blends in: (a) MD and (b) TD of the film.

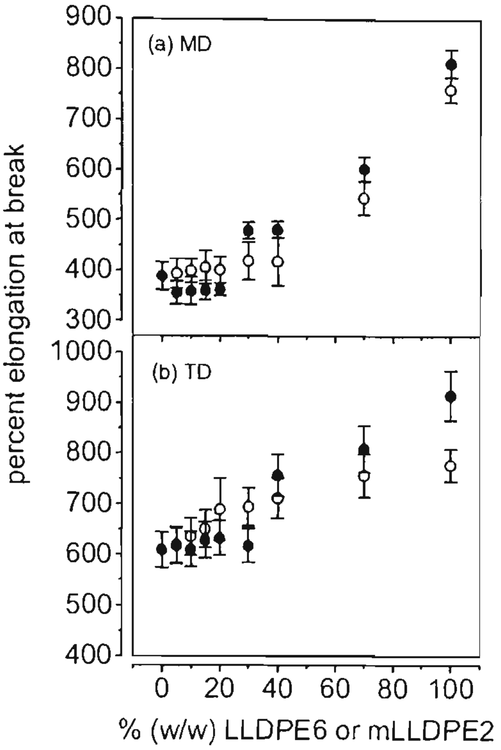

Figure 4.73. Percent elongation at break versus composition for: (•) LDPE2/LLDPE6 blends and (○) LDPE2/mLLDPE2 blends in: (a) MD and (b) TD of the film.

A plot of the dart impact strength versus composition for the film blends is shown in Figure 4.74. The 100% mLLDPE2 film has much higher (more than 200%) dart impact strength than either 100% LDPE2 or 100% LLDPE6. The superior dart impact strength of the mLLDPE2 may be due to the homogeneity of its molecular structure [377,379]. The dart impact strength is a typical example of a physico-mechanical parameter that is expected to exhibit linear variation with blend composition in idealized systems [59,431,583,722]. The observed linearity of dart impact strength with composition supports the notion of blend compatibility suggested previously by the DSC data and the CL data (see Figure 4.23 and Figure 4.24 respectively). Indeed, such behaviour is observed in both of the LDPE2/mLLDPE2 and LDPE2/LLDPE6 blend systems where the dart impact strength of each system increases approximately linearly with increasing levels of LLDPE6 or mLLDPE2. Blends of conventional LLDPE with LDPE [374] generally exhibit lower dart impact strengths than blends with mLLDPE resins and this behaviour is also reflected in the results of the present study where the dart impact strengths of the LLDPE6 and LDPE2 resins are significantly lower than that of the mLLDPE2.

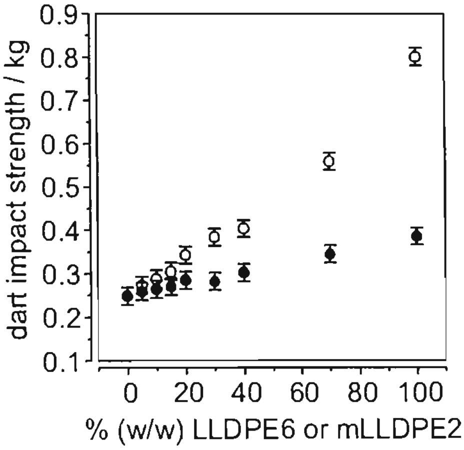

Figure 4.74. Dart impact strength versus composition for: (•) LDPE2/LLDPE6 blends and (o) LDPE2/mLLDPE2 blends.

A plot of tear resistance versus composition for each of the blends is shown in Figure 4.75. Up to and including a blend composition of 40% (w/w) mLLDPE2 or LLDPE6, the MD tear resistance (Figure 4.75(a)), remains relatively constant across the composition range. Above these levels, however, the tear resistance of both blends increases noticeably. In the TD (Figure 4.75(b)) the tear resistance increases approximately linearly up to and including a blend composition of 70% (w/w) mLLDPE2 or LLDPE6. Interestingly, the tear resistance of the 100% mLLDPE2 or LLDPE6 film is slightly lower than that of the blend containing 70% (w/w) which may be due to orientation effects resulting from the film blowing process [663,718].

Optical Properties of LDPE2/LLDPE6 and LDPE2/mLLDPE2 Blends

Figure 4.76 shows plots of the percent haze and the percent gloss versus composition for both of the blends. From this plot it can be seen that the percent haze (Figure 4.76(a)) of blends containing mLLDPE2 is slightly lower than that of blends containing LLDPE6, particularly at a level of 40% (w/w) mLLDPE2. Similarly, the percent gloss of the film (Figure 4.76(b)) increases with increasing levels of mLLDPE2 or LLDPE6 with a maximum at *ca.* 40% (w/w) mLLDPE2. At levels of mLLDPE2 above this maximum there is a noticeable increase in the haze and a corresponding decrease in the gloss. The decline in optical properties that is observed at levels of mLLDPE2 above 40% (w/w) may be due to melt fracture that occurs in the blend during processing conditions that subsequently results in surface imperfections or roughness [723-727].

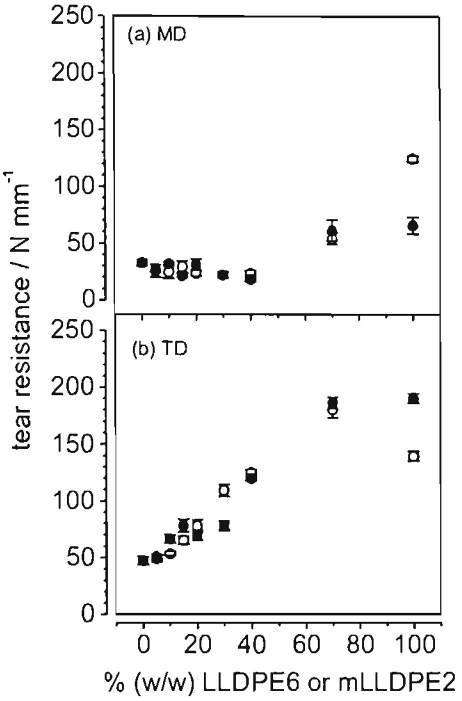

Figure 4.75. Tear resistance versus composition for: (•) LDPE2/ LLDPE6 blends and (o) LDPE2/mLLDPE2 blends in: (a) MD and (b) TD of the film.

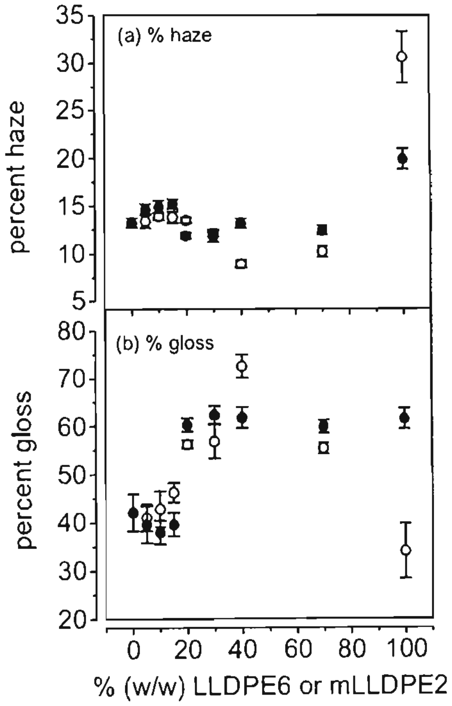

Figure 4.76. Plots of: (a) percent haze and (b) percent gloss versus composition for: (•) LDPE2/LLDPE6 blends and (o) LDPE2/ mLLDPE2 blends.

Optimizing Blend Composition

The normalized areas associated with the *radar* plots for all blend compositions have been calculated and are shown in Figure 4.77(a) and Figure 4.77(b) for the LDPE2/mLLDPE2 and LDPE2/LLDPE6 systems respectively. As expected, the normalized area increases with increasing mLLDPE2 or LLDPE6 content in each of the blends. The normalized MFR values for each of the blends have been superimposed on these plots and, as expected, the values decrease with increasing mLLDPE2 or LLDPE6 content in the blend (see Figure 4.77(b)). The point at which the normalized area sum and normalized MFR intersect will be indicative of a blend with optimal physicomechanical and optical properties as well as optimal processability. For LDPE2/mLLDPE2 blends (see Figure 4.77(a)), the optimal blend composition is *ca.* 35% (w/w) mLLDPE2 whereas for LDPE2/LLDPE6 blends (see Figure 4.77(b)), the optimal blend composition is *ca.* 40% (w/w) LLDPE6. These blend compositions are consistent with other studies where the optimum levels of mLLDPE or LLDPE in a blend with LDPE in the range of 25% to 50% (w/w) are suggested [226,700,702,708].

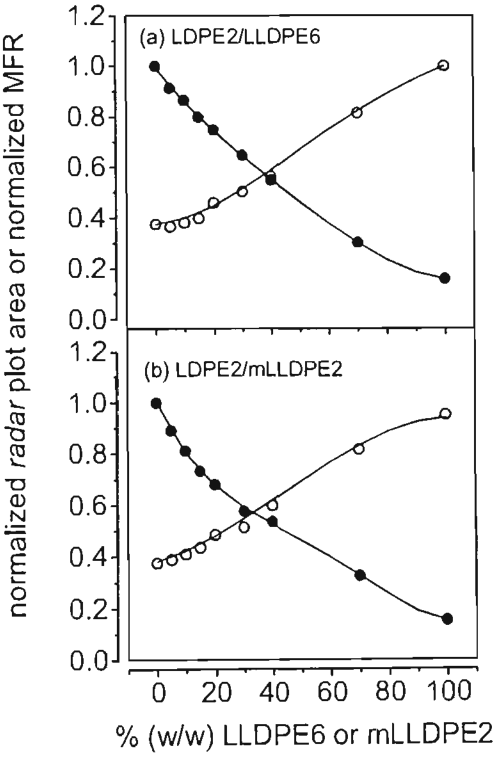

Figure 4.77. Plots of: (o) normalized *radar* plot area and (•) normalized MFR versus composition for: (a) LDPE2/LLDPE6 blends and (b) LDPE2/mLLDPE2 blends.

Downgauging the Film Thickness

The physicomechanical and optical data of the blends containing 20%, 30% or 40% (w/w) mLLDPE or LLDPE at the different gauge lengths were also standardized in order to prepare *radar* plots and calculate the area sums associated with these plots. A blend with a relatively high area sum therefore is deemed to have overall better physicomechanical and optical data than a blend with a relatively low area sum. In the context of the current work, the change in the *radar* plot area ($\Delta A = A_{mLLDPE2}-A_{LLDPE6}$) indicates the overall superiority of an LDPE2/mLLDPE2 film blend over a comparable one that is comprised of LDPE2/LLDPE6. In particular, a large value of ΔA indicates superior overall physicomechanical properties of a given LDPE2/mLLDPE2 blend compared with an LDPE2/LLDPE6 blend.

Figure 4.78 shows plots of ΔA versus composition at constant gauge length for the blends studied in this work. A slight, but general upward trend in ΔA is observed in Figure 4.78(a) and Figure 4.78(b) which suggests that as the composition increases, the superiority of mLLDPE2 over LLDPE6 as a blend constituent in general becomes greater at a given composition. Nonetheless, an interesting observation is that the superiority of mLLDPE2 at a gauge length of 60 μm and 40% (w/w) is far greater than under any other condition (see Figure 4.78(c)). The behaviour illustrated in Figure 4.78 is also reflected in Figure 4.79 where the data are replotted in such a way as to keep the composition constant in order to examine the effect of gauge length. The superiority of mLLDPE2 over LLDPE6 generally increases with increasing gauge length with particular exception of the 40% (w/w) LDPE2/mLLDPE2 blend that exhibits a significant superiority at a small gauge length of 60 μm (see Figure 4.79(a)) and the value of ΔA dramatically decreases when the gauge length is increased. This may be attributed largely to a marked increase in the optical properties imparted by the mLLDPE2 that becomes more pronounced at smaller gauge lengths. Furthermore, the superior optical properties of the 40% (w/w) mLLDPE2 blend are also apparent in the data shown in Figure 4.76.

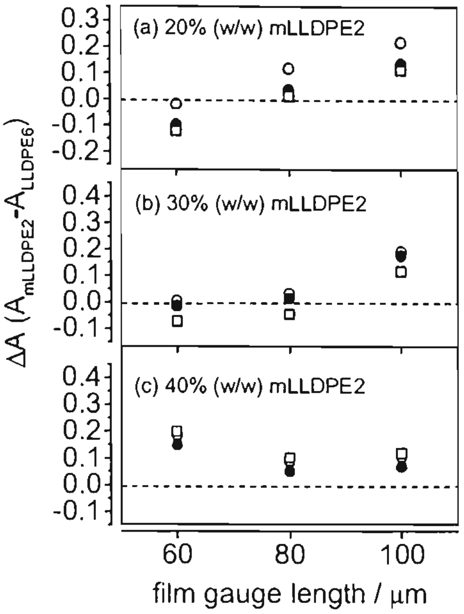

Figure 4.78. Change in *radar* area ($A_{mLLDPE2}$-A_{LLDPE6}) versus LDPE2/mLLDPE2 film gauge length for: (a) 20%, (b) 30%, and (c) 40% (w/w) mLLDPE2 where: (○) 60 μm, (●) 80 μm, and (□) 100 μm LDPE2/LLDPE6 film gauges.

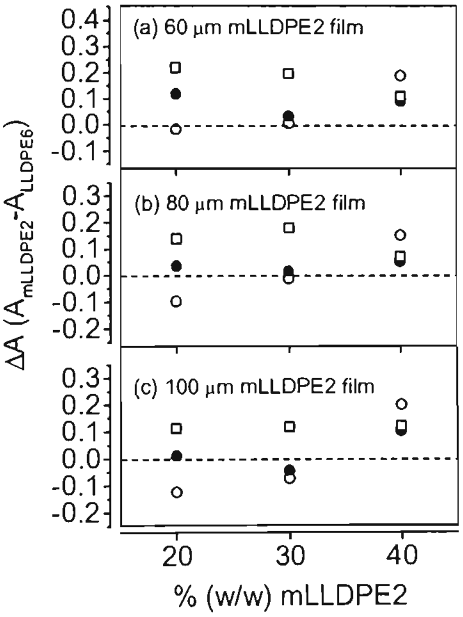

Figure 4.79. Change in *radar* area ($A_{mLLDPE2}$-A_{LLDPE6}) versus composition of mLLDPE2 in the blend for: (a) 60 μm, (b) 80 μm and (c) 100 μm LDPE2/mLLDPE2 film where: (○) 20%, (●) 30% and (□) 40% (w/w) mLLDPE2.

To illustrate further the effects of downgauging, selected *radar* plots are shown in Figure 4.80 through Figure 4.82 which compares a given mLLDPE2 with an LLDPE6 film formulation. In Figure 4.80, the *radar* plots of 60 μm film containing 40% (w/w) mLLDPE2 and 80 μm film containing 20% (w/w) LLDPE6 suggests that a higher level of mLLDPE2 at a lower gauge length increases the overall properties. Figure 4.81 shows the *radar* plots of 80 μm film containing 20% (w/w) mLLDPE2 and 100 μm film containing 20% (w/w) LLDPE6. In this example, the same blend composition with a thinner mLLDPE2 film results in similar overall properties. Figure 4.82 compares the *radar* plots of 60 μm film containing 40% (w/w) mLLDPE2 and 100 μm film containing 40% (w/w) LLDPE. These data suggest that at the same blend composition, a thinner mLLDPE2 film has better overall properties.

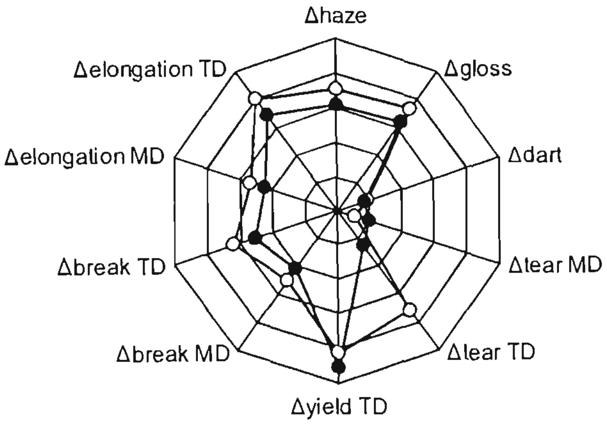

Figure 4.80. *Radar* plots of: (○) 60 μm film containing 40% (w/w) mLLDPE2 and (●) 80 μm film containing 20% (w/w) LLDPE6.

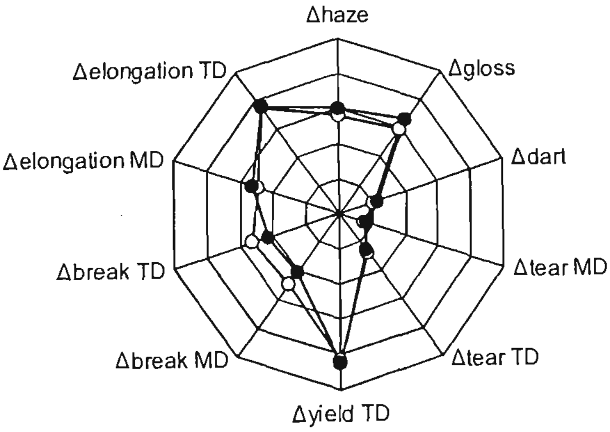

Figure 4.81. *Radar* plots of: (○) 80 μm film containing 20% (w/w) mLLDPE2 and (●) 100 μm film containing 20% (w/w) LLDPE6.

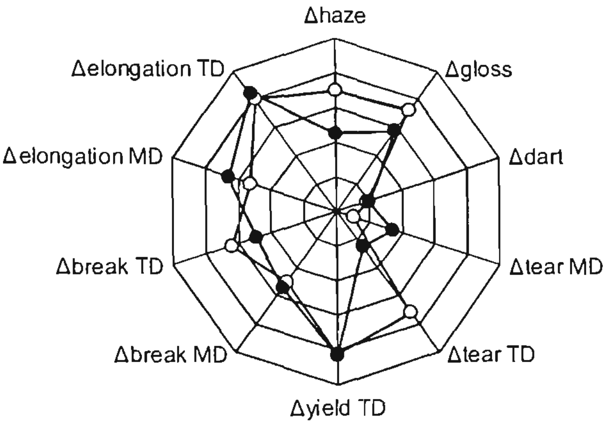

Figure 4.82. *Radar* plots of (○) 60 μm film containing 40% (w/w) mLLDPE2 and (●) 100 μm film containing 40% (w/w) LLDPE6.

Potential Materials and Cost Savings Resulting from Downgauging

In addition to the possible improvements in physicomechanical properties that can be achieved through the use of mPEs in polymer blends, the advantages of the latter also extends to potential weight reductions and the associated cost reductions in such formulations.

The mass of 1 m^2 sections of film based on a common component can be readily calculated using the following mass balance equations:

$$m_a = \rho_1 G_a \chi_1 + \rho_3 G_a (1 - \chi_1) \qquad (4.4)$$

$$m_b = \rho_2 G_b \chi_2 + \rho_3 G_b (1 - \chi_2) \qquad (4.5)$$

where m_a and m_b are the masses of 1 m^2 section of film formulations *a* and *b* respectively, ρ_1, ρ_2, and ρ_3 are the densities of components 1 (mLLDPE2), 2 (LLDPE6), and 3 (LDPE2) respectively, G_a and G_b are the gauge lengths of the film formulations *a* and *b* respectively, and χ_1 and χ_2 are the mass fractions of components 1 and 2 respectively.

The mass difference between formulations *b* and *a* is given by:

$$\Delta m = m_b - m_u \quad (4.6)$$

$$= \rho_2 G_b \chi_2 + \rho_3 G_b (1-\chi_2) - \rho_1 G_u \chi_1 - \rho_3 G_u (1-\chi_1) \quad (4.7)$$

Similar equations can be derived to calculate the cost difference [728]:

$$\Delta C = C_b - C_u \quad (4.8)$$

$$= \rho_2 G_b \chi_2 c_2 + \rho_3 G_b (1-\chi_2) c_3 - \rho_1 G_u \chi_1 c_1 - \rho_3 G_u (1-\chi_1) c_3 \quad (4.9)$$

where C_a and C_b are the costs of 1 m^2 of film formulations *a* and *b* respectively and c_1, c_2, and c_3 are the cost per unit mass of components 1 (mLLDPE2), 2 (LLDPE6), and 3 (LDPE2) respectively.

Some selected examples of calculated mass and cost differences (based on current costs of resins) for various compositions at different gauge lengths are given in Table 4.3. This table serves to illustrate that in many cases the incorporation of mLLDPE2 in a PE blend can achieve savings in material costs whilst simultaneously imparting superior physicomechanical properties at reduced gauge length.

Table 4.3. Selected mass difference and cost difference calculations.

LLDPE6 blend details		**mLLDPE2 blend details**				
%LLDPE6,	**film gauge**	**%mLLDPE2,**	**film gauge**	**ΔA**	**Δm/%**	**ΔC/%**
20%,	80 μm	40%,	60 μm	0.306	25.1	23.6
40%,	100 μm	40%,	60 μm	0.200	40.1	39.0
40%,	100 μm	20%,	100 μm	0.032	0.1	-0.6
20%,	100 μm	20%,	80 μm	0.012	20.1	19.4
30%,	60 μm	20%,	60 μm	-0.146	0.1	-0.7

Note: The mass and cost differences are expressed as a percentage of the respective savings based on a blend containing LLDPE6. A more detailed list of mass difference and cost difference calculations is presented in Appendix 4. Blend compositions are (w/w).

Chapter 5 Conclusions, Recommendations, Future Work

5.1 Conclusions

Several systems of polyethylene blends were prepared where one component was a conventional PE and the second component was a conventional LLDPE or an mLLDPE. New techniques of blend characterization based on traditional DSC analysis and FT-IR spectroscopy, and a relatively new method based on CL were successfully developed and used to investigate the blends. The physicomechanical and optical properties of some of the blends were investigated and the results were used to optimize the composition of some of the film blends and assess the effects of downgauging the film thickness.

Five systems of LDPE/LLDPE blends where the LLDPE component contains C4, C6 or C8 comonomer were prepared and characterized by DSC. A modified form of multi-step isothermal annealing, the TSIA procedure, was developed and investigated in order to characterize the blends. The TSIA procedure appears to segregate effectively the LDPE component from the LLDPE component in all blends studied regardless of the comonomer type with the LLDPE component possessing a higher peak melting temperature after the TSIA treatment presumably due to a decrease in branch density. Furthermore, the TSIA procedure results in the segregation of two or more phases of LLDPE of varying branch density. It has also been shown that the segregation method provides sufficient resolution to suggest that it may form a useful part of a quantitative analytical technique for the characterization of LDPE/LLDPE blends. In particular, this method should have general applicability to blends containing low concentrations of the minor component (e.g. 5% to 10% (w/w)) admixed polymer where conventional treatment prior to DSC analysis produces thermograms that lack resolution.

Four systems of PE blends where one component is a conventional LDPE or HDPE and the second component is a conventional LLDPE or an mLLDPE were prepared and investigated by FT-IR spectroscopy. An equation based on the ratio of two absorbance peaks in an FT-IR spectrum was derived and has been successfully applied to the quantitative analysis of the PE blends. The associated analytical method relies on both the inherent differences and similarities of the PE components in the blend to obtain a suitable absorbance ratio for use in the equation. In selecting optimal peaks for the application of this method to PE blends, it has been confirmed that one of the peaks must be distinct to one of the components whereas the other peak should be common to both components. If one of the components is a copolymer (such as LLDPE or mLLDPE), the peak relating to the SCB is deemed suitable for use as a peak that is distinct to that component. A number of peaks have been found to be suitable for selection as the common peak but care should be exercised in the choice of that peak in order to optimize the linearity of the equation. Under certain circumstances peaks that are not spectrally distinct can be used successfully in the application of the method. It is envisaged that the devised method has particular merit in the routine analysis of PE blends provided that the absorption properties have been previously calibrated.

The technique of chemiluminescence monitoring was successfully applied to four systems of PE blends where one component is a conventional LDPE or HDPE and the second component is a conventional LLDPE or an mLLDPE. The CL data obtained for the blends was found to be consistent with the thermal and physicomechanical properties of the blends and the CL technique has the potential to produce information on important aspects of blends such as blend miscibility. Decreased blend miscibility is reflected in the CL data as a departure from the idealized behaviour that is observed in the case of more miscible blends. Furthermore, in the case of non-ideal systems that exhibit immiscibility between the components, it appears that the immiscibility in the solid state is reflected to some extent in the behaviour of the melt. The preliminary experiments conducted to determine the level of consistency of CL results with regard to both variability between instruments and variability between techniques, indicate a high degree of correlation exists in each case. However, differences in temperature calibration between CL apparatus can result in an offset in the derived OIt values.

Following the successful development of characterization techniques, the various blends that were studied were subjected to physicomechanical and optical property testing. For blends involving HDPE, significant improvements in the Izod impact strength were achieved even by blending with small amounts of mLLDPE. The tensile properties of the HDPE/mLLDPE blends were consistent with those of HDPE with conventional LLDPE with considerable increases in percent elongation observed for the blends. The variation in tensile properties of blends of low MW LDPE with mLLDPE is similar to that of the HDPE/mLLDPE blends with significant improvements in percent elongation observed. The instrumented impact test results measured at room temperature and at -20°C for the LDPE/mLLDPE blends showed little variation in energy-to-peak, energy-to-break and ratio of energies with increasing levels of mLLDPE. The ductility of the blends, however, increases with increasing levels of mLLDPE and the relative ductility is greater at -20°C than at room temperature for each of the blends.

For film blends of mLLDPE with conventional LLDPE, the yield strength decreases and the break strength increases with increasing levels of mLLDPE in the blend. Unlike the previous blends of HDPE or LDPE with mLLDPE, the percent elongation at break decreases with increasing levels of mLLDPE in the LLDPE/mLLDPE blends. The dart impact strength is shown to increase significantly with increasing levels of mLLDPE in the blend. The tear resistance shows little variation with increasing levels of mLLDPE although the tear resistance in the TD is consistently greater than that in the MD at the same composition. The optical properties of the film suggest that the addition of mLLDPE to LLDPE generally has little effect on the overall clarity of the film blends. An alternative interpretation of the data, however, suggests the addition of a small amount of LLDPE to mLLDPE noticeably improves the optical properties of the latter.

In order to assess the effects of blending mLLDPE on the properties of LDPE, two systems of LDPE/mLLDPE film blends were prepared and the physicomechanical and optical properties were systematically and successfully studied. The melt flow properties of these blends were also studied in order to assess the ease at which the blends can be processed. It was found that the addition of mLLDPE to LDPE improves most of the properties under consideration in this work and that the LDPE material having a higher polydispersity produces blends that have generally superior properties. A novel adaptation of conventional *radar* plots, involving the calculation of the area enclosed by the polygon on such a plot, enables one to identify a level at which mLLDPE can be incorporated in LDPE to produce optimal overall properties. In the case of the LDPE materials studied, a level of mLLDPE of between 20% and 30% (w/w) appears to be that required to achieve optimization.

The potential to downgauge LDPE/mLLDPE film blends while maintaining or improving physicomechanical and optical properties compared with analogous LDPE/LLDPE blends was investigated. At constant gauge length, the optimal blend compositions for LDPE/mLLDPE blends and LDPE/LLDPE blends were found to be *ca.* 35% (w/w) mLLDPE and *ca.* 40% (w/w) LLDPE respectively. When the gauge length is varied, the physicomechanical and optical properties of a given blend generally improve with increasing levels of mLLDPE or with increasing film thickness. Of the complete matrix of gauge lengths studied in the current work, more that 68% of LDPE/mLLDPE blends had better overall properties than the LDPE/LLDPE blend formulations with most of the LDPE/mLLDPE blends containing 30% or 40% (w/w) mLLDPE. The best results for downgauging were achieved at higher levels of mLLDPE with no LLDPE formulation out-performing any blend containing 40% (w/w) mLLDPE at any gauge length. Downgauging a film containing 40% (w/w) mLLDPE to a film thickness of 60 μm can achieve significantly better properties than a similar blend containing 40% (w/w) LLDPE at 100 μm film thickness. If such a formulation containing mLLDPE were to be used in place of a formulation containing LLDPE, the potential materials or cost savings are estimated to be *ca.* 40% and the resultant film would have similar properties.

5.2 Recommendations

A systematic approach is required in order to develop polyolefin blends that have desirable physicomechanical and optical properties and that are commercially viable. The development or implementation of suitable blend characterization techniques is often an appropriate first step as it enables the analysis of structural compatibility. The use of compatibilizers can be investigated if necessary but providing the blend is structurally acceptable, the blend can be further assessed by a suitable suite of physicomechanical or optical tests over an appropriate range of compositions. The tests should encompass the assessment of the properties that would be considered important for the end-use of the resulting polymer blend. For example, if a blend is required for a high impact resistant film packaging application, the tests should include those that measure impact resistance such as free-falling dart impact testing.

Following the collection of the physicomechanical and optical data, an effective approach to data analysis is required. The current work has demonstrated that the use of conventional *radar* plots and associated *radar* area sum calculations can enable the simultaneous and convenient analysis of a large amount of data. The normalized area calculations can be adapted to reflect the more significant properties with appropriate weighting factors applied to these *radar* areas. A blend with a relatively high normalized area sum is deemed to have overall better physicomechanical and optical properties than a blend with a comparatively low area sum.

In order to optimize the blend composition, a parameter that is indicative of a detriment to the blend over the range of compositions should be identified and normalized over the same composition range. For example, this parameter could be based on decreased processability with increasing blend composition or could be based on possible increasing costs of blend components. By superimposing this parameter with a plot of normalized *radar* area sums, the point at which these two plots intersect will be indicative of a blend with optimal physicomechanical and optical properties as well as optimal processability or associated costs. Indeed one can propose that a three-dimensional plot of this nature could also be used to optimize the controlling parameters.

5.3 Scope for Future Work

The potential of the analytical techniques based on DSC, FT-IR and CL developed in this work could be applied to blends of different polymers in order to assess the applicability of these methods to characterize blends other than those of polyethylenes.

The use of *radar* plots and associated area sums as a means of identifying and optimizing functional, potentially commercial blends could be further investigated and developed into a computerized assessment tool.

The development of an extensive database of general polymer blends would be valuable in order to collate and centralize the vast amount of data that are available in this field. Such a database would have potentially commercial and industrial appeal, particularly in the area of material selection and product development.

Although a complete analysis of the cost savings associated with blending is outside the scope of the current work and was not subsequently pursued, future studies could assess more extensively the cost benefits of blending existing polymers.

The development of new polymer materials with customized properties by blending two or more existing polymers has almost unlimited potential for further development. Combinations of polymers in binary blends alone are limited only by blend compatibility but when combined with the use additives such as compatibilizers the range of potentially useful materials based on existing or recycled polymers is enormous.

The future of polymer blending technology lies in the propensity to develop commercially useful or specialized engineering materials that can be quickly and easily characterized and have optimum physicomechanical properties.

Appendix 1 List of ASTM Test Methods

The following list details the ASTM methods (in order of designation number) used for the physical, mechanical and optical property tests (see Section 3.3 and Section 3.4).

ASTM Method **D 256 - 97**, "Standard Test Method for Determining the Izod Pendulum Impact Resistance of Plastics", Plastics (I), 08.01, pp. 1-20, 1998.

ASTM Method **D 638 - 98**, "Standard Test Method for Tensile Properties of Plastics", Plastics (I), 08.01, pp. 45-57, 1998.

ASTM Method **D 792 - 98**, "Standard Test Method for Density and Specific Gravity (Relative Density) of Plastics by Displacement", Plastics (I), 08.01, pp. 157-161, 1998.

ASTM Method **D 882 - 97**, "Standard Test Method for Tensile Properties of Thin Plastic Sheeting", Plastics (I), 08.01, pp. 163-171, 1998.

ASTM Method **D 1003 - 97**, "Standard Test Method for Haze and Luminous Transmittance of Transparent Plastics", Plastics (I), 08.01, pp. 199-204, 1998.

ASTM Method **D 1238 - 98**, "Standard Test Method for Flow Rates of Thermoplastics by Extrusion Plastometry", Plastics (I), 08.01, pp. 258-267, 1998.

ASTM Method **D 1505 - 98**, "Standard Test Method for Density of Plastics by the Density-Gradient Technique", Plastics (I), 08.01, pp. 304-310, 1998.

ASTM Method **D 1709 - 98**, "Standard Test Method for Impact Resistance of Plastic Film by the Free-Falling Dart Method", Plastics (I), 08.01, pp. 381-388, 1998.

ASTM Method **D 1922 - 94a**, "Standard Test Method for Propogation Tear Resistance of Plastic Film and Thin Sheeting by Pendulum Method", Plastics (I), 08.01, pp. 455-460, 1998.

ASTM Method **D 1928 - 96**, "Standard Practice for Preparation of Compression-Molded Polyethylene Test Sheets and Test Specimens", Plastics (I), 08.01, pp. 461-467, 1998.

ASTM Method **D 1996 - 97**, "Standard Test Method for Determination of Phenolic Antioxidants and Erucamide Slip Additives in Low-Density Polyethylene Using Liquid Chromatography (LC)", Plastics (I), 08.01, pp. 481-486, 1998.

ASTM Method **D 2457 - 97**, "Standard Test Method for Specular Gloss of Plastic Films and Solid Plastics", Plastics (II), 08.02, pp. 9-13, 1998.

ASTM Method **D 3417 - 97**, "Standard Test Method for Enthalpies of Fusion and Crystallization of Polymers by Differential Scanning Calorimetry (DSC)", Plastics (II), 08.02, pp. 325-328, 1998.

ASTM Method **D 3763 - 98**, "Standard Test Method for High Speed Puncture Properties of Plastics Using Load and Displacement Sensors", Plastics (II), 08.02, pp. 430-438, 1998.

ASTM Method **D 5524 - 94**, "Standard Test Method for Determination of Phenolic Antioxidants in High-Density Polyethylene Using Liquid Chromatography", Plastics (III), 08.03, pp. 552-556, 1996.

ASTM Method **D 5815 - 95**, "Standard Test Method for Determination of Phenolic Antioxidants and Erucamide Slip Additives in Linear Low-Density Polyethylene Using Liquid Chromatography (LC)", Plastics (III), 08.03, pp. 633-637, 1996.

Appendix 2 Supplemental LDPE/LLDPE Figures

Supplemental figures for blend characterization by DSC (see Section 4.1).

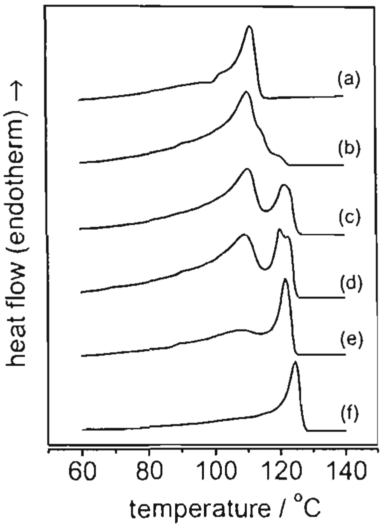

Figure A2.1. DSC melting thermograms of LDPE1/LLDPE3 blends containing: (a) 0%, (b) 5%, (c) 25%, (d) 30%, (e) 60% and (f) 100% LLDPE3 prior to the TSIA procedure. Blend compositions are (w/w).

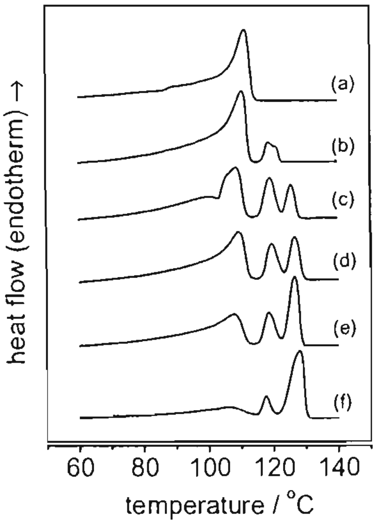

Figure A2.2. DSC melting thermograms of LDPE1/LLDPE3 blends containing: (a) 0%, (b) 5%, (c) 25%, (d) 30%, (e) 60% and (f) 100% LLDPE3 after the TSIA procedure. Blend compositions are (w/w).

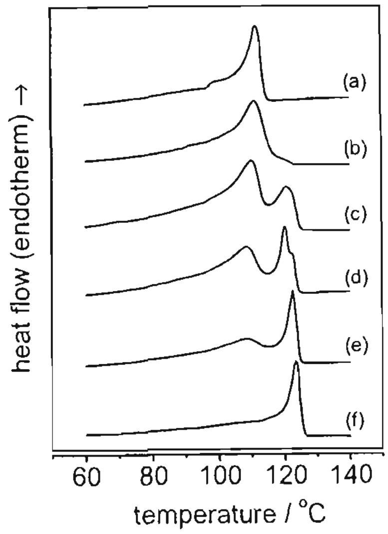

Figure A2.3. DSC melting thermograms of LDPE1/LLDPE4 blends containing: (a) 0%, (b) 5%, (c) 25%, (d) 30%, (e) 60% and (f) 100% LLDPE4 prior to the TSIA procedure. Blend compositions are (w/w).

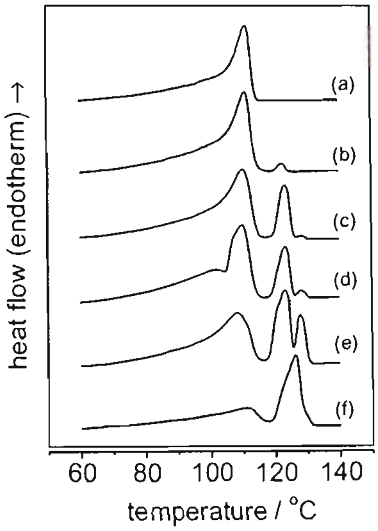

Figure A2.4. DSC melting thermograms of LDPE1/LLDPE4 blends containing: (a) 0%, (b) 5%, (c) 25%, (d) 30%, (e) 60% and (f) 100% LLDPE4 after the TSIA procedure. Blend compositions are (w/w).

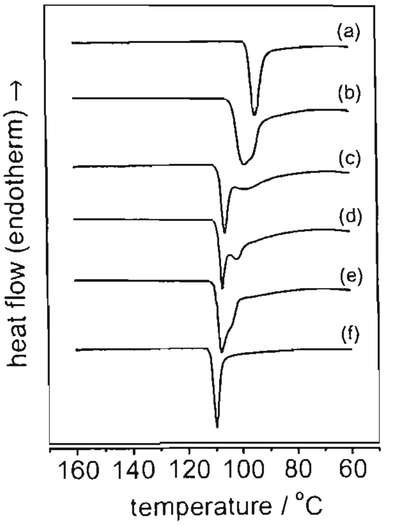

Figure A2.5. Crystallization thermograms of LDPE1/LLDPE2 blends containing: (a) 0%, (b) 5%, (c) 25%, (d) 30%, (e) 60% and (f) 100% LLDPE2. Compositions are (w/w).

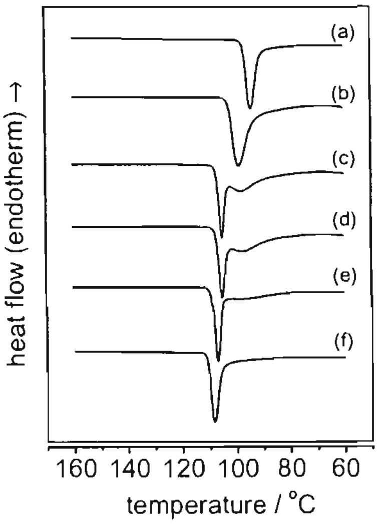

Figure A2.6. Crystallization thermograms of LDPE1/LLDPE3 blends containing: (a) 0%, (b) 5%, (c) 25%, (d) 30%, (e) 60% and (f) 100% LLDPE3. Compositions are (w/w).

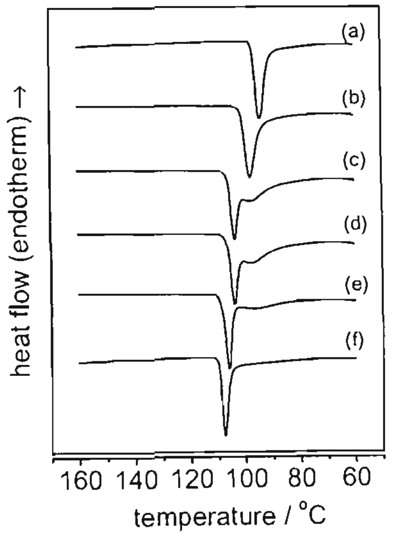

Figure A2.7. Crystallization thermograms of LDPE1/LLDPE4 blends containing: (a) 0%, (b) 5%, (c) 25%, (d) 30%, (e) 60% and (f) 100% LLDPE4. Compositions are (w/w).

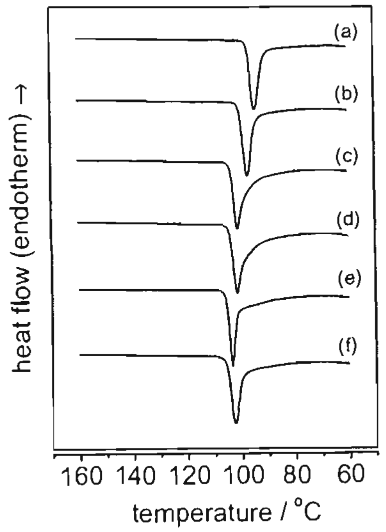

Figure A2.8. Crystallization thermograms of LDPE1/LLDPE5 blends containing: (a) 0%, (b) 5%, (c) 25%, (d) 30%, (e) 60% and (f) 100% LLDPE1. Compositions are (w/w).

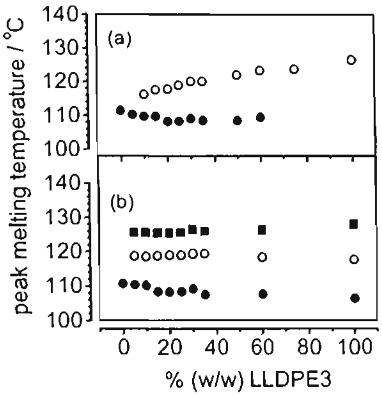

Figure A2.9. Peak melting temperature versus composition for the LDPE1/LLDPE3 blends: (a) before the TSIA treatment and (b) after the TSIA treatment: (●) LDPE1, (o) LLDPE3 peak 1 and (■) LLDPE3 peak 2.

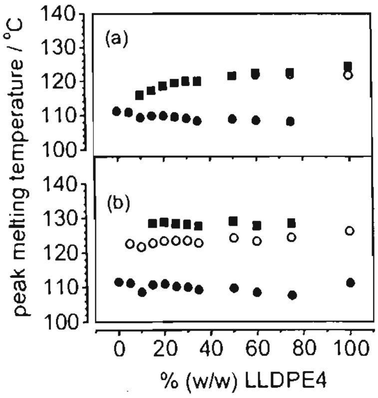

Figure A2.10. Peak melting temperature versus composition for the LDPE1/LLDPE4 blends: (a) before the TSIA treatment and (b) after the TSIA treatment: (●) LDPE1, (o) LLDPE2 peak 1 and (■) LLDPE2 peak 2.

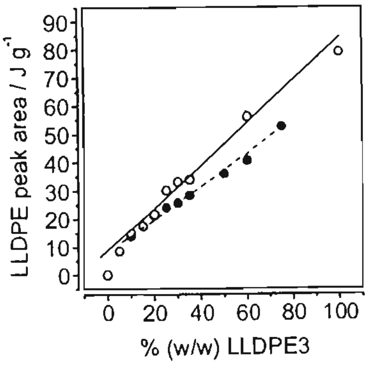

Figure A2.11. Integrated area under the LLDPE peak versus composition for the LDPE1/LLDPE3 blends: (●) before the TSIA treatment and (o) after the TSIA treatment.

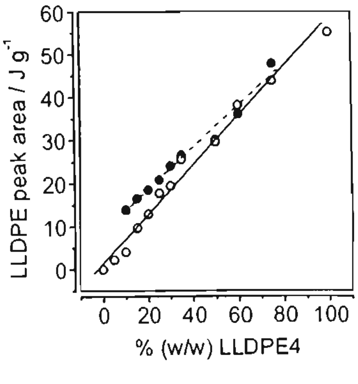

Figure A2.12. Integrated area under the LLDPE peak versus composition for the LDPE1/LLDPE4 blends: (●) before the TSIA treatment and (o) after the TSIA treatment.

Appendix 3 Supplemental DSC Themograms

Supplemental DSC thermograms for the study of blend miscibility by CL and DSC techniques (Section 4.1) and melting behaviour of LDPE/mLLDPE blends (Section 4.4.4).

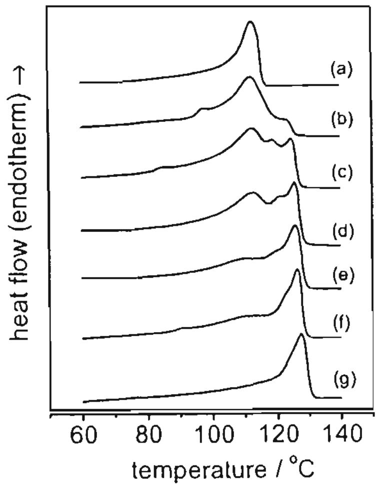

Figure A3.1. DSC endotherms of selected LDPE2/LLDPE6 blends. The blends contain: (a) 0%, (b) 10%, (c) 20%, (d) 30%, (e) 50%, (f) 70% and (g) 100 % LLDPE6. Blend compositions are (w/w).

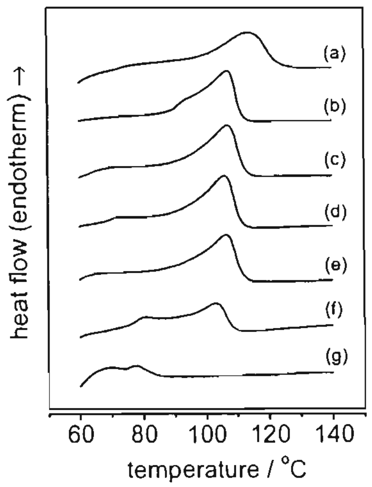

Figure A3.2. DSC endotherms of selected LDPE4/mLLDPE4 blends. Blends contain: (a) 0%, (b) 10%, (c) 25%, (d) 35%, (e) 50%, (f) 75% and (g) 100% mLLDPE4. Blend compositions are (w/w).

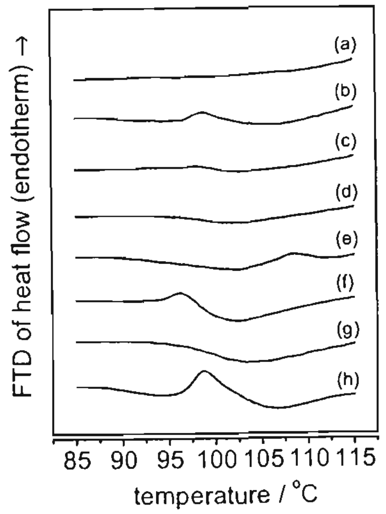

Figure A3.3. First-time derivative of DSC endotherms of selected HDPE1/mLLDPE5 blends over the temperature range 85-115°C. The blends contain: (a) 0%, (b) 10%, (c) 20%, (d) 35%, (e) 50%, (f) 65%, (g) 85% and (h) 100% mLLDPE5. Compositions are (w/w).

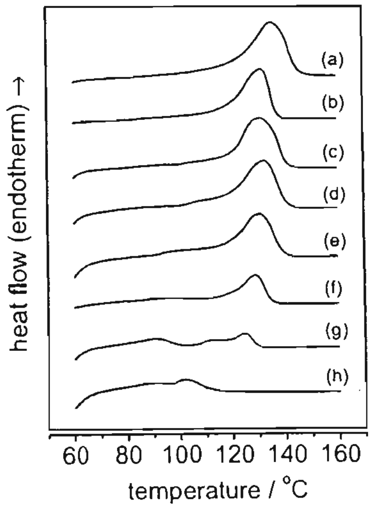

Figure A3.4. DSC endotherms of selected HDPE2/mLLDPE5 blends. Blends contain: (a) 0%, (b) 10%, (c) 20%, (d) 35%, (e) 50%, (f) 65%, (g) 85% and (h) 100% mLLDPE5. Blend compositions are (w/w).

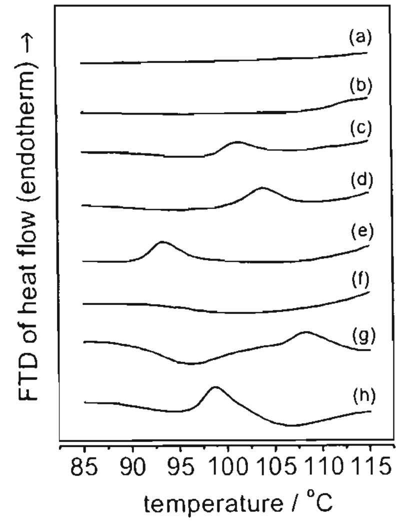

Figure A3.5. First-time derivative of DSC endotherms of selected HDPE2/mLLDPE5 blends in the temperature range 85°C to 115°C. The blends contain: (a) 0%, (b) 10%, (c) 20%, (d) 35%, (e) 50%, (f) 65%, (g) 85% and (h) 100% mLLDPE5. Blend compositions are (w/w).

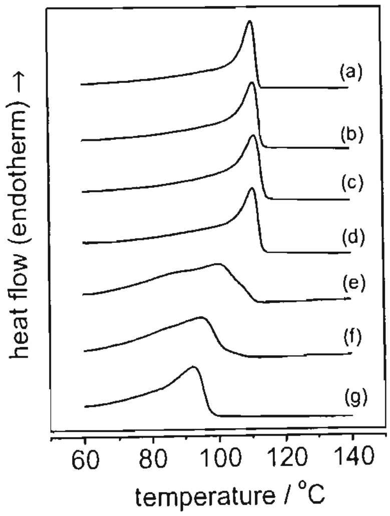

Figure A3.6. DSC endotherms of selected LDPE3/mLLDPE1 blends. Blends contain: (a) 0%, (b) 10%, (c) 20%, (d) 50%, (e) 75%, (f) 90% and (g) 100% mLLDPE1. Blend compositions are (w/w).

Appendix 4 Mass and Cost Difference Calculations

The following table lists the mass difference and cost difference calculations for the complete array of compositions and gauge lengths that were prepared to study the effect of downgauging on the properties of LDPE film blends (see Section 4.4.5).

Table A4.1. Mass difference and cost difference calculations from highest to lowest ΔA.

PE Blend Details						
%LLDPE6,	film gauge	%mLLDPE2,	film gauge	ΔA	Δm/%	ΔC/%
20%,	60 μm	40%,	60 μm	0.386	0.2	-1.8
20%,	60 μm	30%,	100 μm	0.324	-66.5	-68.8
20%,	60 μm	40%,	100 μm	0.306	-66.4	-69.7
20%,	80 μm	40%,	60 μm	0.306	25.1	23.6
20%,	60 μm	40%,	80 μm	0.288	-33.1	-35.8
20%,	100 μm	40%,	60 μm	0.281	40.1	38.9
30%,	60 μm	40%,	60 μm	0.257	0.2	-1.7
30%,	80 μm	40%,	60 μm	0.240	25.1	23.7
20%,	80 μm	30%,	100 μm	0.244	-24.8	-26.6
20%,	80 μm	40%,	100 μm	0.226	-24.8	-27.3
20%,	80 μm	40%,	80 μm	0.208	0.2	-1.8
40%,	100 μm	40%,	60 μm	0.200	40.1	39.0
20%,	100 μm	30%,	100 μm	0.219	0.1	-1.3
20%,	60 μm	20%,	100 μm	0.218	-66.5	-68.0
20%,	100 μm	40%,	100 μm	0.200	0.2	-1.8
30%,	60 μm	30%,	100 μm	0.195	-66.4	-68.7
40%,	60 μm	40%,	60 μm	0.188	0.2	-1.6
20%,	100 μm	40%,	80 μm	0.183	20.1	18.5
30%,	60 μm	40%,	100 μm	0.177	-66.4	-69.5
30%,	100 μm	40%,	60 μm	0.180	40.1	39.0
30%,	80 μm	30%,	100 μm	0.178	-24.8	-26.5
30%,	60 μm	40%,	80 μm	0.159	-33.1	-35.6
30%,	80 μm	40%,	100 μm	0.159	-24.8	-27.1
20%,	60 μm	30%,	80 μm	0.163	-33.2	-35.1
40%,	80 μm	40%,	60 μm	0.151	25.1	23.8
30%,	80 μm	40%,	80 μm	0.142	0.2	-1.7
40%,	100 μm	30%,	100 μm	0.138	0.1	-1.1
40%,	100 μm	40%,	100 μm	0.120	0.2	-1.6
20%,	80 μm	20%,	100 μm	0.138	-24.9	-26.0
40%,	100 μm	40%,	80 μm	0.102	20.1	18.7
40%,	60 μm	30%,	100 μm	0.127	-66.4	-68.5
20%,	60 μm	30%,	60 μm	0.133	0.1	-1.3
40%,	60 μm	40%,	100 μm	0.108	-66.4	-69.3
30%,	100 μm	30%,	100 μm	0.118	0.1	-1.2
30%,	100 μm	40%,	100 μm	0.100	0.2	-1.7
20%,	60 μm	20%,	80 μm	0.118	-33.2	-34.4
40%,	60 μm	40%,	80 μm	0.090	-33.1	-35.4

Note: The mass and cost differences are expressed as a percentage of the respective savings based on a blend containing LLDPE6. Blend compositions are (w/w).

Table A4.1. Continued.

PE Blend Details						
%LLDPE6,	film gauge	%mLLDPE2,	film gauge	ΔA	Δm/%	ΔC/%
20%,	100 μm	20%,	100 μm	0.112	0.1	-0.8
30%,	100 μm	40%,	80 μm	0.082	20.1	18.6
40%,	80 μm	30%,	100 μm	0.089	-24.8	-26.3
40%,	80 μm	40%,	100 μm	0.070	-24.8	-27.0
30%,	60 μm	20%,	100 μm	0.089	-66.5	-67.8
20%,	80 μm	30%,	80 μm	0.083	0.1	-1.3
40%,	80 μm	40%,	80 μm	0.053	0.2	-1.6
30%,	80 μm	20%,	100 μm	0.071	-24.9	-25.9
20%,	100 μm	30%,	80 μm	0.057	20.1	19.0
20%,	80 μm	30%,	60 μm	0.054	25.1	24.0
40%,	100 μm	20%,	100 μm	0.032	0.1	-0.6
30%,	60 μm	30%,	80 μm	0.034	-33.2	-34.9
20%,	80 μm	20%,	80 μm	0.038	0.1	-0.8
20%,	100 μm	30%,	60 μm	0.028	40.1	39.2
40%,	60 μm	20%,	100 μm	0.020	-66.5	-67.6
30%,	80 μm	30%,	80 μm	0.016	0.1	-1.2
30%,	100 μm	20%,	100 μm	0.012	0.1	-0.7
20%,	100 μm	20%,	80 μm	0.012	20.1	19.4
30%,	60 μm	30%,	60 μm	0.005	0.1	-1.2
40%,	100 μm	30%,	80 μm	-0.024	20.1	19.1
30%,	60 μm	20%,	80 μm	-0.011	-33.2	-34.2
40%,	80 μm	20%,	100 μm	-0.017	-24.9	-25.7
30%,	80 μm	30%,	60 μm	-0.013	25.1	24.1
20%,	60 μm	20%,	60 μm	-0.017	0.1	-0.8
30%,	80 μm	20%,	80 μm	-0.029	0.1	-0.7
40%,	60 μm	30%,	80 μm	-0.035	-33.2	-34.8
30%,	100 μm	30%,	80 μm	-0.044	20.1	19.0
40%,	100 μm	30%,	60 μm	-0.053	40.1	39.4
40%,	100 μm	20%,	80 μm	-0.069	20.1	19.5
40%,	80 μm	30%,	80 μm	-0.073	0.1	-1.1
40%,	60 μm	30%,	60 μm	-0.064	0.1	-1.1
30%,	100 μm	30%,	60 μm	-0.073	40.1	39.3
40%,	60 μm	20%,	80 μm	-0.080	-33.2	-34.1
30%,	100 μm	20%,	80 μm	-0.088	20.1	19.5
20%,	80 μm	20%,	60 μm	-0.097	25.1	24.4
40%,	80 μm	30%,	60 μm	-0.102	25.1	24.2
40%,	80 μm	20%,	80 μm	-0.118	0.1	-0.6
20%,	100 μm	20%,	60 μm	-0.123	40.1	39.5
30%,	60 μm	20%,	60 μm	-0.146	0.1	-0.7
30%,	80 μm	20%,	60 μm	-0.164	25.1	24.5
40%,	100 μm	20%,	60 μm	-0.204	40.1	39.7
40%,	60 μm	20%,	60 μm	-0.215	0.1	-0.6
30%,	100 μm	20%,	60 μm	-0.223	40.1	39.6
40%,	80 μm	20%,	60 μm	-0.253	25.1	24.6

Note: The mass and cost differences are expressed as a percentage of the respective savings based on a blend containing LLDPE6. Blend compositions are (w/w).

Appendix 5 Contents of Attached CD-Rom

The CD-Rom attached to this thesis (see inside back cover) contains the following folders and files (PDF files or Excel files, sorted alphabetically):

Folders and files	**Contents**
Chapters	
Chapter 0.pdf	Title page to beginning of Introduction
Chapter 1.pdf	Introduction
Chapter 2.pdf	Literature Review
Chapter 3.pdf	Experimental
Chapter 4.pdf	Results and Discussion
Chapter 5.pdf	Conclusions
Chapter 6.pdf	Appendix 1 to Appendix 5 & References
Data Files	
Data B1 Blends.xls	Blends of LDPE1 with LLDPE1 to LLDPE5
Data B2 Blends.xls	Blends of LDPE2, LDPE3 and mLLDPE1
Data B3 Blends.xls	Blends of LDPE2, LLDPE6 and mLLDPE2
Data B4 Blends.xls	Blends of LLDPE6 and mLLDPE2
Data B5 Blends.xls	Blends of LDPE4, mLLDPE3 and mLLDPE4
Data B6 Blends.xls	Blends of HDPE1, HDPE2 and mLLDPE5
Data FT-IR and CL.xls	FT-IR data for B2, B3, B5 and B6 blends and CL data for B3 through B6 blends
References	
ReferenceAuthor.pdf	Reference list with titles sorted by first author
ReferenceNumerical.pdf	Same as previous, ordered numerically
Thesis	
Figures.pdf	Figures separated from text
Thesis.pdf	Complete thesis

Note: Excel workbooks best viewed at 1024 x 768 screen resolution.

References

1. J.A. Brydson in "Plastics Materials", Butterworth-Heinemann, Oxford, 1999, pp. 1-18.
2. W.F. Smith in "Principles of Materials Science and Engineering", McGraw-Hill, Inc., New York, 1986, pp. 299-393.
3. H. Morawetz in "Polymers: The Origins and Growth of a Science", John Wiley & Sons, Inc., New York, 1985, pp. 53-59.
4. D. Feldman and A. Barbalata in "Synthetic Polymers", Chapman & Hall, London, 1996, pp. 338-350.
5. D. Feldman and A. Barbalata in "Synthetic Polymers", Chapman & Hall, London, 1996, pp. 3-57.
6. J.A. Brydson, "Plastics Materials", Butterworth-Heinemann, Oxford, 1999.
7. S. Katz, "Classic Plastics", Thames and Hudson, London, 1984.
8. G.T. Austin in "Shreve's Chemical Process Industries", McGraw-Hill Inc., Sydney, 1984, pp. 633-665.
9. I.M. Campbell in "Introduction to Synthetic Polymers", Oxford University Press Inc., New York, 1994, pp. 1-17.
10. F.W. Billmeyer, Jr. in "Textbook of Polymer Science", John Wiley & Sons, New York, 1984, pp. 3-21.
11. E.G. Couzens and V.E. Yarsley in "Plastics in the Modern World", Penguin Books Ltd, Middlesex, 1968, pp. 62-74.
12. F.M. McMillan, "The Chain Straighteners", The MacMillan Press Ltd, London, 1979.
13. D.J. Williams, "Polymer Science and Engineering", Prentice-Hall, Inc., Englewood Cliffs, 1971.
14. H.F. Mark in "Applied Polymer Science", R.W. Tess and G.W. Poehlein (eds.), American Chemical Society, Washington DC, 1985, pp. 1-23.
15. C.C. Winding and G.D. Hiatt, "Polymeric Materials", McGraw-Hill Book Company Inc., New York, 1961.
16. H.-G. Elias in "An Introduction to Polymer Science", VCH Publishers, Inc., New York, 1997, pp. 1-9.
17. J.A. Brydson in "Plastics Materials", Butterworth-Heinemann, Oxford, 1999, pp. 205-246.
18. S. Hosoda, *Polym. J.*, **20**, 383-397 (1988).
19. F.M. Mirabella, Jr. and E.A. Ford, *J. Polym. Sci. Polym. Phys.*, **25**, 777-790 (1987).
20. G. Liu, Y. Chen and H. Li, *J. Appl. Polym. Sci.*, **92**, 3894-3900 (2004).
21. H. Ueda, F.E. Karasz and R.J. Farris, *Polym. Eng. Sci.*, **26**, 1483-1488 (1986).
22. T. Tinçer and M. Coşkun, *Polym. Eng. Sci.*, **33**, 1243-1250 (1993).
23. A.R. Khare, S.P. Westphal, M.T.K. Ling, C. Qin and L. Woo, *Thermochim. Acta*, **357-358**, 155-160 (2000).
24. R.A. Shanks, J. Li and L. Yu, *Polymer*, **41**, 2133-2139 (2000).

25. A.C. Manaure and A.J. Müller, *Macromol. Chem. Phys.*, **201**, 958-972 (2000).

26. R.A. Shanks and G. Amarasinghe, *J. Therm. Anal. Calorim.*, 59, 471-482 (2000).

27. B.K. Kim, K.J. Kim, S.J. Park and H.M. Jeong, *J. Polym. Eng.*, 11, 297-314 (1992).

28. A.C. Manaure, R.A. Morales, J.J. Sánchez and A.J. Müller, *J. Appl. Polym. Sci.*, 66, 2481-2493 (1997).

29. V. Tanrattanakul and W. Udomkichdecha, *J. Appl. Polym. Sci.*, **82**, 650-660 (2001).

30. J. Li, R.A. Shanks and Y. Long, *J. Appl. Polym. Sci.*, **87**, 1179-1189 (2003).

31. T.C. Yu and G.J. Wagner, *SPE'RETEC Polyolefins VIII Conference*, February (1993).

32. K. Nitta, K. Suzuki and A. Tanaka, *J. Mater. Sci.*, **35**, 2719-2727 (2000).

33. K. Jordens, G.L. Wilkes, J. Janzen, D.C. Rohlfing and M.B. Welch, *Polymer*, **41**, 7175-7192 (2000).

34. M.L. Dias, V.V. Barbi, R.A. Pereira and E.B. Mano, *Mat.Res. Innov.*, 4, 82-88 (2001).

35. P. Starck and B. Löfgren, *Eur. Polym. J.*, **38**, 97-107 (2002).

36. K.-H. Nitta and A. Tanaka, *Polymer*, **42**, 1219-1226 (2001).

37. P.S. Chum, W.J. Kruper and M.J. Guest, *Adv. Mat.*, **12**, 1759-1767 (2000).

38. M. Razavi-Nouri and J.N. Hay, *Polymer*, **42**, 8621-8627 (2001).

39. W.J. Wang, Z.B. Ye, H. Fan, B.G. Li and S.P. Zhu, *Polymer*, **45**, 5497-5504 (2004).

40. J.F. Vega, A. Muñoz-Escalona, A. Santamaría, M.E. Muñoz and P. Lafuente, *Macromolecules*, **29**, 960-965 (1996).

41. L. Woo, M.T.K. Ling and S.P. Westphal, *Thermochim. Acta*, **272**, 171-179 (1996).

42. J.J. Janimak and G.C. Stevens, *Thermochim. Acta*, **332**, 125-142 (1999).

43. D. Yan, W.-J. Wang and S. Zhu, *Polymer*, **40**, 1737-1744 (1999).

44. R.J. Crawford in "Plastics Engineering", Butterworth-Heinemann, Oxford, 1998, pp. 1-40.

45. L.A. Utracki in "Polymer Alloys and Blends", Carl Hanser Verlag, Munich, 1989, pp. 1-28.

46. L.A. Utracki, "Polymer Alloys and Blends", Carl Hanser Verlag, Munich, 1989.

47. L.A. Utracki, D.J. Walsh and R.A. Weiss in "Multiphase Polymers: Blends and Ionomers", L.A. Utracki and R.A. Weiss (eds.), American Chemical Society, Washington DC, 1989, pp. 1-35.

48. M. Mehrabzadeh and F. Farahmand, *J. Appl. Polym. Sci.*, **80**, 2573-2577 (2001).

49. Z. Kruliš, B.V. Kokta, Z. Horák, D. Michálková and I. Fortelný, *Macromol. Mater. Eng.*, **286**, 156-160 (2001).

50. H.V. Smith, *Polym-Plast. Technol. Eng.*, **12**, 141-147 (1979).

51. R.S. Stein in "Emerging Technologies in Plastics Recycling", G.D. Andrews and P.M. Subramanian (eds.), American Chemical Society, Washington DC, 1992, pp. 39-48.

52. O.B. Ushakova, V.F. Potapov and V.N. Kuleznev, *J. Polym. Eng.*, **12**, 109-119 (1993).

53. N. Kukaleva, G.P. Simon and E. Kosior, *Polym. Eng. Sci.*, 43, 26-39 (2003).

54. J. Scheirs, "Polymer Recycling", John Wiley & Sons, Chichester, 1998.

55. W. Pearson in "Emerging Technologies in Plastics Recycling", G.D. Andrews and P.M. Subramanian (eds.), American Chemical Society, Washington DC, 1992, pp. 1-14.

56. J. George, R. Joseph, S. Thomas and K.T. Varughese, *J. Appl. Polym. Sci.*, **57**, 449-465 (1995).

57. A. Rudin in "The Elements of Polymer Science and Engineering", Academic Press, Inc., New York, 1982, pp. 428-464.

58. T. Bremner, A. Rudin and D.G. Cook, *J. Appl. Polym. Sci.*, **41**, 1617-1627 (1990).

59. P. Vadhar and T. Kyu, *Polym. Eng. Sci.*, **27**, 202-209 (1987).

60. L.A. Utracki, *Polym. Eng. Sci.*, **35**, 2-17 (1995).

61. S.-R. Hu, T. Kyu and R.S. Stein, *J. Polym. Sci. Polym. Phys.*, **25**, 71- 87 (1987).

62. C. Whitehouse, M.L. Liu and P. Gao, *Polymer*, **40**, 1421-1431 (1999).

63. D. Abraham, K.E. George and D.J. Francis, *Eur. Polym. J.*, **26**, 197-200 (1990).

64. B. Schlund and L.A. Utracki, *Polym. Eng. Sci.*, **27**, 359-366 (1987).

65. A.J. Müller and V. Balsamo, *Adv. Polym. Blends Alloys Technol.*, **5**, 1-21 (1994).

66. I.S. Bhardwaj, V. Kumar and K. Palanivelu, *Thermochim. Acta*, **131**, 241-246 (1988).

67. B.S. Tanem and A. Stori, *Polymer*, **42**, 5389-5399 (2001).

68. T. Kyu, S.-R. Hu and R.S. Stein, *J. Polym. Sci. Polym. Phys.*, **25**, 89- 103 (1987).

69. M. Guimarães, F.M.B. Coutinho, M.C.G. Rocha and M.E.F. Garcia, *J. Appl. Polym. Sci.*, **81**, 1991-1995 (2001).

70. B.S. Tanem and A. Stori, *Polymer*, **42**, 6609-6618 (2001).

71. A.A. Donatelli, *J. Appl. Polym. Sci.*, **23**, 3071-3076 (1979).

72. S. Sánchez-Valdes, C. Guerrero-Salazar, L.F. Ramos De Valle, Q. Lopez, I. Yañez-Flores, F. Orona-Villarreal and R. Ramirez-Vargas, *J. Polym. Eng.*, **17**, 257-268 (1997).

73. G.D. Mendenhall, *Angew. Chem., Int. ed. Eng.*, **29**, 362-373 (1990).

74. A.R. Cooper, *Polym. Eng. Sci.*, **27**, 1170-1181 (1987).

75. D. Campbell and J.R. White, "Polymer Characterization", Chapman and Hall, London, 1989.

76. C. Reckinger, B.C. Larbi and J. Rault, *J. Macromol. Sci.-Phys.*, **B23**, 511-526 (1985).

77. H.H. Song, R.S. Stein, D.-Q. Wu, M. Ree, J.C. Phillips, A. LeGrand and B. Chu, *Macromolecules*, **21**, 1180-1182 (1988).

78. H.H. Song, D.Q. Wu, B. Chu, M. Satkowski, M. Ree, R.S. Stein and J.C. Phillips, *Macromolecules*, **23**, 2380-2384 (1990).

79. J. Janicki and A. Wlochowicz, *J. de Physique IV*, **3**, 21-24 (1993).

80. T.A. Ezquerra, Z. Roslaniec, E. López-Cabarcos and F.J. Baltá-Calleja, *Macromolecules*, **28**, 4516-4524 (1995).

81. K. Tashiro, K. Imanishi, Y. Izumi, M. Kobayashi, K. Kobayashi, M. Satoh and R.S. Stein, *Macromolecules*, **28**, 8477-8483 (1995).

82. G.D. Wignall, J.D. Londono, J.S. Lin, R.G. Alamo, M.J. Galante and L. Mandelkern, *Macromolecules*, **28**, 3156-3167 (1995).

83. R. Thomann, J. Kressler, S. Setz, C. Wang and R. Mülhaupt, *Polymer*, **37**, 2627-2634 (1996).

84. R. Hu, W.S. Lambert and J.D. Barnes, *Polym. Eng. Sci.*, **37**, 1475-1479 (1997).

85. A. Marigo, R. Zannetti and F. Milani, *Eur. Polym. J.*, **33**, 595-598 (1997).

86. Y. Akpalu, L. Kielhorn, B.S. Hsiao, R.S. Stein, T.P. Russell, J. Van Egmond and M. Muthukumar, *Macromolecules*, **32**, 765-770 (1999).

87. R. Androsch, *Polymer*, **40**, 2805-2812 (1999).

88. S. Sasaki, K. Tashiro, M. Kobayashi, Y. Izumi and K. Kobayashi, *Polymer*, **40**, 7125-7135 (1999).

89. G.D. Wignall, R.G. Alamo, J.D. Londono, L. Mandelkern, M.H. Kim, J.S. Lin and G.M. Brown, *Macromolecules*, **33**, 551-561 (2000).

90. A.M.E. Baker and A.H. Windle, *Polymer*, **42**, 681-698 (2001).

91. H. Sato, Y. Katsumoto, S. Sasao, K. Matsukawa, Y. Kita, H.W. Siesler and Y. Ozaki, *Macromol. Symp.*, **184**, 339-348 (2002).

92. Siddaramaiah, T. Jeevananda, K.S. Jagadeesh, H. Somashekarappa and R. Somashekar, *J. Appl. Polym. Sci.*, **90**, 2938-2944 (2003).

93. R.E. Prud'homme, *J. Polym. Sci., Polym. Phys. Ed.*, **20**, 307-317 (1982).

94. T. Kyu and P. Vadhar, *J. Appl. Polym. Sci.*, **32**, 5575-5584 (1986).

95. M. Ree, T. Kyu and R.S. Stein, *J. Polym. Sci. Polym. Phys.*, **25**, 105-126 (1987).

96. J.M. Rego López and U.W. Gedde, *Polymer*, **30**, 22-26 (1989).

97. T. Ogita, Y. Kawahara, C. Sawatari, F. Ozaki and M. Matsuo, *Polym. J.*, **23**, 871-884 (1991).

98. K. Tashiro, M.M. Satkowski, R.S. Stein, Y. Li, B. Chu and S.L. Hsu, *Macromolecules*, **25**, 1809-1815 (1992).

99. A. Larena and G. Pinto, *Polym. Eng. Sci.*, **33**, 742-747 (1993).

100. U. Dayal, *J. Appl. Polym. Sci.*, **53**, 1557-1562 (1994).

101. A.K. Gupta, S.K. Rana and B.L. Deopura, *J. Appl. Polym. Sci.*, **51**, 231-239 (1994).

102. M. Okamoto and T. Inoue, *Polymer*, **36**, 2739-2744 (1995).

103. J.P. Penning and R.St.J. Manley, *Macromolecules*, **29**, 77-83 (1996).

104. S.K. Rana, *J. Appl. Polym. Sci.*, **61**, 951-957 (1996).

105. I. Hénaut, B. Vergnes, J.F. Agassant and J.-M. Haudin, *Int. Polym. Proc.*, **13**, 199-208 (1998).

106. S.K. Rana, *J. Appl. Polym. Sci.*, **69**, 2599-2607 (1998).

107. A. Faldi and J.B.P. Soares, *Polymer*, **42**, 3057-3066 (2001).

108. L. Pan, T. Inoue, H. Hayami and S. Nishikawa, *Polymer*, **43**, 337-343 (2002).

109. C.K. Chai, Q. Auzoux, H. Randrianatoandro, P. Navard and J.-M. Haudin, *Polymer*, **44**, 773-782 (2003).

110. R.S. Stein in "Polymer Blends", D.R. Paul and S. Newman (eds.), Academic Press, Inc., New York, 1978, pp. 393-444.

111. U.W. Gedde, S. Eklund and J.-F. Jansson, *Polymer*, **24**, 1532-1540 (1983).

112. R.H. Glaser and L. Mandelkern, *J. Polym. Sci. Polym. Phys.*, **26**, 221-234 (1988).

113. P. Aaltonen and B. Löfgren, *Macromolecules*, **28**, 5353-5357 (1995).

114. J.A. Deiber, M.B. Peirotti and A. Gappa, *J. Elastomers Plast.*, **29**, 290-313 (1997).

115. R.L. Morgan, M.J. Hill, P.J. Barham and C.J. Frye, *Polymer*, **38**, 1903-1909 (1997).

116. Y.C. Kim and K.S. Yang, *Polym. J.*, **31**, 579-584 (1999).

117. J.C.M. Suarez, E.B. Mano and C.M.C. Bonelli, *Polym. Eng. Sci.*, **39**, 1398-1403 (1999).

118. S.H. Hamid, *J. Appl. Polym. Sci.*, **78**, 1591-1596 (2000).

119. I.A. Hussein, K. Ho, S.K. Goyal, E. Karbashewski and M.C. Williams, *Polym. Deg. Stab.*, **68**, 381-392 (2000).

120. J.C.M. Suarez, E.B. Mano and R.A. Pereira, *Polym. Deg. Stab.*, **69**, 217-222 (2000).

121. P.M. Wood-Adams and J.M. Dealy, *Macromolecules*, **33**, 7481-7488 (2000).

122. V. Karmore and G. Madras, *Ind. Eng. Chem. Res.*, **40**, 1306-1311 (2001).

123. R.N. Shroff and H. Mavridis, *Macromolecules*, **34**, 7362-7367 (2001).

124. A. Malmberg, C. Gabriel, T. Steffl, H. Münstedt and B. Löfgren, *Macromolecules*, **35**, 1038-1048 (2002).

125. Y. Gao, H. Huang, Z. Yao, D. Shi, Z. Ke and J. Yin, *J. Polym. Sci. Polym. Phys.*, **41**, 1837-1849 (2003).

126. G.N. LeBlanc, *American Laboratory*, September, 32-37 (2003).

127. C.X. He, S. Costeux and P. Wood-Adams, *Polymer*, **45**, 3747-3754 (2004).

128. N. Sombatsompop, K. Sungsanit and C. Thongpin, *J. Appl. Polym. Sci.*, **92**, 3167-3172 (2004).

129. F. Vilaplana, V. Morera-Escrich, P. Hierro-Navarro, B. Monrabal and A. Ribes-Greus, *J. Appl. Polym. Sci.*, **94**, 1803-1814 (2004).

130. W.J. Wang, S. Kharchenko, K. Migler and S.P. Zhu, *Polymer*, **45**, 6495-6505 (2004).

131. J. Schelton, G.D. Wignall, D.G.H. Ballard and G.W. Longman, *Polymer*, **18**, 1111-1120 (1977).

132. J.C. Nicholson, T.M. Finerman and B. Crist, *Polymer*, **31**, 2287-2293 (1990).

133. R.G. Alamo, J.D. Londono, L. Mandelkern, F.C. Stehling and G.D. Wignall, *Macromolecules*, **27**, 411-417 (1994).

134. W.W. Graessley, R. Krishnamoorti, N.P. Balsara, R.J. Butera, L.J. Fetters, D.J. Lohse, D.N. Schulz and J.A. Sissano, *Macromolecules*, **27**, 3896-3901 (1994).

135. K. Tashiro, K. Imanishi, M. Izuchi, M. Kobayashi, Y. Itoh, M. Imai, Y. Yamaguchi, M. Ohashi and R.S. Stein, *Macromolecules*, **28**, 8484-8490 (1995).

136. K. Sakurai, W.J. MacKnight, D.J. Lohse, D.N. Schulz, J.A. Sissano, J.-S. Lin and M. Agamalyan, *Polymer*, **37**, 4443-4453 (1996).

137. C. Schipp, M.J. Hill, P.J. Barham, V.M. Cloke, J.S. Higgins and L. Oiarzabal, *Polymer*, **37**, 2291-2297 (1996).

138. G.D. Wignall, R.G. Alamo, J.D. Londono, L. Mandelkern and F.C. Stehling, *Macromolecules*, **29**, 5332-5335 (1996).

139. R.G. Alamo, W.W. Graessley, R. Krishnamoorti, D.J. Lohse, J.D. Londono, L. Mandelkern, F.C. Stehling and G.D. Wignall, *Macromolecules*, **30**, 561-566 (1997).

140. M.M. Agamalian, R.G. Alamo, J.D. Londono, L. Mandelkern, F.C. Stehling and G.D. Wignall, *Polym. Mater. Sci. Eng.*, **78**, 74-75 (1998).

141. H.S. Jeon, J.H. Lee, N.P. Balsara and M.C. Newstein, *Macromolecules*, **31**, 3340-3352 (1998).

142. H.S. Jeon, J.H. Lee and N.P. Balsara, *Macromolecules*, **31**, 3328-3339 (1998).

143. G.C. Reichart, W.M. Graessley, R.A. Register and D.J. Lohse, *Macromolecules*, **31**, 7886-7894 (1998).

144. M.M. Agamalian, R.G. Alamo, M.H. Kim, J.D. Londono, L. Mandelkern and G.D. Wignall, *Macromolecules*, **32**, 3093-3096 (1999).

145. M.M. Agamalian, R.G. Alamo, J.D. Londono, L. Mandelkern and G.D. Wignall, *J. Appl. Crystallogr.*, **33**, 843-846 (2000).

146. S. Coutry and S.J. Spells, *Polymer*, **44**, 1949-1956 (2003).

147. C.T. Lo, S. Seifert, P. Thiyagarajan and B. Narasimhan, *Polymer*, **45**, 3671-3679 (2004).

148. H. Wang, *J. Polym. Sci. Polym. Phys.*, **42**, 3133-3147 (2004).

149. K. Kimura, T. Shigemura and S. Yuasa, *J. Appl. Polym. Sci.*, **29**, 3161-3179 (1984).

150. D. Vaillant, J. Lacoste and G. Dauphin, *Polym. Deg. Stab.*, **45**, 355-360 (1994).

151. Y. Sugiura, Y. Makimura, Y. Kita and M. Matsuo, *Colloid Polym. Sci.*, **273**, 633-641 (1995).

152. C.H. Lee, C.E. Lee, J.H. Han and K.S. Suh, *Jpn. J. Appl. Phys.*, **35**, 2415-2148 (1996).

153. K. Kuwabara, H. Kaji, F. Horii, D.C. Bassett and R.H. Olley, *Macromolecules*, **30**, 7516-7521 (1997).

154. S. Percec, *Polym. Adv. Technol.*, **8**, 707-711 (1997).

155. G.B. Rojaš, J.G. Fatou, Ma.C. Martinez and O. Laguna, *Eur. Polym. J.*, **33**, 725-728 (1997).

156. H.P. Blom, J.W. Teh, T. Bremner and A. Rudin, *Polymer*, **39**, 4011-4022 (1998).

157. Y. Feng and X. Jin, *Polym.-Plast. Technol. Eng.*, **37**, 271-283 (1998).

158. M. Geppi, C. Forte, E. Passaglia and B. Mendez, *Macromol. Chem. Phys.*, **199**, 1957-1963 (1998).

159. J. Grobelny and D. Sěk, *Polymer*, **39**, 2143-2147 (1998).

160. G.B. Galland, R.F. de Souza, R.S. Mauler and F.F. Nunes, *Macromolecules*, **32**, 1620-1625 (1999).

161. P. Pietikäinen, P. Starck and J.V. Seppälä, *J. Polym. Sci. Polym. Chem.*, **37**, 2379-2389 (1999).

162. J.C.M. Suarez, E.B. Mano and M.I.B. Tavares, *J. Appl. Polym. Sci.*, **78**, 899-909 (2000).

163. M.I.B. Tavares, *Polym. Test.*, **19**, 899-904 (2000).

164. J. Murín, J. Uhrin and I. Chodák, *Macromol. Symp.*, **170**, 115-121 (2001).

165. J. Uhrin, J. Murín, L. Ševčovič and I. Chodák, *Macromol. Symp.*, **170**, 123-129 (2001).

166. B.R. de Gáscue, B. Méndez, J.L. Manosalva, L. Lopez, V.R.S. Quiteria and A.J. Müller, *Polymer*, **43**, 2151-2159 (2002).

167. C.-S. Wu, S.-M. Lai and H.-T. Liao, *J. Appl. Polym. Sci.*, **85**, 2905-2912 (2002).

168. C.-S. Wu, H.-T. Liao and S.-M. Lai, *Polym.-Plast. Technol. Eng.*, **41**, 645-661 (2002).

169. L. Ma, M. Azuma, C.Q. He, T. Suzuki, Y.Z. Bin and M. Matsuo, *Macromolecules*, **37**, 7673-7682 (2004).

170. J. Dlugosz, G.V. Fraser, D. Grubb, A. Keller, J.A. Odell and P.L. Goggin, *Polymer*, **17**, 471-480 (1976).

171. M.T. Conde Braña, J.I. Iragorri Sainz, B. Terselius and U.W. Gedde, *Polymer*, **30**, 410-415 (1989).

172. F. Defoor, G. Groeninckx, P. Schouterden and B. Van der Heijden, *Polymer*, **33**, 5186-5190 (1992).

173. A. Garton, D.N. Batchelder and C. Cheng, *Appl. Spectrosc.*, **47**, 922-927 (1993).

174. M.J. Hill, L. Oiarzabal and J.S. Higgins, *Polymer*, **35**, 3332-3337 (1994).

175. Y. Liu and R.W. Truss, *J. Appl. Polym. Sci.*, **60**, 1461-1473 (1996).

176. G.H. Michler, *J. Macromol. Sci.-Phys.*, **B35**, 329-355 (1996).

177. C.-F. Ou and C.-C. Lin, *J. Appl. Polym. Sci.*, **61**, 1447-1454 (1996).

178. A.A. Patel, J. Feng, M.A. Winnik, G.J. Vancso and C.B.D. McBain, *Polymer*, **37**, 5577-5582 (1996).

179. M. Patrick, V. Bennett and M.J. Hill, *Polymer*, **37**, 5335-5341 (1996).

180. C. Marcott, G.M. Story, A.E. Dowrey, R.C. Reeder and I. Noda, *Mikrochim. Acta*, **14**, 157-163 (1997).

181. J.M. Chalmers, N.J. Everall, K. Hewitson, M.A. Chesters, M. Pearson, A. Grady and B. Ruzicka, *Analyst*, **123**, 579-586 (1998).

182. P. Laokijcharoen and A.Y. Coran, *Rubber Chem. Technol.*, **71**, 966-974 (1998).

183. P. Montes, Y.A. Rafiq and M.J. Hill, *Polymer*, **39**, 6669-6672 (1998).

184. K. Tashiro, S. Sasaki, N. Gose and M. Kobayashi, *Polym. J.*, **30**, 485-491 (1998).

185. R.L. Morgan, M.J. Hill, P.J. Barham, A. Van der Pol, B. Kip, J. van Ruiten and L. Markwort, *J. Macromol. Sci.-Phys.*, **B38**, 419-437 (1999).

186. D. Raghavan, X. Gu, T. Nguyen, M. VanLandingham and A. Karim, *Macromolecules*, **33**, 2573-2583 (2000).

187. D.S. Moore and R.O. Hudson, *Spectroscopy*, **16**, 20-23 (2001).

188. K.M. Drummond, R.A. Shanks and F. Cser, *J. Appl. Polym. Sci.*, **83**, 777-784 (2002).

189. P. Schmidt, J. Dybal, J. Scudla, M. Raab, J. Kratochvil, K.-J. Eichhorn, S.-L. Quintana and J.M. Pàstor, *Macromol. Symp.*, **184**, 107-122 (2002).

190. D. Vesely in "Polymer Blends and Alloys", P.S. Hope and M. J. Folkes (eds.), Blackie Academic & Professional, London, 1999, pp. 103-125.

191. M.L. Arnal, J.J. Sánchez and A.J. Müller, *Polymer*, **42**, 6877-6890 (2001).

192. A.J. Müller, M.L. Arnal, A.L. Spinelli, E. Cañizales, C.C. Puig and H. Wang, *Macromol. Chem. Phys.*, **204**, 1497-1513 (2003).

193. L.I. Minkova, Ts. Miteva, D. Sek, B. Kaczmarczyk, P.L. Magagnini, M. Paci, F.P. La Mantia and R. Scaffaro, *J. Appl. Polym. Sci.*, **62**, 1613-1625 (1996).

194. Y. Xie, Q. Zhang and X. Fan, *J. Appl. Polym. Sci.*, **89**, 2686-2691 (2003).

195. A. Prasad, *Polym. Eng. Sci.*, **38**, 1716-1728 (1998).

196. P. Micic, S.N. Bhattacharya and G. Field, *Int. Polym. Proc.*, **12**, 110-115 (1997).

197. P.L. Joskowicz, A.J. Müller, J. Barrera and A.J. Müller, *Macromol. Chem. Phys.*, **196**, 385-398 (1995).

198. K.M. Drummond, J.L. Hopewell and R.A. Shanks, *J. Appl. Polym. Sci.*, **78**, 1009-1016 (2000).

199. Y.-T. Shieh and H.-C. Chuang, *J. Appl. Polym. Sci.*, **81**, 1808-1816 (2001).

200. T. Tsukame, Y. Ehara, Y. Shimizu, M. Kutsuzawa, H. Saitoh and Y. Shibasaki, *Thermochim. Acta*, **299**, 27-32 (1997).

201. A.C.-Y. Wong and A.D.E. Sy, *J. Mater. Sci.*, **30**, 5672-5680 (1995).

202. M.J. Hill and C.C. Puig, *J. Appl. Polym. Sci.*, **65**, 1921-1931 (1997).

203. P. Micic, S.N. Bhattacharya and G. Field, *Int. Polym. Proc.*, **11**, 14- 20 (1996).

204. H. Lee, K. Cho, T.-K. Ahn, S. Choe, I.-J. Kim, I. Park and B.H. Lee, *J. Polym. Sci. Polym. Phys.*, **35**, 1633-1642 (1997).

205. T. Tsukame, M. Kutsuzawa, H. Sekine, H. Saitoh and Y. Shibasaki, *J. Therm. Anal. Calorim.*, **57**, 847-851 (1999).

206. C.C. Puig, *Polymer*, **42**, 6579-6585 (2001).

207. N.K. Datta and A.W. Birley, *Plast. Rubber Process. Appl.*, **2**, 237-245 (1982).

208. F.-C. Chiu, Q. Fu, Y. Peng and H.-H. Shih, *J. Polym. Sci. Polym. Phys.*, **40**, 325-337 (2002).

209. M. Zhang, D.T. Lynch and S.E. Wanke, *Polymer*, **42**, 3067-3075 (2001).

210. P. Starck, *Polym. Int.*, **40**, 111-122 (1996).

211. P. Starck, A. Malmberg and B. Löfgren, *J. Appl. Polym. Sci.*, **83**, 1140-1156 (2002).

212. F. Chen, R.A. Shanks and G. Amarasinghe, *Polym. Int.*, **53**, 1795-1805 (2004).

213. H.-L. Chen, J.C. Hwang and C.-C. Chen, *Polymer*, **37**, 5461-5467 (1996).

214. W. Liu, S. Kim, J. Lopez, B. Hsiao, M.Y. Keating, I.H. Lee, B. Landes and R.S. Stein, *J. Therm. Anal. Calorim.*, **59**, 245-255 (2000).

215. M.L. Arnal, V. Balsamo, G. Ronca, A. Sánchez, A.J. Müller, E. Cañizales and C. Urbina de Navarro, *J. Therm. Anal. Calorim.*, **59**, 451-470 (2000).

216. J.-T. Xu, X.-R. Xu and L. Feng, *Eur. Polym. J.*, **36**, 685-693 (1999).

217. C.C. Puig, M.V. Aviles, P. Joskowicz and A. Diaz, *J. Appl. Polym. Sci.*, 79, 2022-2028 (2001).

218. M. Zhang, D.T. Lynch and S.E. Wanke, *J. Appl. Polym. Sci.*, **75**, 960-967 (2000).

219. R.L. Morgan, M.J. Hill and P.J. Barham, *Polymer*, **40**, 337-348 (1999).

220. S. Haghighat and A.W. Birley, *Adv. Polym. Technol.*, **10**, 143-151 (1990).

221. J.Z. Liang and J.N. Ness, *Polym. Test.*, **16**, 173-184 (1997).

222. D. Abraham, K.E. George and D.J. Francis, *Int. J. Polym. Mat.*, **18**, 197-211 (1992).

223. F.P. La Mantia, A. Valenza and D. Acierno, *Eur. Polym. J.*, **22**, 647-652 (1986).

224. N.K. Datta and A.W. Birley, *Plast. Rubber Process. Appl.*, **3**, 237-242 (1983).

225. G.J. Field, P. Micic and S.N. Bhattacharya, *Polym. Int.*, **48**, 461-466 (1999).

226. U. Yilmazer, *J. Appl. Polym. Sci.*, **42**, 2379-2384 (1991).

227. P. Micic, S.N. Bhattacharya and G. Field, *Int. Polym. Proc.*, **13**, 50- 57 (1998).

228. S. Haghighat and A.W. Birley, *Plast. Rubber Process. Appl.*, **13**, 197-200 (1990).

229. M. Yamaguchi and S. Abe, *J. Appl. Polym. Sci.*, **74**, 3153-3159 (1999).

230. J.-T. Xu, X.-R. Xu, L. Chen, L. Feng and W. Chen, *Polymer*, **42**, 3867-3874 (2001).

231. K. Tashiro, R.S. Stein and S.L. Hsu, *Macromolecules*, **25**, 1801-1808 (1992).

232. F. Defoor, G. Groeninckx, P. Schouterden and B. Van der Heijden, *Polymer*, **33**, 3878-3883 (1992).

233. T. Usami, Y. Gotoh and S. Takayama, *Macromolecules*, **19**, 2722-2726 (1986).

234. R.A. Shanks and G. Amarasinghe, *Polymer*, **41**, 4579-4587 (2000).

235. J. Scheirs in "Compositional and Failure Analysis of Polymers: A Practical Approach", John Wiley & Sons, Chichester, 2000, pp. 198-200.

236. G. Amarasinghe, F. Chen, A. Genovese and R.A. Shanks, *J. Appl. Polym. Sci.*, **90**, 681-692 (2003).

237. M.L. Arnal, E. Cañizales and A.J. Müller, *Polym. Eng. Sci.*, **42**, 2048-2063 (2002).

238. E.C. Kelusky, C.T. Elston and R.E. Murray, *Polym. Eng. Sci.*, **27**, 1562-1571 (1987).

239. F. Chen, R.A. Shanks and G. Amarasinghe, *Polymer*, **42**, 4579-4587 (2001).

240. C.A. Fonseca and I.R. Harrison, *Thermochim. Acta*, **313**, 37-41 (1998).

241. D.L. Wilfong and G.W. Knight, *J. Polym. Sci. Polym. Phys.*, **28**, 861-870 (1990).

242. A.J. Müller, Z.H. Hernández, M.L. Arnal and J.J. Sánchez, *Polym. Bull.*, **39**, 465-472 (1997).

243. L.J.D. Britto, J.B.P. Soares, A. Penlidis and B. Monrabal, *J. Polym. Sci. Polym. Phys.*, **37**, 539-552 (1999).

244. C. Gabriel and D. Lilge, *Polymer*, **42**, 297-303 (2001).

245. C. Wang, M.C. Chu, T.L. Lin, S.-M. Lai, H.-H. Shih and J.C. Yang, *Polymer*, **42**, 1733-1741 (2001).

246. R. Quijada, A. Narvaez, M. Dal Pizzol, S. Liberman, A. Arli and G.B. Galland, *J. Appl. Polym. Sci.*, 79, 221-227 (2001).

247. J.B.P. Soares and A.E. Hamielec, *Polymer*, **36**, 1639-1654 (1995).

248. C.J. Neves, E. Monteiro and A.C. Habert, *J. Appl. Polym. Sci.*, **50**, 817-824 (1993).

249. A. Nesarikar, B. Crist and A. Davidovich, *J. Polym. Sci. Polym. Phys.*, **32**, 641-646 (1994).

250. M.Y. Keating and E.F. McCord, *Thermochim. Acta*, **243**, 129-145 (1994).

251. E. Karbashewski, L. Kale, A. Rudin, W.J. Tchir, D.G. Cook and J.O. Pronovost, *J. Appl. Polym. Sci.*, **44**, 425-434 (1992).

252. P. Starck, P. Lehmus and J.V. Seppälä, *Polym. Eng. Sci.*, 39, 1444-1455 (1999).

253. A. Barbalata, T. Bohossian and G. Delmas, *J. Appl. Polym. Sci.*, **46**, 411-420 (1992).

254. J.-T. Xu and L. Feng, *Eur. Polym. J.*, **36**, 867-878 (2000).

255. J. Borrajo, C. Cordon, J.M. Carella, S. Toso and G. Goizueta, *J. Polym. Sci. Polym. Phys.*, **33**, 1627-1632 (1995).

256. Q. Fu, F.-C. Chiu, T. He, J. Liu and E.T. Hsieh, *Macromol. Chem. Phys.*, **202**, 927-932 (2001).

257. Q. Gao and J.I. Scheinbeim, *Macromolecules*, **33**, 7564-7572 (2000).

258. S. Choe, Y.-J. Cha, H.-S. Lee, J.S. Yoon and H.J. Choi, *Polymer*, **36**, 4977-4982 (1995).

259. K. Tashiro, M. Izuchi, M. Kobayashi and R.S. Stein, *Macromolecules*, **27**, 1221-1227 (1994).

260. J. Prinos, D.N. Bikiaris, S. Theologidis and C. Panayiotou, *Polym. Eng. Sci.*, **38**, 954-964 (1998).

261. E.G. Koulouri, A.X. Georgaki and J.K. Kallitsis, *Polymer*, **38**, 4185-4192 (1997).

262. L. Li, T. Tang and B. Huang, *Angew. Makromol. Chem.*, **241**, 77-93 (1996).

263. N. Mekhilef, A. Aït-Kadi and A. Ajji, *Polym. Eng. Sci.*, **32**, 894-902 (1992).

264. S.-L. Quintana, P. Schmidt, J. Dybal, J. Kratochvil, J.M. Pastor and J.C. Merino, *Polymer*, **43**, 5187-5195 (2002).

265. P. Schmidt, J. Baldrian, J. Scudla, J. Dybal, M. Raab and K.-J. Eichhorn, *Polymer*, **42**, 5321-5326 (2001).

266. Q. Wei, D. Chionna, E. Galoppini and M. Pracella, *Macromol. Chem. Phys.*, **204**, 1123-1133 (2003).

267. W. Camacho and S. Karlsson, *Polym. Eng. Sci.*, **41**, 1626-1635 (2001).

268. C.M.C. Bonelli, A.F. Martins, E.B. Mano and C.L. Beatty, *J. Appl. Polym. Sci.*, **80**, 1305-1311 (2001).

269. M. Pracella, L. Rolla, D. Chionna and A. Galeski, *Macromol. Chem. Phys.*, **203**, 1473-1485 (2002).

270. M.M. Coleman and P.C. Painter, *Appl. Spectrosc. Rev.*, **20**, 255-346 (1984).

271. S. Ultsch and H.G. Fritz, *Plast. Rubber Process. Appl.*, **13**, 81-91 (1990).

272. K. Tashiro, M. Izuchi, F. Kaneuchi, C. Jin, M. Kobayashi and R.S. Stein, *Macromolecules*, **27**, 1240-1244 (1994).

273. L. Marquez, I. Rivero and A.J. Müller, *Macromol. Chem. Phys.*, **200**, 330-337 (1999).

274. H. Hagemann, R.G. Snyder, A.J. Peacock and L. Mandelkern, *Macromolecules*, **22**, 3600-3606 (1989).

275. J.V. Gulmine, P.R. Janissek, H.M. Heise and L. Akcelrud, *Polym. Test.*, **21**, 557-563 (2002).

276. E. Földes, A. Tóth, E. Kálmán, E. Fekete and Á. Tomasovszky-Bobák, *J. Appl. Polym. Sci.*, **76**, 1529-1541 (2000).

277. L. Rintoul, H. Panayiotou, S. Kokot, G.A. George, G. Cash, R. Frost, T. Bui and P. Fredericks, *Analyst*, **123**, 571-577 (1998).

278. M.G. Sowa, D. Fischer, H.H. Eysel and H.H. Mantsch, *J. Mol. Struct.*, **379**, 77-85 (1996).

279. I.C. McNeill and M.H. Mohammed, *Polym. Deg. Stab.*, **49**, 263-273 (1995).

280. F.A.A. Khabbaz, *J. Appl. Polym. Sci.*, **79**, 2309-2316 (2001).

281. D.N. Bikiaris, J. Prinos and C. Panayiotou, *Polym. Deg. Stab.*, **56**, 1-9 (1997).

282. T. Corrales, F. Catalina, C. Peinado, N.S. Allen and E. Fontan, *J. Photochem. Photobiol., A Chem.*, **147**, 213-224 (2002).

283. W.R. Waldman and M.-A. De Paoli, *Polym. Deg. Stab.*, **60**, 301-308 (1998).

284. A.V. Prasad, P.N. Thanki and R.P. Singh, *J. Macromol. Sci., Pure Appl. Chem.*, **A34**, 349-359 (1997).

285. E. Epacher, J. Tolvéth, K. Stoll and B. Pukánszky, *J. Appl. Polym. Sci.*, **74**, 1596-1605 (1999).

286. G.A. George, M. Celina, A.M. Vassallo and P.A. Cole-Clarke, *Polym. Deg. Stab.*, **48**, 199-210 (1995).

287. A. Garton, "Infrared Spectroscopy of Polymer Blends, Composites and Surfaces", Hanser Publishers, Munich, 1992.

288. J.C. Henniker in "Infrared Spectrometry of Industrial Polymers", Academic Press, Inc., London, 1967, pp. 128-145.

289. J.C. Henniker in "Infrared Spectrometry of Industrial Polymers", Academic Press, Inc., London, 1967, pp. 146-159.

290. F. Apruzzese, R. Reshadat and S.T. Balke, *Appl. Spectrosc.*, **56**, 1268-1274 (2002).

291. F. Rugg, J. Smith and L. Waterman, *J. Polym. Sci.*, **11**, 11953).

292. R.A. Ozzetti, A.P. de Oliveira Filho, U. Schuchardt and D. Mandelli, *J. Appl. Polym. Sci.*, **85**, 734-745 (2002).

293. E. Cernia, C. Mancini and G. Montaudo, *J. Polym. Sci., B, Polym. Lett.*, **1**, 371-377 (1963).

294. R. Brüll, H. Pasch, H.G. Raubenheimer, R. Sanderson, A.J. van Reenen and U.M. Wahner, *Macromol. Chem. Phys.*, **202**, 1281-1288 (2001).

295. E.J. Markel, W.Q. Weng, A.J. Peacock and A.H. Dekmezian, *Macromolecules*, **33**, 8541-8548 (2000).

296. M. Buback, M. Busch, T. Dröge, F.-O. Mähling and C. Prellberg, *Eur. Polym. J.*, **33**, 375-379 (1997).

297. R.M. Paroli, J. Lara, J.-J. Hechler, K.C. Cole and I.S. Butler, *Appl. Spectrosc.*, **41**, 319-320 (1987).

298. J.E. Forrette and A.L. Rozek, *J. Appl. Polym. Sci.*, **18**, 2973-2981 (1974).

299. C. Tosi and T. Simonazzi, *Angew. Makromol. Chem.*, **32**, 153-161 (1973).

300. R.G. Davidson, *Mater. Forum*, **10**, 126-133 (1987).

301. C.E. Miller, *Appl. Spectrosc.*, **47**, 222-228 (1993).

302. R. Satoto, W.S. Subowo, R. Yusiasih, Y. Takane, Y. Wantanabe and T. Hatakeyama, *Polym. Deg. Stab.*, **56**, 275-279 (1997).

303. S.T. Wellinghoff, J.L. Koenig and E. Baer, *J. Polym. Sci., Polym. Phys. Ed.*, **15**, 1913-1925 (1977).

304. M. Sargent and J.L. Koenig, *Adv. Chem. Ser.*, **236**, 191-219 (1993).

305. K. Yoshino, X.H. Yin, K. Tada, T. Kawai, M. Hamaguchi, H. Araki, R. Sugimoto, N. Uchikawa, T. Asanuma, M. Kawahigashi and H. Kato, *IEEE Trans. Dielectr. Electr. Insul.*, **3**, 331-344 (1996).

306. T. Usami and S. Takayama, *Polym. J.*, **16**, 731-738 (1984).

307. C. Baker and W.F. Maddams, *Makromol. Chem.*, **177**, 437-448 (1976).

308. W.F. Maddams, D.B. Morris and H.A. Willis, *Polymer Comm.*, **30**, 180-181 (1989).

309. B. Wolf, S. Kenig, J. Klopstock and J. Miltz, *J. Appl. Polym. Sci.*, **62**, 1339-1345 (1996).

310. C. Baker, W.F. Maddams, G.S. Park and B. Robertson, *Makromol. Chem.*, **165**, 321-323 (1973).

311. R. Popli and L. Mandelkern, *J. Polym. Sci. Polym. Phys.*, **25**, 441-483 (1987).

312. J.P. Blitz and D.C. McFaddin, *J. Appl. Polym. Sci.*, **51**, 13-20 (1994).

313. W.F. Maddams and J. Woolmington, *Makromol. Chem.*, **186**, 1665-1670 (1985).

314. ASTM Method D 5576 - 94, "Standard Practice for Determination of Structural Entities in Polyolefins by Infrared Spectroscopy", pp. 580-582, 1998.

315. M.A. McRae and W.F. Maddams, *Makromol. Chem.*, **177**, 449-459 (1976).

316. A.H. Willbourn, *J. Polym. Sci.*, **34**, 569-597 (1959).

317. Y.S. Kim, C.I. Chung, S.Y. Lai and K.S. Hyun, *J. Appl. Polym. Sci.*, **59**, 125-137 (1996).

318. X.-R. Xu, J.-T. Xu, L. Feng and W. Chen, *J. Appl. Polym. Sci.*, **77**, 1709-1715 (2000).

319. T.M. Liu and W.E. Baker, *Polym. Eng. Sci.*, **32**, 944-955 (1992).

320. E. Nishio, M. Morimoto and K. Nishikada, *Appl. Spectrosc.*, **44**, 1639-1640 (1990).

321. D.S. Bag, S.N. Ghosh and S. Maiti, *Eur. Polym. J.*, **34**, 855-861 (1998).

322. J.N. Hay and X.-Q. Zhou, *Polymer*, **34**, 2282-2288 (1993).

323. K.C. Cole, Y. Thomas, E. Pellerin, M.M. Dumoulin and R.M. Paroli, *Appl. Spectrosc.*, **50**, 774-780 (1996).

324. G.C. Pandey, *Process Control Qual.*, **7**, 173-177 (1995).

325. ASTM Method D 3124 - 98, "Standard Test Method for Vinylidene Unsaturation in Polyethylene by Infrared Spectrophotometry", pp. 249-252, 1998.

326. ASTM Method D 2238 - 92, "Standard Test Method for Absorbance of Polyethylene Due to Methyl Groups at 1378 cm^{-1}", 08.01, pp. 523-529, 1998.

327. R. Setnescu, S. Jipa and Z. Osawa, *Polym. Deg. Stab.*, 60, 377-383 (1998).

328. Z. Osawa, M. Kato and M. Terano, *Macromol. Rapid Commun.*, **18**, 667-671 (1997).

329. P.K. Fearon, N. Marshall, N.C. Billingham and S.W. Bigger, *J. Appl. Polym. Sci.*, 79, 733-741 (2001).

330. P.K. Fearon, D.J. Whiteman, N.C. Billingham and S.W. Bigger, *J. Appl. Polym. Sci.*, 79, 1986-1993 (2001).

331. J. Boxhammer, *Macromol. Symp.*, **178**, 11-24 (2002).

332. L. Zlatkevich in "Polymer Stabilization and Degradation", P.P. Klemchuk (ed.), ACS Symposium Series 280, American Chemical Society, Washington DC, 1985, pp. 387-409.

333. K. Jacobson, B. Stenberg, B. Terselius and T. Reitberger, *Polym. Deg. Stab.*, **68**, 53-60 (2000).

334. D.R. Kohler and C. Kröhnke, *Polym. Deg. Stab.*, **62**, 385-393 (1998).

335. M. Celina and G.A. George, *Polym. Deg. Stab.*, **50**, 89-99 (1995).

336. K. Jacobson, P. Eriksson, T. Reitberger and B. Stenberg, *Adv. Polym. Sci.*, **169**, 151-176 (2004).

337. G.N. Foster, S.H. Wasserman and D.J. Yacka, *Angew. Makromol. Chem.*, **252**, 11-32 (1997).

338. F. Gugumus, *Polym. Deg. Stab.*, **52**, 131-144 (1996).

339. F. Gugumus, *Polym. Deg. Stab.*, **52**, 145-157 (1996).

340. F. Gugumus, *Polym. Deg. Stab.*, **52**, 159-170 (1996).

341. F. Gugumus, *Polym. Deg. Stab.*, **53**, 161-187 (1996).

342. F. Gugumus, *Polym. Deg. Stab.*, **55**, 21- 43 (1997).

343. N.S. Allen, M. Edge, D. Holdsworth, A. Rahaman, F. Catalina, E. Fontan, A.M. Escalona and F.F. Sibon, *Polym. Deg. Stab.*, **67**, 57-67 (2000).

344. F.P. La Mantia and A. Valenza, *Angew. Makromol. Chem.*, **216**, 45-65 (1994).

345. P. Ghosh, B. Chattopadhyay and A.K. Sen, *Eur. Polym. J.*, **32**, 1015-1021 (1996).

346. I. Ray, S. Roy, T.K. Chaki and D. Khastgir, *J. Elastomers Plast.*, **26**, 168-182 (1994).

347. L. Matisová-Rychlá, J. Rychlý, Z. Fodor, K. Barabas, M. Iring and F. Tudos, *Int. J. Polym. Mat.*, **13**, 227-235 (1990).

348. L. Matisová-Rychlá, I. Chodák, J. Rychlý and J. Bussink, *J. Appl. Polym. Sci.*, **49**, 1887-1891 (1993).

349. H. Kihara and S. Hosoda, *Polym. J.*, **22**, 763-770 (1990).

350. T. Memetea, Z. Vuluga and C. Hagiopol, *Int. J. Polym. Mat.*, **15**, 187-195 (1991).

351. B. Mattson, A. Kron, T. Reitberger, A.Y. Craig and R.H. Fleming, *Polym. Test.*, **11**, 357-372 (1992).

352. R.H. Fleming and A.Y. Craig, *Polym. Deg. Stab.*, 37, 173-180 (1992).

353. S. Hosoda, Y. Seki and H. Kihara, *Polymer*, **34**, 4602-4606 (1993).

354. G. Ablblad, B. Stenberg, B. Terselius and T. Reitberger, *Polym. Test.*, **16**, 59-73 (1997).

355. L.R. Mason and A.B. Reynolds, *J. Appl. Polym. Sci.*, **66**, 1691-1702 (1997).

356. L. Audouin-Jirackova and J. Verdu, *J. Polym. Sci. Polym. Chem.*, **25**, 1205-1217 (1987).

357. S. Hosoda and H. Kihara, *Antec '88*, **34**, 941-944 (1988).

358. O. Zenjiro, T. Kenji and K. Fujiko, *Materials Life*, **2**, 162-166 (1990).

359. K. Naito and T.K. Kwei, *J. Polym. Sci., Polym. Chem. Ed.*, **17**, 2935-2946 (1979).

360. N. Nugay and T. Tinçer, *Eur. Polym. J.*, 30, 473-477 (1994).

361. A.P. Plochocki in "Polymer Blends and Alloys", P.S. Hope and M. J. Folkes (eds.), Blackie Academic & Professional, London, 1978, pp. 319-368.

362. R.A. Rubeck and H.M. Baker, *Polymer*, **23**, 1680-1684 (1982).

363. J.I. Iragorri, J.M. Rego, I. Katime, M.T. Conde Braña and U.W. Gedde, *Polymer*, **33**, 461-466 (1990).

364. L.A. Hamielec, *Polym. Eng. Sci.*, **26**, 111-115 (1986).

365. A. Siegmann and Y. Nir, *Polym. Eng. Sci.*, **27**, 1182-1186 (1987).

366. A.D. Channell and E.Q. Clutton, *Polymer*, **33**, 4108-4112 (1992).

367. F.M. Mirabella, Jr., S.P. Westphal, P.L. Fernando, E.A. Ford and J.G. Williams, *J. Polym. Sci. Polym. Phys.*, **26**, 1995-2005 (1988).

368. A.D. Channell, E.Q. Clutton and G. Capaccio, *Polymer*, **35**, 3893-3898 (1994).

369. T.M. Liu and W.E. Baker, *Polym. Eng. Sci.*, **31**, 751-763 (1991).

370. D.M. Kaylon and F.H. Moy, *Polym. Eng. Sci.*, **28**, 1551-1558 (1988).

371. L.E. Bailey, D.G. Cook, J. Pronovost and A. Rudin, *Polym. Eng. Sci.*, **34**, 1485-1491 (1994).

372. M.A. Spalding, D.E. Kirkpatrick and K.S. Hyun, *Polym. Eng. Sci.*, **33**, 423-430 (1993).

373. A.C.-Y. Wong, *Polym. Eng. Sci.*, **31**, 1549-1552 (1991).

374. C.S. Speed, *Plast. Eng.*, **July**, 39-42 (1982).

375. J.A. Parker, D.C. Bassett, R.H. Olley and P. Jaaskelainen, *Polymer*, **35**, 4140-4145 (1994).

376. J.C.W. Chien and D. He, *J. Polym. Sci. Polym. Chem.*, **29**, 1585-1593 (1991).

377. J.H. Schut, *Plast. World*, **53**, 12-13 (1995).

378. J.H. Schut, *Plast. World*, **53**, 18-20 (1995).

379. R.D. Leaversuch, *Mod. Plast. Int.*, **70**, 18-19 (1995).

380. C.-T. Lue, *J. Plast. Film Sheeting*, **15**, 131-139 (1999).

381. E. Martuscelli, M. Pracella, G. Della Volpe and P. Greco, *Makromol. Chem.*, **185**, 1041-1061 (1984).

382. W.-Y. Chiu and S.J. Fang, *J. Appl. Polym. Sci.*, **30**, 1473-1489 (1985).

383. M. Levij and F.H.J. Maurer, *Polym. Eng. Sci.*, **28**, 670-678 (1988).

384. G. Rizzo and G. Spadaro, *Eur. Polym. J.*, **24**, 303-306 (1988).

385. G. Spadaro and G. Rizzo, *Eur. Polym. J.*, **25**, 1189-1192 (1989).

386. V. Flaris, A. Wasiak and W. Wenig, *J. Mater. Sci.*, **28**, 1685-1688 (1993).

387. M.R. Arroyo and M.A. López-Manchado, *Angew. Makromol. Chem.*, **226**, 129-141 (1995).

388. P. Zamotaev, I. Chodák, O. Mityukhin and I. Chorváth, *J. Appl. Polym. Sci.*, **56**, 935-946 (1995).

389. I. Fortelný, Z. Kruliš, D. Michálková and Z. Horák, *Angew. Makromol. Chem.*, **238**, 97-104 (1996).

390. J.Z. Liang and J.N. Ness, *Polym. Test.*, **16**, 379-389 (1997).

391. E. Vaccaro, A.T. Dibenedetto and S.J. Huang, *J. Appl. Polym. Sci.*, **63**, 275-281 (1997).

392. A.G. Andreopoulos, P.A. Tarantili and P. Anastassakis, *J. Macromol. Sci., Pure Appl. Chem.*, **A35**, 751-761 (1998).

393. L. Dong, R.H. Olley and D.C. Bassett, *J. Mater. Sci.*, **33**, 4043-4048 (1998).

394. J.Z. Liang and J.N. Ness, *Polym. Test.*, **17**, 179-189 (1998).

395. Ch. Tselios, D.N. Bikiaris, V. Maslis and C. Panayiotou, *Polymer*, **39**, 6807-6817 (1998).

396. M. Yamaguchi, *J. Appl. Polym. Sci.*, **70**, 457-463 (1998).

397. G. Barra, C. D'Aniello, L. Guadagno and V. Vittoria, *J. Mater. Sci.*, **34**, 4601-4606 (1999).

398. Ch. Tselios, D.N. Bikiaris, P. Savidis, C. Panayiotou and A. Larena, *J. Mater. Sci.*, **34**, 385-394 (1999).

399. C.M. Tai, R.K.Y. Li and C.N. Ng, *Polym. Test.*, **19**, 143-154 (2000).

400. J. Li, R.A. Shanks, R.H. Olley and G.R. Greenway, *Polymer*, **42**, 7685-7694 (2001).

401. S. Bertin and J.-J. Robin, *Eur. Polym. J.*, **38**, 2255-2264 (2002).

402. P.C. Guschi and J.U. Otaigbe, *J. Appl. Polym. Sci.*, **90**, 3445-3456 (2003).

403. C. Li, Y. Zhang and Y. Zhang, *Polym. Test.*, **22**, 191-195 (2003).

404. C. Li, W. Li, H. Wang, D. Zhang and Z. Li, *J. Appl. Polym. Sci.*, **88**, 2804-2809 (2003).

405. D.W. Bartlett, J.W. Barlow and D.R. Paul, *J. Appl. Polym. Sci.*, **27**, 2351-2360 (1982).

406. J.H. Cho, K.S. Choi and S.Y. Kim, *Int. J. Polym. Mat.*, **21**, 19-29 (1993).

407. M. Shibayama, A. Izutani, A. Ishikawa, K. Tanaka and S. Nomura, *Polymer*, **35**, 271-280 (1994).

408. H.P. Blom, J.W. Teh and A. Rudin, *J. Appl. Polym. Sci.*, **58**, 995-1006 (1995).

409. W. Zhu, X. Zhang, Z. Feng and B. Huang, *J. Appl. Polym. Sci.*, **58**, 551-557 (1995).

410. W. Zhu, X. Zhang, B. Huang and Z. Feng, *J. Appl. Polym. Sci.*, **58**, 515-521 (1995).

411. H.P. Blom, J.W. Teh and A. Rudin, *J. Appl. Polym. Sci.*, **61**, 959-968 (1996).

412. H.P. Blom, J.W. Teh and A. Rudin, *J. Appl. Polym. Sci.*, **60**, 1405-1417 (1996).

413. B.K. Kim and C.H. Choi, *J. Appl. Polym. Sci.*, **60**, 2199-2206 (1996).

414. S.J. Mahajan, B.L. Deopura and Y. Wang, *J. Appl. Polym. Sci.*, **60**, 1527-1538 (1996).

415. R.L. McEvoy and S. Krause, *Macromolecules*, **29**, 4258-4266 (1996).

416. W. Zheng, Y. Leng and X. Zhu, *Plast. Rubber Compos. Process. Appl.*, **25**, 490-494 (1996).

417. R.L. McEvoy and S. Krause, *J. Appl. Polym. Sci.*, **64**, 2221-2235 (1997).

418. C. Albano, G. Sánchez and A. Ismayel, *Polym. Bull.*, **41**, 91-98 (1998).

419. H.P. Blom, J.W. Teh and A. Rudin, *J. Appl. Polym. Sci.*, **70**, 2081-2095 (1998).

420. U. Plawky and W. Wenig, *J. Mater. Sci.*, **33**, 1611-1618 (1998).

421. H. Sano, H. Yui, H. Li and T. Inoue, *Polymer*, **39**, 5265-5267 (1998).

422. F. Hernández-Sánchez, R. Olayo and A. Manzur, *Polym. Bull.*, **42**, 481-488 (1999).

423. R. Hettema, J. Van Tol and L.P.B.M. Janssen, *Polym. Eng. Sci.*, **39**, 1628-1641 (1999).

424. U. Niebergall, J. Bohse, S. Seidler, W. Grellmann and B.L. Schürmann, *Polym. Eng. Sci.*, **39**, 1109-1118 (1999).

425. C.-S. Ha, H.-D. Park and W.-J. Cho, *J. Appl. Polym. Sci.*, **76**, 1048-1053 (2000).

426. J.I. Kim, S.H. Ryu and Y.W. Chang, *J. Appl. Polym. Sci.*, **77**, 2595-2602 (2000).

427. J. Li, R.A. Shanks and Y. Long, *J. Appl. Polym. Sci.*, **76**, 1151-1164 (2000).

428. C. Zhang, X.-S. YI, S. Asai and M. Sumita, *J. Mater. Sci.*, **35**, 673-683 (2000).

429. A.M.C. Souza and N.R. Demarquette, *Polymer*, **43**, 3959-3967 (2002).

430. A.M.C. Souza and N.R. Demarquette, *Polymer*, **43**, 1313-1321 (2002).

431. M. Taşdemir and H. Yildirim, *J. Appl. Polym. Sci.*, **83**, 2967-2975 (2002).

432. J. Finlay, M.J. Hill, P.J. Barham, K. Byrne and A. Woogara, *J. Polym. Sci. Polym. Phys.*, **41**, 1384-1392 (2003).

433. N. Kukaleva, G.P. Simon and E. Kosior, *Polym. Eng. Sci.*, **43**, 431-443 (2003).

434. S. Jose, A.S. Aprem, B. Francis, M.C. Chandy, P. Werner, V. Alstaedt and S. Thomas, *Eur. Polym. J.*, **40**, 2105-2115 (2004).

435. M.M. Dumoulin, C. Farha and L.A. Utracki, *Polym. Eng. Sci.*, **24**, 1319-1326 (1984).

436. P.-L. Yeh and A.W. Birley, *Plast. Rubber Process. Appl.*, **5**, 249-252 (1985).

437. M.M. Dumoulin, P.J. Carreau and L.A. Utracki, *Polym. Eng. Sci.*, **27**, 1627-1633 (1987).

438. Y. Long, Z.H. Stachurski and R.A. Shanks, *Polym. Int.*, **26**, 143-146 (1991).

439. V. Flaris, W. Wenig and Z.H. Stachurski, *Mater. Forum*, **16**, 181-184 (1992).

440. Y. Long, Z.H. Stachurski and R.A. Shanks, *Mater. Forum*, **16**, 173-179 (1992).

441. Y. Long, Z.H. Stachurski and R.A. Shanks, *Mater. Forum*, **16**, 259-265 (1992).

442. X.-Q. Zhou and J.N. Hay, *Polymer*, **34**, 4710-4716 (1993).

443. M. Bains, S.T. Balke, D. Reck and J. Horn, *Polym. Eng. Sci.*, **34**, 1260-1268 (1994).

444. V. Flaris, M.D. Zipper, G.P. Simon and A.J. Hill, *Polym. Eng. Sci.*, **35**, 28-33 (1995).

445. Y. Liu and R.W. Truss, *J. Polym. Sci. Polym. Phys.*, **33**, 813-822 (1995).

446. P.C. Cheung and S.T. Balke, *Ind. Eng. Chem. Res.*, **36**, 1191-1201 (1997).

447. L. Li, L. Chen, P. Bruin and M.A. Winnik, *J. Polym. Sci. Polym. Phys.*, **35**, 979-991 (1997).

448. F. Cser, F. Rasoul and E. Kosior, *Polym. Eng. Sci.*, **39**, 1100-1108 (1999).

449. H.-G. Jeong and K.-J. Lee, *Adv. Polym. Technol.*, **18**, 43-51 (1999).

450. N. Kukaleva, M. Jollands, F. Cser and E. Kosior, *J. Appl. Polym. Sci.*, **76**, 1011-1018 (2000).

451. I. Coccorullo, G. Gorrasi and R. Panatani, *J. Appl. Polym. Sci.*, **82**, 2237-2244 (2001).

452. J. Li, R.A. Shanks and Y. Long, *Polymer*, **42**, 1941-1951 (2001).

453. J. Li, R.A. Shanks and Y. Long, *J. Appl. Polym. Sci.*, **82**, 628-639 (2001).

454. K. Prehphet and W. Paecharoenchai, *J. Appl. Polym. Sci.*, **82**, 2140-2149 (2001).

455. A.C. Chang, T. Inge, L. Tau, A. Hiltner and E. Baer, *Polym. Eng. Sci.*, **42**, 2202-2212 (2002).

456. P. Pieroni, D. Ercoli, G. Goizueta and N. Capiati, *J. Elastomers Plast.*, **34**, 131-143 (2002).

457. G. Gorrasi, R. Pucciariello, V. Villani, V. Vittoria and S. Belviso, *J. Appl. Polym. Sci.*, **90**, 3338-3346 (2003).

458. A.P. Gupta, U.K. Saroop and M. Verma, *Polym.-Plast. Technol. Eng.*, **42**, 357-372 (2003).

459. S. Zhu, Y. Zhang and Y. Zhang, *J. Appl. Polym. Sci.*, **89**, 3248-3255 (2003).

460. A.P. Gupta, U.K. Saroop and M. Verma, *Polym.-Plast. Technol. Eng.*, **43**, 937-950 (2004).

461. P.P. Kundu, J. Biswas, H. Kim, S.E. Shim, S. Choe and D.S. Lee, *Adv. Polym. Technol.*, **23**, 230-238 (2004).

462. B.C. Poon, S.P. Chum, A. Hiltner and E. Baer, *J. Appl. Polym. Sci.*, **92**, 109-115 (2004).

463. M.C. Schwarz, J.W. Barlow and D.R. Paul, *J. Appl. Polym. Sci.*, **35**, 2053-2067 (1988).

464. B. Brahimi, A. Aït-Kadi and A. Ajji, *Polym. Eng. Sci.*, **34**, 1202-1210 (1994).

465. Z. Bartczak, N.P. Krasnikova and A. Galeski, *J. Appl. Polym. Sci.*, **62**, 167-179 (1996).

466. M.N. Bureau, H. El Kadi, J. Denault and J.I. Dickson, *Polym. Eng. Sci.*, **37**, 377-390 (1997).

467. S. Karrad, J.-M.L. Cuesta and A. Crespy, *Plast. Rubber Compos. Process. Appl.*, **26**, 193-198 (1997).

468. M.N. Bureau, J.I. Dickson and J. Denault, *J. Mater. Sci.*, **33**, 1405-1419 (1998).

469. S.C. Tjong and S.A. Xu, *J. Appl. Polym. Sci.*, **68**, 1099-1108 (1998).

470. S.-A. Xu and C.-M. Chan, *Polym. J.*, **30**, 552-558 (1998).

471. L. Abis, L. Abbondanza, R. Braglia, L. Castellani, G. Giannotta and R. Po, *Macromol. Chem. Phys.*, **201**, 1732-1741 (2000).

472. Z. Bartczak, A. Galeski and M. Pluta, *J. Appl. Polym. Sci.*, **76**, 1746-1761 (2000).

473. J. Li, C.-M. Chan, B. Gao and J. Wu, *Macromolecules*, 33, 1022-1029 (2000).

474. S.A. Xu and S.C. Tjong, *J. Appl. Polym. Sci.*, 77, 2024-2033 (2000).

475. S.-A. Xu and S.C. Tjong, *Polym. J.*, **32**, 208-214 (2000).

476. J. Wu, B. Guo, C.-M. Chan, J. Li and H.-S. Tang, *Polymer*, **42**, 8857-8865 (2001).

477. B. Chen, X. Li, S. Xu, T. Tang, B. Zhou and B. Huang, *Polymer*, **43**, 953-961 (2002).

478. G. Chen, S. Guo and H. Li, *J. Appl. Polym. Sci.*, **86**, 23-32 (2002).

479. Y. Hu, C. Qi, W. Liu, B. Wang, H. Zheng, X. Sun and X. Zheng, *J. Appl. Polym. Sci.*, **90**, 1507-1514 (2003).

480. H. Padilla-Lopez, M.O. Vazquez, R. Gonzalez-Nunez and D. Rodrigue, *Polym. Eng. Sci.*, **43**, 1646-1656 (2003).

481. G. Chen, S. Guo and Y. Li, *J. Appl. Polym. Sci.*, **92**, 3153-3158 (2004).

482. A. Chirawithayaboon and S. Kiatkamjornwong, *J. Appl. Polym. Sci.*, **91**, 742-755 (2004).

483. H.M. Lee and O.O. Park, *J. Rheol.*, **38**, 1405-1425 (1994).

484. T. Li, V.A. Topolkaraev, A. Hiltner, E. Baer, X.Z. Ji and R.P. Quirk, *J. Polym. Sci. Polym. Phys.*, **33**, 667-683 (1995).

485. L.-Y. Yang, T.G. Smith and D. Bigio, *J. Appl. Polym. Sci.*, **58**, 117-127 (1995).

486. L.-Y. Yang, D. Bigio and T.G. Smith, *J. Appl. Polym. Sci.*, **58**, 129-141 (1995).

487. H. Feng, J. Tian and C. Ye, *J. Appl. Polym. Sci.*, **61**, 2265-2271 (1996).

488. T. Li, V.A. Topolkaraev, A. Hiltner and E. Baer, *Adv. Chem. Ser.*, **252**, 319-334 (1996).

489. T. Li, C. Carfagna, Jr., V.A. Topolkaraev, A. Hiltner, E. Baer, X.-Z. Ji and R.P. Quirk, *Adv. Chem. Ser.*, **252**, 335-350 (1996).

490. M.L. Arnal and A.J. Müller, *Macromol. Chem. Phys.*, **200**, 2559-2576 (1999).

491. J. Francis and K.E. George, *J. Elastomers Plast.*, **24**, 151-166 (1992).

492. J. Francis, K.E. George and R. Joseph, *Eur. Polym. J.*, **28**, 1289-1293 (1992).

493. M. Aglietto, E. Benedetti, G. Ruggeri, M. Pracella, A. D'Alessio and F. Ciardelli, *Macromol. Symp.*, **98**, 1101-1122 (1995).

494. Q.-Y. Zhou, B.-H. Zhang, M.-D. Song and B.-L. He, *Eur. Polym. J.*, **32**, 1145-1150 (1996).

495. P. He, H. Huang, W. Xiao, S. Huang and S. Cheng, *J. Appl. Polym. Sci.*, **64**, 2535-2541 (1997).

496. H. Liang and B.D. Favis, *Ind. Eng. Chem. Res.*, **36**, 1211-1217 (1997).

497. R. Xu and H.P. Schreiber, *J. Appl. Polym. Sci.*, **70**, 1597-1604 (1998).

498. M. Bani-Hani, D. Banu, J. Campanelli and D. Feldman, *J. Appl. Polym. Sci.*, **74**, 1156-1168 (1999).

499. H. Liang, R. Xu, B.D. Favis and H.P. Schreiber, *Polymer*, **40**, 4419-4423 (1999).

500. H. Liang, B.D. Favis, Y.S. Yu and A. Eisenberg, *Macromolecules*, **32**, 1637-1642 (1999).

501. W.-D. Wang, H. Liang, B.D. Favis and H.P. Schreiber, *J. Appl. Polym. Sci.*, **81**, 1891-1901 (2001).

502. T.D. Traugott, J.W. Barlow and D.R. Paul, *J. Appl. Polym. Sci.*, **28**, 2947-2959 (1983).

503. S.A. Jabarin, E.A. Lofgren and S.B. Shah in "Emerging Technologies in Plastics Recycling", American Chemical Society, Washington DC, 1992, pp. 215-231.

504. C.C. Chen and J.L. White, *Polym. Eng. Sci.*, **33**, 923-930 (1993).

505. P. Sambaru and S.A. Jabarin, *Polym. Eng. Sci.*, **33**, 827-837 (1993).

506. C. Chen and F.S. Lai, *Polym. Eng. Sci.*, 34, 472-476 (1994).

507. S.S. Dagli and K.M. Kamdar, *Polym. Eng. Sci.*, **34**, 1709-1719 (1994).

508. L. Mascia and F. Bellahdeb, *Adv. Polym. Technol.*, **13**, 99-109 (1994).

509. B. Boutevin, J.M. Lusinchi, Y. Pietrasanta and J.-J. Robin, *Polym. Eng. Sci.*, **36**, 879-884 (1996).

510. G. Kumaravel and S.A. Jabarin, *Adv. Polym. Technol.*, **15**, 191-204 (1996).

511. S. Basu and D.D. Kale, *Macromol. Symp.*, **118**, 329-334 (1997).

512. S. Kim, C.E. Park, J.H. An, D. Lee and J. Kim, *Polym. J.*, **29**, 274-278 (1997).

513. Y. Pietrasanta, J.-J. Robin, N. Torres and B. Boutevin, *Macromol. Chem. Phys.*, **200**, 142-149 (1999).

514. D.H. Kim, K.Y. Park, S.K. Do and J.Y. Kim, *J. Macromol. Sci., Pure Appl. Chem.*, **A37**, 1141-1157 (2000).

515. D.-H. Kim, K.-Y. Park, J.-Y. Kim and K.-D. Suh, *J. Appl. Polym. Sci.*, **78**, 1017-1024 (2000).

516. F. Pazzagli and M. Pracella, *Macromol. Symp.*, **149**, 225-230 (2000).

517. T. Demir and T. Tinçer, *J. Appl. Polym. Sci.*, **79**, 827-835 (2001).

518. C. Guerrero, T. Lozano, V. González and E. Arroyo, *J. Appl. Polym. Sci.*, **82**, 1382-1390 (2001).

519. P. Laurienzo, B. Immirzi and M. Malinconico, *Macromol. Mater. Eng.*, **286**, 248-253 (2001).

520. J.M. Lusinchi, B. Boutevin, N. Torres and J.-J. Robin, *J. Appl. Polym. Sci.*, **79**, 874-880 (2001).

521. M.a. Pluta, Z. Bartczak, A. Pawlak, A. Galeski and M. Pracella, *J. Appl. Polym. Sci.*, **82**, 1423-1436 (2001).

522. A. Retolaza, J.I. Eguiazábal and J. Nazábal, *Polym. Eng. Sci.*, **42**, 2072-2083 (2002).

523. R.M. Meri, I. Jablonskis, J. Zicans, M. Kalnins and A.K. Bledzki, *Mech. Compos. Mater.*, **40**, 247-252 (2004).

524. F.P. La Mantia and A. Valenza, *Eur. Polym. J.*, **25**, 553-556 (1989).

525. H. Raval, S. Devi, Y.P. Singh and M.H. Mehta, *Polymer*, **32**, 493-500 (1991).

526. M.M. Nir, A. Ram and J. Miltz, *Polym. Eng. Sci.*, **35**, 1878-1883 (1995).

527. P.L. Beltrame, A. Castelli, M. Di Pasquantonio, M. Canetti and A. Seves, *J. Appl. Polym. Sci.*, **60**, 579-590 (1996).

528. E.F. Silva and B.G. Soares, *J. Appl. Polym. Sci.*, **60**, 1687-1694 (1996).

529. B. Jurkowski and Y.A. Olkhov, *J. Appl. Polym. Sci.*, **65**, 1807-1811 (1997).

530. K. Kelar and B. Jurkowski, *Polymer*, **41**, 1055-1062 (2000).

531. S. Filippi, V. Chiono, G. Polacco, M. Paci, L.I. Minkova and P. Magagnini, *Macromol. Chem. Phys.*, **203**, 1512-1525 (2002).

532. C. Harrats, R. Fayt and R. Jérôme, *Polymer*, **43**, 5347-5354 (2002).

533. B. Jurkowski, Y.A. Olkhov, K. Kelar and O.M. Olkhova, *Eur. Polym. J.*, **38**, 1229-1236 (2002).

534. L. Minkova, Hr. Yordanov and S. Filippi, *Polymer*, **43**, 6195-6204 (2002).

535. C. Jiang, S. Filippi and P. Magagnini, *Polymer*, **44**, 2411-2422 (2003).

536. V. Chiono, S. Filippi, H. Yordanov, L. Minkova and P. Magagnini, *Polymer*, **44**, 2423-2432 (2003).

537. F.P. La Mantia, R. Scaffaro, A. Valenza, A. Marchetti and S. Filippi, *Macromol. Symp.*, **198**, 173-182 (2003).

538. P. Leewajanakul, R. Pattanaolarn, J.W. Ellis, M. Nithitanakul and B.P. Grady, *J. Appl. Polym. Sci.*, **89**, 620-69 (2003).

539. L. Minkova, H. Yordanov, S. Filippi and N. Grizzuti, *Polymer*, **44**, 7925-7932 (2003).

540. R. Scaffaro, F.P. La Mantia, L. Canfora, G. Polacco, S. Filippi and P. Magagnini, *Polymer*, **44**, 6951-6957 (2003).

541. Hr. Yordanov and L. Minkova, *Eur. Polym. J.*, **39**, 951-958 (2003).

542. L. Canfora, S. Filippi and F.P. La Mantia, *Polym. Eng. Sci.*, **44**, 1732-1737 (2004).

543. S. Filippi, H. Yordanov, L. Minkova, G. Polacco and M. Talarico, *Macromol. Mater. Eng.*, **289**, 512-523 (2004).

544. F.P. La Mantia, *Polym. Deg. Stab.*, **37**, 145-148 (1992).

545. P.S. Hope, J.G. Bonner and A.F. Miles, *Plast. Rubber Compos. Process. Appl.*, **22**, 147-158 (1994).

546. T. Li, S. Henry, M.S. Silverstein, A. Hiltner and E. Baer, *J. Appl. Polym. Sci.*, **52**, 301-314 (1994).

547. D.R. Rueda, F.J. Baltá-Calleja, A. Viksne and L. Malers, *J. Mater. Sci.*, **29**, 1109-1114 (1994).

548. D.R. Rueda, L. Malers, A. Viksne and F.J. Baltá-Calleja, *J. Mater. Sci.*, **31**, 3915-3920 (1996).

549. C. Albano, G. Sánchez and A. Ismayel, *J. Macromol. Sci., Pure Appl. Chem.*, **A35**, 1349-1361 (1998).

550. S. Tall, S. Karlsson and A.-C. Albertsson, *Polym. Polym. Compos.*, **6**, 261-267 (1998).

551. G.A. Marques and J.A.S. Tenório, *Waste Manag.*, **20**, 265-269 (2000).

552. F. Elmaghor, L. Zhang and H. Li, *J. Appl. Polym. Sci.*, **88**, 2756-2762 (2003).

553. D. Rana, C.H. Lee, K. Cho, B.H. Lee and S. Choe, *J. Appl. Polym. Sci.*, **69**, 2441-2450 (1998).

554. L.A. Utracki in "Multiphase Polymers: Blends and Ionomers", L.A. Utracki and R.A. Weiss (eds.), American Chemical Society, Washington,DC, 1989, pp. 153-210.

555. B.H. Clampitt, *Anal. Chem.*, **35**, 577-579 (1963).

556. B.H. Clampitt, *J. Polym. Sci., Part A, Gen. Pap.*, **3**, 671-679 (1965).

557. T. Sato and M. Takahashi, *J. Appl. Polym. Sci.*, **13**, 2665-2676 (1969).

558. D.R. Norton and A. Keller, *J. Mater. Sci.*, **19**, 447-456 (1984).

559. D.C. Yang, J.M. Brady and E.L. Thomas, *J. Mater. Sci.*, **23**, 2546-2552 (1988).

560. T. Malavasic and V. Musil, *J. Therm. Anal.*, **34**, 503-508 (1988).

561. M.P. Farr and I.R. Harrison, *ACS Div. Polym. Sci., Polym. Prepr.*, **31**, 257-258 (1989).

562. M.T. Conde Braña and U.W. Gedde, *Polymer*, **33**, 3123-3136 (1992).

563. U.W. Gedde, *Prog. Colloid Polym. Sci.*, **87**, 8-15 (1992).

564. M.J. Hill, S.J. Morgan and P.J. Barham, *Thermochim. Acta*, **238**, 17-39 (1994).

565. J. Minick, A. Moet and E. Baer, *Polymer*, **36**, 1923-1932 (1995).

566. C.C. Puig, *Polym. Bull.*, **36**, 361-367 (1996).

567. C.C. Puig, *Polym. Bull.*, **38**, 715-720 (1997).

568. A. Alizadeh, A. Muñoz-Escalona, B. Vallejo and J. Martínez-Salazar, *Polymer*, **38**, 1207-1214 (1997).

569. A. Viksne, L. Malers and A.K. Bledzki, *Angew. Makromol. Chem.*, **249**, 47-57 (1997).

570. Z.J. Fan, M.C. Williams and P. Choi, *Polymer*, **43**, 1497-1502 (2002).

571. Q. Fu, Y. Men and G. Strobl, *Polymer*, **44**, 1927-1933 (2003).

572. S.J. Mumby, P. Sher and J. van Ruiten, *Polymer*, **36**, 2921-2927 (1995).

573. M.J. Hill, P.J. Barham, A. Keller and C.C.A. Rosney, *Polymer*, **32**, 1384-1393 (1991).

574. M.J. Hill and P.J. Barham, *Polymer*, **33**, 4891-4897 (1992).

575. C.C. Puig, M.J. Hill and J.A. Odell, *Polymer*, **34**, 3402-3407 (1993).

576. M.J. Hill, *Polymer*, **35**, 1991-1993 (1994).

577. C.C. Puig, J.A. Odell, M.J. Hill, P.J. Barham and M.J. Folkes, *Polymer*, **35**, 2452-2457 (1994).

578. M.J. Hill, P.J. Barham and A. Keller, *Polymer*, **33**, 2530-2541 (1992).

579. M.J. Hill and P.J. Barham, *Polymer*, **33**, 4099-4107 (1992).

580. B. Crist and M.J. Hill, *J. Polym. Sci. Polym. Phys.*, **35**, 2329-2353 (1997).

581. A. Garcia-Rejon and C. Alvarez, *Polym. Eng. Sci.*, **27**, 640-646 (1987).

582. C. Tran, *Macromol. Symp.*, **112**, 137-139 (1996).

583. K. Cho, B.H. Lee, K.-M. Hwang, H. Lee and S. Choe, *Polym. Eng. Sci.*, **38**, 1969-1975 (1998).

584. G.H. Edward, *Br. Polym. J.*, **18**, 88-93 (1986).

585. M. Pracella, E. Benedetti and F. Galleschi, *Thermochim. Acta*, **162**, 163-177 (1990).

586. J.A. Gonzalez Orozco, J.M. Rego and I. Katime, *J. Appl. Polym. Sci.*, **42**, 1943-1948 (1991).

587. B.S. Tanem and A. Stori, *Thermochim. Acta*, **345**, 73-80 (2000).

588. P. Kurian, K.E. George and D.J. Francis, *Angew. Makromol. Chem.*, **193**, 39-49 (1991).

589. A.K. Gupta, S.K. Rana and B.L. Deopura, *J. Appl. Polym. Sci.*, **46**, 99- 108 (1992).

590. A.K. Gupta, S.K. Rana and B.L. Deopura, *J. Appl. Polym. Sci.*, **44**, 719-726 (1992).

591. Y. Zhao, S. Liu and D. Yang, *Macromol. Chem. Phys.*, **198**, 1427-1436 (1997).

592. S.Y. Lee, J.Y. Jho and W. Huh, *J. Ind. Eng. Chem.*, **4**, 258-262 (1998).

593. P. Choi, *Polymer*, **41**, 8741-8747 (2000).

594. S.K. Rana, *J. Appl. Polym. Sci.*, **83**, 2604-2608 (2002).

595. M.S. Bischel, M.R. Vanlandingham, R.F. Eduljee, J.W. Gillespie, Jr. and J.M. Schultz, *J. Mater. Sci.*, **35**, 221-228 (2000).

596. M.D. Failla and L. Mandelkern, *Macromolecules*, **26**, 7167-7175 (1993).

597. I.A. Hussein, *Macromolecules*, **36**, 2024-2031 (2003).

598. I.A. Hussein, *Polym. Int.*, **53**, 1327-1335 (2004).

599. L.Y. Zhao and P. Choi, *J. Appl. Polym. Sci.*, **91**, 1927-1931 (2004).

600. F.P. La Mantia, A. Valenza and D. Acierno, *Polym. Bull.*, **15**, 381-387 (1986).

601. J.A. Gonzalez Orozco, J.M. Rego and I. Katime, *J. Appl. Polym. Sci.*, **42**, 1879-1886 (1991).

602. M.J. Hill, R.L. Morgan and P.J. Barham, *Polymer*, **38**, 3003-3009 (1997).

603. P.J. Barham, M.J. Hill, G. Goldbeck-Wood and J. van Ruiten, *Polymer*, **34**, 2981-2988 (1993).

604. M.J. Hill, P.J. Barham and J. van Ruiten, *Polymer*, **34**, 2975-2980 (1993).

605. M.J. Hill and P.J. Barham, *Polymer*, **35**, 1802-1808 (1994).

606. M.J. Hill and P.J. Barham, *Polymer*, **38**, 5595-5601 (1997).

607. R.L. Morgan, M.J. Hill, P.J. Barham, A. Van der Pol, B.J. Kip, R. Ottjes and J. van Ruiten, *Polymer*, **42**, 2121-2135 (2001).

608. B.S. Tanem and A. Stori, *Polymer*, **42**, 5689-5694 (2001).

609. B.S. Tanem and A. Stori, *Polymer*, **42**, 4309-4319 (2001).

610. A. Tabtiang, B. Parchana, R.A. Venables and T. Inoue, *J. Polym. Sci. Polym. Phys.*, **39**, 380-389 (2001).

611. H. Kwag, D. Rana, K. Cho, J. Rhee, T. Woo, H. Byung and S. Choe, *Polym. Eng. Sci.*, **40**, 1672-1681 (2000).

612. M. Hess, B.L. Lopez and C. Gartner, *Macromol. Symp.*, **174**, 277-294 (2001).

613. M.J.O.C. Guimarães, F.M.B. Coutinho, M.C.G. Rocha, M. Farah and R.E.S. Bretas, *J. Appl. Polym. Sci.*, **86**, 2240-2246 (2002).

614. J. Wang, D. Pang and B. Huang, *Polym. Bull.*, **24**, 241-246 (1990).

615. C. Liu, J. Wang and J. He, *Polymer*, **43**, 3811-3818 (2002).

616. M.W.C. Guimaraes, F.M.B. Coutinho, M.C.G. Rocha, A. Farah and R.E.S. Bretas, *Polym. Test.*, **22**, 843-847 (2003).

617. M.S. Bischel, J.M. Schultz and K.M. Kit, *Polymer*, **39**, 2123-2127 (1998).

618. V. Musil, B. Pregrad and B. Zerjal, *Int. Polym. Proc.*, **2**, 182-184 (1988).

619. C.L.P. Shan, J.B.P. Soares and A. Penlidis, *Polymer*, **43**, 7345-7365 (2002).

620. C.L.P. Shan, J.B.P. Soares and A. Penlidis, *Polymer*, **44**, 177-185 (2003).

621. E. Karbashewski, L. Kale, A. Rudin and W.J. Tchir, *J. Appl. Polym. Sci.*, **47**, 1143-1154 (1993).

622. A.K. Gupta, S.K. Rana and B.L. Deopura, *J. Appl. Polym. Sci.*, **49**, 477-485 (1993).

623. Y. Wang, H. Zou, Q. Fu, G. Zhang and K. Shen, *J. Appl. Polym. Sci.*, **85**, 236-243 (2002).

624. J. Schellenberg and G. Fienhold, *Polym. Eng. Sci.*, **38**, 1413-1419 (1998).

625. Z. Zhou, X. Lu and N. Brown, *Polymer*, **34**, 2520-2523 (1993).

626. Z. Zhou and N. Brown, *Polymer*, **35**, 3619-3623 (1994).

627. N. Brown and Z. Zhou, *Macromolecules*, **28**, 1807-1811 (1995).

628. J. Rhee and B. Crist, *J. Polym. Sci. Polym. Phys.*, **32**, 159-169 (1994).

629. M. Huggard, *J. Fire Sci.*, **14**, 393-408 (1996).

630. C. Goin, *Proc. Int. Conf. Fire Saf.*, **23**, 199-207 (1997).

631. S.K. Bhateja and E.H. Andrews, *Polym. Eng. Sci.*, **23**, 888-894 (1983).

632. M. Okamoto, A. Kojima and T. Kotaka, *Polymer*, **39**, 2149-2153 (1998).

633. J.-T. Yeh and H.-C. Wu, *Polym. J.*, **30**, 1-10 (1998).

634. J.-T. Yeh and S.-S. Chang, *Polym. Eng. Sci.*, **42**, 1558-1567 (2002).

635. C. Sawatari and M. Matsuo, *Polymer*, **30**, 1603-1614 (1989).

636. Y. Bin, L. Ma, R. Adachi, H. Kurosu and M. Matsuo, *Polymer*, **42**, 8125-8135 (2001).

637. Y. Bin, M. Fukuda, H. Kurosu and M. Matsuo, *Macromol. Symp.*, **147**, 1-14 (1999).

638. J.-T. Yeh and S.-S. Chang, *J. Appl. Polym. Sci.*, **79**, 1890-1901 (2001).

639. J.T. Yeh and S.S. Chang, *J. Mater. Sci.*, **35**, 3227-3236 (2000).

640. J.-T. Yeh, S.-S. Chang and M.-S. Yen, *J. Appl. Polym. Sci.*, **70**, 149-159 (1998).

641. J.-T. Yeh, Y.-L. Lin and C.-C. Fan-Chiang, *Macromol. Chem. Phys.*, **197**, 3531-3540 (1996).

642. J.-T. Yeh, Y.-T. Lin and K.-N. Chen, *J. Appl. Polym. Sci.*, **89**, 3728-3738 (2003).

643. C. Nakafuku and K. Nishimura, *J. Appl. Polym. Sci.*, **87**, 1962-1968 (2003).

644. L. Minkova and M. Mikhailov, *Colloid Polym. Sci.*, **265**, 1-7 (1987).

645. M. Mihailov and L. Minkova, *Colloid Polym. Sci.*, **265**, 681-685 (1987).

646. L. Minkova and M. Mikhailov, *Colloid Polym. Sci.*, **267**, 577-582 (1989).

647. L. Minkova and M. Mikhailov, *Colloid Polym. Sci.*, **268**, 1018-1023 (1990).

648. Y.L. Huang and N. Brown, *Polymer*, 33, 2989-2997 (1992).

649. M.M. Dumoulin, L.A. Utracki and J. Lara, *Polym. Eng. Sci.*, **24**, 117-126 (1984).

650. A.B. Boscoletto, R. Franco, M. Scapin and M. Tavan, *Eur. Polym. J.*, 33, 97-105 (1997).

651. Y. Zhao, W. Zhang and D. Yang, *J. Mater. Sci. Lett.*, **12**, 1309-1312 (1993).

652. S.-G. Lee and T.-J. Kang, *Polym. Bull.*, **40**, 95-102 (1998).

653. A.J. Müller, V. Balsamo, F. Da Silva, C.M. Rosales and A.E. Sáez, *Polym. Eng. Sci.*, **34**, 1455-1463 (1994).

654. B. Tremblay, *Polym. Eng. Sci.*, **32**, 65- 72 (1992).

655. J.J. Gunderson and D.R. Parikh, *ACS Div. Polym. Sci., Polym. Prepr.*, **30**, 233-234 (1989).

656. F. Martinez and N. Barrera, *Tappi J.*, **74**, 165-171 (1991).

657. J.-H. Oh, *J. Reinf. Plast. Compos.*, **18**, 662-672 (1999).

658. J.P. García-Villaluenga, B. Seoane, V. Compañ and R. Diaz-Calleja, *Polymer*, **38**, 3827-3836 (1997).

659. A. Ghaneh-Fard, P.J. Carreau and P.G. Lafleur, *Int. Polym. Proc.*, **12**, 136-146 (1997).

660. D.Y. Chiu, G.E. Ealer, F.H. Moy and J.O. Bühler-Vidal, *J. Plast. Film Sheeting*, **15**, 153-178 (1999).

661. R.K. Krishnaswamy and A.M. Sukhadia, *Polymer*, **41**, 9205-9217 (2000).

662. R.K. Krishnaswamy and M.J. Lamborn, *Polym. Eng. Sci.*, **40**, 2385-2396 (2000).

663. J. Lu, H.-J. Sue and T.P. Rieker, *J. Mater. Sci.*, **35**, 5169-5178 (2000).

664. P.P. Kundu, J. Biswas, H. Kim and S. Choe, *Eur. Polym. J.*, **39**, 1585-1593 (2003).

665. A. Ajji, J. Auger, J. Huang and L. Kale, *Polym. Eng. Sci.*, **44**, 252-260 (2004).

666. G.M. McNally, C. Bermingham and W.R. Murphy, *Chem. Eng. Res. Des.*, **71**, 223-231 (1993).

667. D.M. Simpson and D.G. O'Neil, *Tappi J.*, **78**, 170-174 (1995).

668. Y. Hong, S.J. Coombs, J.J. Cooper-White, M.E. Mackay, C.J. Hawker, E. Malmström and N. Rehnberg, *Polymer*, **41**, 7705-7713 (2000).

669. D. Rana, H.L. Kim, H. Kwag, J. Rhee, K. Cho, T. Woo, B.H. Lee and S. Choe, *J. Appl. Polym. Sci.*, **76**, 1950-1964 (2000).

670. D. Rana, H.L. Kim, H. Kwag and S. Choe, *Polymer*, **41**, 7067-7082 (2000).

671. D. Rana, K. Cho, T. Woo, B.H. Lee and S. Choe, *J. Appl. Polym. Sci.*, **74**, 1169-1177 (1999).

672. M.J. Hill and P.J. Barham, *Polymer*, **41**, 1621-1625 (2000).

673. P. Micic, S.N. Bhattacharya and G. Field, *Polym. Eng. Sci.*, **38**, 1685-1693 (1998).

674. G.A. Campbell and A.K. Babel, *Macromol. Symp.*, **101**, 199-206 (1996).

675. E.W. Kuijk, P.P. Tas and P. Neuteboom, *J. Reinf. Plast. Compos.*, **18**, 508-517 (1999).

676. P. Micic and S.N. Bhattacharya, *Polym. Int.*, **49**, 1580-1589 (2000).

677. J. Lu and H.-J. Sue, *J. Polym. Sci. Polym. Phys.*, **40**, 507-518 (2002).

678. J. Li, R.A. Shanks and Y. Long, *J. Appl. Polym. Sci.*, **88**, 12-16 (2003).

679. A.C.-Y. Wong, *Plast. Rubber Compos. Process. Appl.*, **20**, 159-164 (1993).

680. D. Abraham, K.E. George and D.J. Francis, *Angew. Makromol. Chem.*, **200**, 15-25 (1992).

681. I.A. Hussein and M.C. Williams, *Polym. Eng. Sci.*, **41**, 696-701 (2001).

682. J.-Z. Liang, *Polym. Test.*, **21**, 69-74 (2002).

683. A. Ajji, P. Sammut and M.A. Huneault, *J. Appl. Polym. Sci.*, **88**, 3070-3077 (2003).

684. I.A. Hussein and M.C. Williams, *Polym. Eng. Sci.*, **44**, 660-672 (2004).

685. S.K. Isac and K.E. George, *J. Appl. Polym. Sci.*, **81**, 2545-2549 (2001).

686. A. Ghijsels, J.J.S.M. Ente and J. Raadsen, *Int. Polym. Proc.*, 7, 44-50 (1992).

687. D. Acierno, D. Curto, F.P. La Mantia and A. Valenza, *Polym. Eng. Sci.*, **26**, 28-33 (1986).

688. B. Tremblay, *J. Non-Newton. Fluid Mech.*, **43**, 1-29 (1992).

689. L.A. Utracki and B. Schlund, *Polym. Eng. Sci.*, **27**, 367-379 (1987).

690. B. Schlund and L.A. Utracki, *Polym. Eng. Sci.*, **27**, 380-386 (1987).

691. L.A. Utracki and B. Schlund, *Polym. Eng. Sci.*, **27**, 1512-1522 (1987).

692. B. Schlund and L.A. Utracki, *Polym. Eng. Sci.*, **27**, 1523-1529 (1987).

693. D. Abraham, K.E. George and D.J. Francis, *J. Appl. Polym. Sci.*, **62**, 59- 65 (1996).

694. X.-R. Xu, J.-T. Xu, L. Chen, R. Liu and L. Feng, *J. Appl. Polym. Sci.*, **80**, 123-129 (2001).

695. M.H. Wagner, S. Kheirandish and M. Yamaguchi, *Rheol. Acta.*, **44**, 198-218 (2004).

696. H.S. Lee and M.M. Denn, *Polym. Eng. Sci.*, **40**, 1132-1142 (2000).

697. M. Herranen and A. Savolainen, *Rheol. Acta.*, **23**, 461-464 (1984).

698. K. Ho, L. Kale and S. Montgomery, *J. Appl. Polym. Sci.*, **85**, 1408-1418 (2002).

699. F.P. La Mantia and D. Acierno, *Eur. Polym. J.*, **21**, 811-813 (1985).

700. A. Majumdar and D.D. Kale, *J. Appl. Polym. Sci.*, **81**, 53-57 (2001).

701. I.A. Hussein, T. Hameed, B.F.A. Sharkh and K. Mezghani, *Polymer*, **44**, 4665-4672 (2003).

702. H.-H. Shih, C.-M. Wong, Y.-C. Wang, C.-J. Huang and C.-C. Wu, *J. Appl. Polym. Sci.*, **73**, 1769-1773 (1999).

703. C.M. Beagan, G.M. McNally and W.R. Murphy, *J. Plast. Film Sheeting*, **15**, 329-340 (1999).

704. J.-T. Xu, X.-R. Xu, Q. Zheng, L. Feng and W. Chen, *Eur. Polym. J.*, **38**, 365-375 (2002).

705. T. Hameed and I.A. Hussein, *Polymer*, **43**, 6911-6929 (2002).

706. F. Chen, R.A. Shanks and G. Amarasinghe, *J. Appl. Polym. Sci.*, **81**, 2227-2236 (2001).

707. R.W. Halle, *Tappi J.*, **83**, 85-85 (2000).

708. W. Hellmuth, *Kunststoffe: Plast Europe*, **86**, 1821-1822 (1996).

709. F.M. Mirabella and A. Bafna, *J. Polym. Sci. Polym. Phys.*, **40**, 1637-1643 (2002).

710. D.E. Axelson, G.C. Levy and L. Mandelkern, *Macromolecules*, **12**, 41-52 (1979).

711. F.A. Kunrath, R.S. Mauler, R.F. de Souza and O.L.Jr. Casagrande, *Macromol. Chem. Phys.*, **203**, 2058-2068 (2002).

712. J. Schellenberg and B. Wagner, *J. Therm. Anal. Calorim.*, **52**, 275-292 (1998).

713. N.C. Billingham, O.J. Hoad, F. Chenard and D.J. Whiteman, *Macromol. Symp.*, **115**, 203-214 (1997).

714. M. Celina, G.A. George, D.J. Lacey and N.C. Billingham, *Polym. Deg. Stab.*, **47**, 311-317 (1995).

715. Z. Zhou, N. Brown and B. Crist, *J. Polym. Sci. Polym. Phys.*, **33**, 1047-1051 (1995).

716. F. Raue and G.W. Ehrenstein, *J. Elastomers Plast.*, **31**, 194-204 (1999).

717. S.L. Sakellarides and A.J. McHugh, *Polym. Eng. Sci.*, **25**, 1179-1187 (1985).

718. Y.-M. Kim and J.-K. Park, *J. Appl. Polym. Sci.*, **61**, 2315-2324 (1996).

719. G.H. Meeten in "Optical Properties of Polymers", Elsevier Applied Science Publishers, London, 1986, pp. 265-333.

720. A.B. Sabbagh and A.J. Lesser, *J. Polym. Sci. Polym. Phys.*, **37**, 2651-2663 (1999).

721. R.M. Patel, T.I. Butler, K.L. Walton and G.W. Knight, *Polym. Eng. Sci.*, **34**, 1506-1514 (1994).

722. C.K. Samios and N.K. Kalfoglou, *Polymer*, **39**, 3863-3870 (1998).

723. E. Andreassen, A. Larsen, K. Nord-Varhaug, M. Skar and H. Oysaed, *Polym. Eng. Sci.*, **42**, 1082-1097 (2002).

724. A.M. Sukhadia, D.C. Rohlfing, M.B. Johnson and G.L. Wilkes, *J. Appl. Polym. Sci.*, **85**, 2396-2411 (2002).

725. M.B. Johnson, G.L. Wilkes, A.M. Sukhadia and D.C. Rohlfing, *J. Appl. Polym. Sci.*, **77**, 2845-2864 (2000).

726. M. Kojima, J.H. Magill, J.S. Lin and S.N. Magonov, *Chem. Mater.*, **9**, 1145-1153 (1997).

727. A. Bafna, G. Beaucage, F.M. Mirabella, G. Skillas and S. Sukumaran, *J. Polym. Sci. Polym. Phys.*, **39**, 2923-2936 (2001).

728. L.A. Utracki in "Polymer Alloys and Blends", Carl Hanser Verlag, Munich, 1989, pp. 1-30.